Fall 2002

Iron phosphate glass for the vitrification of INEEL sodium bearing waste and Hanford low activity waste

Robert Douglas Leerssen

Department:

Iron Phosphate Glass for the Vitrification of INEEL Sodium Bearing Waste and Hanford Low Activity Waste

by

Robert Douglas Leerssen

A THESIS

Presented to the Faculty of the Graduate School of the

UNIVERSITY OF MISSOURI-ROLLA

In Partial Fulfillment of the Requirements for the Degree

MASTER OF SCIENCE IN CERAMIC ENGINEERING

2002

Approved by

_____	_____
Delbert E. Day, Advisor	Richard K. Brow

_____

David J. Wronkiewicz

PUBLICATION THESIS OPTION

This thesis has been prepared in the style used for publication in the Journal of Nuclear Materials. Pages 1 through 105 are intended to be submitted for publication in that journal. Appendices have been added for purposes of normal thesis writing.

ABSTRACT

The current study investigates the feasibility of using iron phosphate glass for the immobilization of nuclear wastes that have limited solubility in the current borosilicate glass used for vitrification. These wastes contain elements such as sulfur and phosphorus, which have proven problematic (causing phase separation at >1 wt%) for vitrification in borosilicate glasses, as well as having a high soda content (50-75 wt%) which also limits wasteloading.

Simulated Sodium Bearing Waste (SBW) based on the composition at Idaho National Engineering and Environmental Laboratory (INEEL) was vitrified using iron phosphate glass at waste loadings up to 45 wt%, at a melting temperature of 1000°C. The alumina content (27.5 wt%) in the SBW aided in making the final wasteform chemically durable.

The Low Activity Waste (LAW) streams at the Hanford, WA site contain from 7.42 to 11.50 wt% sulfate, making them ill-suited for vitrification in borosilicate glass at high wasteloadings. Wasteloadings of up to 30 wt%, at melting temperatures of 950°C were possible in iron phosphate glasses. Sulfate content of up to 4.5 wt% was found for these iron phosphate glasses with no evidence of a sulfate layer on the melt surface or sulfate segregation within the glass. The retention of sulfate decreased with increasing time and temperature. For melting temperatures below 1000°C and times less than 4 hours more than 50 wt% of the sulfate was retained. The chemical durability of the glass improved as the wt% of sulfate was reduced.

The high soda content of the SBW and LAW limited the wasteloading that was possible. A total soda content of approximately 23 wt% in the wasteform (45 wt% SBW, or 30 wt% LAW) was found to be the maximum where these iron phosphate glasses formed durable glasses.

The iron phosphate glasses which contained 45 wt% SBW or 30 wt% LAW crystallized upon slow cooling (<1 °C/min) from the melting temperature to room temperature as well as when heat-treated at 600°C for 24 hours. When crystallized, the iron phosphate wasteforms containing SBW or LAW had higher dissolution rates than the corresponding glassy wasteform.

ACKNOWLEDGMENTS

I would like, first of all, to thank Dr. Delbert Day, my advisor, for his guidance and support throughout this project, and patience while I wrote this thesis. Thanks are also due to Dr. Richard Brow and Dr. David Wronkiewicz for agreeing to be on my committee and for their time and valuable suggestions.

Thanks also to my undergraduate assistants, Natalie Vanderpiegel and Steve Jung, for their countless hours of sample preparation and measurements. I would like to thank Dr. Cheol-Woon Kim for viscosity measurements, Dr. Dongmei Zhu for electrical conductivity, and Drs. Signo Reis, and Mevlüt Karabulut for Mössbauer analysis.

Special thanks go to my parents, Doug and Martha, who have supported and encouraged me through the years, and made it possible for me to attend UMR. Thanks also to my sister Jennifer, as well as the rest of my family, who all knew I could do this even when I questioned it myself.

Thanks to all the guys at the Ole' Teke house and especially my pledge brothers who made my time in Rolla so enjoyable that I wanted to stay around a little longer.

Most importantly, I would like to thank my wife Becky for her endless support, and for understanding my time commitment and stress. Without her encouragement, this work would not have been possible.

Funding for this research has been provided by the United States Department of Energy.

TABLE OF CONTENTS

Page

LIST OF TABLES

Page

Iron phosphate glass for the vitrification of INEEL sodium bearing waste

Iron phosphate glass for the vitrification of Hanford low activity waste with high sulfur content

LIST OF ILLUSTRATIONS

Page

Iron phosphate glass for the vitrification of INEEL sodium bearing waste

LIST OF ILLUSTRATIONS (cont.)

Page

Iron phosphate glass for the vitrification of Hanford low activity waste with high sulfur content

LIST OF ILLUSTRATIONS (cont.)

Page

LIST OF ILLUSTRATIONS (cont.)

Page

LIST OF ILLUSTRATIONS (cont.)

Page

Iron phosphate glass for the vitrification of INEEL sodium bearing waste

R.D. Leerssen, D.E. Day*

Ceramic Engineering Department and Graduate Center for Materials Research, University of Missouri-Rolla, MO 65409

Abstract

Simulated Sodium Bearing Waste (SBW) based on the composition from Idaho National Engineering and Environmental Laboratory (INEEL) was vitrified using iron phosphate glass at waste loadings up to 45 wt%, at a melting temperature of 1000°C. The properties that have been measured include chemical durability, density, melt viscosity, melt AC electrical conductivity, thermal expansion, and Mössbauer spectra. The high sodium content of the waste limited the wasteloading to 45% (22.6 wt% Na_2O) for chemically durable waste glasses. Dissolution rates for these iron phosphate glasses containing SBW were found to be below 8×10^{-9} g/cm^2/min after 14 days in 90°C water and the Product Consistency Test (PCT) mass release was less than 1 g/m^2. The alumina (27.5 wt%) in the SBW aided in making the final wasteform chemically durable. These glasses crystallized upon slow cooling (<1 °C/min) from the melting temperature (1050°C) as well as when heat-treated at 600°C for 24 hours. When crystallized, the iron phosphate wasteforms containing SBW had dissolution rates that on average were 10 times higher than the corresponding glassy wasteform.

PACS codes: 28.41.Kw

Key words: iron phosphate glass; sodium bearing waste; chemical durability

---

*Corresponding Author: Delbert E. Day, Graduate Center for Materials Research, University of Missouri – Rolla, 1870 Miner Circle, Rolla, MO 65401, email: day@umr.edu

1. Introduction

The use of glass to vitrify nuclear waste has been determined to be an effective means of ensuring that the radionuclides present in the waste are not released into the biosphere. This research has been ongoing since the early 1960's, and currently borosilicate glasses are the only approved glasses for waste vitrification.

When the vitrification of nuclear waste from the processing of weapons was first contemplated forty years ago, phosphate-based glasses were considered [1]. These glasses were formed by adding phosphoric acid directly to a liquid waste stream, calcining the resulting phosphate composition, and melting the resulting calcine to form a glass. Because of the high soda content and small concentrations of other components in the waste, these sodium phosphate melts were chemically corrosive toward the furnace refractories and the resulting glass had a poor chemical durability. The poor glass properties found in this early work led to the suspension of research into the use of phosphate glasses for nuclear waste vitrification in the U.S. [1, 2].

Research on phosphate glass continued in Germany until the late 1970's in the form of melting small marbles of sodium-aluminophosphate glass to be embedded in a metal matrix to avoid devitrification [1, 3]. Researchers in Russia also continued to work with phosphate glasses, melting aluminophosphate glasses using a joule-heated ceramic melter in the early 1970's, and more recently using induction melting. Currently Russia is the only country utilizing phosphate glasses to vitrify nuclear waste. Over 10,000 m^3 (2150 tons) of high level waste (HLW) glass was melted in two joule heated melters from 1987 to 1997, when the last melter was shut down [4].

In the mid 1980's, interest in phosphate glasses in the U.S. was renewed with the discovery of chemically durable lead-iron phosphate glasses by Sales and Boatner [5]. These glasses were shown to have a good chemical durability and low processing temperature (900 to 1050°C) which are advantages for vitrifying nuclear waste. A concern for the use of lead containing glasses is that lead causes the wasteform to be classified as a mixed waste, which is subject to additional disposal regulations [6].

Another system that shows great promise for the vitrification of nuclear waste is iron phosphate glass. Like the lead-iron phosphates, these glasses have properties

favorable for vitrifying nuclear waste. Iron phosphate glass has been studied in detail recently and there have been numerous studies detailing their effectiveness as nuclear waste vitrification host glasses as well as their chemical durability, mechanical strength and structural properties [7-12].

Research has been undertaken to find glasses which can incorporate those wastes that are not well suited for vitrification in the current borosilicate glasses [3, 13, 14]. These wastes include those that are high in sodium, phosphorus, sulfur, chromium, or heavy metals [15, 16].

Beginning in the early 1960's, radioactive wastes that had been collected from reprocessing nuclear fuel were calcined at the Idaho Nuclear Technology and Engineering Center. During this time, secondary radioactive wastes from decontamination, laboratory activities and fuel storage activities were collected and stored in liquid form. These liquid wastes are collectively called sodium-bearing wastes (SBW). About 1.3 million gallons of these wastes are now temporarily stored in stainless steel tanks at the Idaho National Engineering and Environmental Laboratory (INEEL) [16-19]. The Batt Settlement Agreement, reached in August 1995, between the U.S. Navy, the State of Idaho and the U.S. Department of Energy (DOE), requires the removal of the SBW liquid wastes from the INEEL storage tanks by the end of 2013 [4, 20]. The waste loading for SBW in the borosilicate glass currently used is limited to 20 wt% due to the high sulfate concentration in the waste [21] that forms a sulfate layer on the surface of the melt, which attacks the refractory lining of the melter.

In the present work, the vitrification of SBW at INEEL in iron phosphate glasses was investigated. Iron phosphate glasses containing from 25 to 75 weight percent SBW were melted and tested. From these glasses, selected compositions were chosen for closer investigation.

The objectives of the present work were: (1) determine the maximum amount of SBW that can be vitrified in iron phosphate glass, (2) determine the chemical durability of iron phosphate wasteforms as a function of composition, (3) identify compositions of iron phosphate glassy wasteforms with the maximum wasteloading and acceptable chemical durability and (4) evaluate the chemical durability of glassy and deliberately crystallized iron phosphate wasteforms.

2. Experimental Procedure

2.1. Simulated waste formulation

The composition of the SBW for the present research is a slightly modified (simplified) version of the composition from a Savannah River Site report and a Tanks Focus Area presentation [16, 22]. Table 1 gives the original composition as well as the simplified version that was used. In the present work, the waste composition was simplified from the original by ignoring several of the components that were below 0.5 wt% and increasing the remaining components accordingly. One exception is chromium oxide, which was increased to address concerns about chromium solubility in the glass [15] and to illustrate that even higher levels of chromium do not adversely affect the properties of the glass. These slight compositional differences are not expected to affect the overall properties of the wasteform, nor the results reported herein.

Due to the high nitrate content of the wastes at INEEL, the nitrate forms of the raw materials were used when possible. Table 1 lists the raw materials used for the SBW composition. This supply of simulated waste was mixed by tumbling in a plastic container and stored in a sealed container until used. The calculated weight loss on ignition for the SBW was 52.1%.

2.2. Glass preparation

Batches that produced 100g of glass were prepared by mixing reagent grade Fe_2O_3 and P_2O_5 dry crystalline powders with varying amounts of SBW. The simulated SBW and additives were dry mixed and melted in a high purity alumina crucible (CoorsTek 65505) in an electric furnace. The melting conditions were: air atmosphere at the lowest temperature possible (generally between 1000 and 1100°C) in an uncovered crucible for 2 hours.

The batch was placed in the crucible in several small amounts at temperatures ranging from 400 to 900°C, adding more as the batch melted. To ensure that the melt was homogeneous, each liquid was stirred three times during melting (at approximately

60 minutes, 90 minutes and 10 minutes prior to pouring the melt) using a silica rod. The melt was poured into steel molds to form 1 cm × 1 cm × 10 cm rectangular bars, which were annealed at 400°C for approximately 2 hours and then cooled overnight to room temperature in the annealing furnace. The resulting glasses were black in color and opaque.

After all of the trial glasses were melted and preliminary chemical durability measurements had been performed (single sample, not well polished), three glass compositions were chosen for more comprehensive study. These compositions include 40 wt% SBW (SBW40), 45 wt% SBW (SBW45) and 50 wt% SBW (SBW50). A 200g batch of each composition was melted in an alumina crucible. The calculated compositions of these three iron phosphate glasses are given in Table 2.

Since P_2O_5 was used as a raw material, an additional 5 wt% of the required amount was added in order to compensate for potential volatilization losses during melting.

2.3. Property measurements

Samples for property measurements were cut from the annealed glass bars. The density of each glass was measured on five samples by the Archimedes method using kerosene as the suspension liquid. The average linear thermal expansion coefficient, α, and dilatometric softening temperature, T_d, were measured using an Orton model 1600 auto-recording dilatometer. T_d was determined as the peak of the expansion curve, and α was calculated from the slope of the expansion curve, using the most linear region of the curve between 100 and 375°C.

Some of the annealed glass was deliberately crystallized by heat treatment between 540 and 600ºC for 24 hours. Some of the crystallized samples were ground to -200 mesh powder and the crystal phases were determined from X-Ray Diffraction (XRD) patterns that were collected over a 2θ range from 10 to 90 degrees, at a scan rate of 1º/min using a Scintag PADX x-ray diffractometer using copper *K*α radiation with a wavelength of 1.5418Å.

One SBW45 melt was slow cooled over a period of 24 hours to simulate the Canister Centerline Cooling rate (CCC) for a glass at the center of the current wasteform containers. The cooling rate chosen was approximately 40°C/hr from the melt temperature of 1050°C to room temperature. This rate is about twice the rate used previously for an iron phosphate glass [23] and about 20 times faster that the actual CCC rate of about 2°C/hr [24], but the higher rate was considered acceptable for the purposes of the present study. The objective of this cooling experiment was to determine if there was a difference in the phases that crystallized from the slowly cooled melt as compared to the phases crystallizing when the same glass was reheated from room temperature to a temperature (540-600°C) where crystallization occurs.

A Netzsch Differential Thermal Analysis/Thermal Gravimetric Analysis instrument (DTA/TGA) was used to determine the glass crystallization temperature and any weight loss in the sample. Approximately 40 mg of glass was heated in an alumina crucible to 800ºC at a rate of 10ºC/min in air.

A JEOL T330A Scanning electron microscope (SEM) was used to examine the surface of glassy, crystallized and chemically corroded samples. The samples were affixed to the SEM mounts with carbon tape and sputter coated with gold/palladium to form a conductive layer.

Inductively Coupled Plasma – Emission Spectroscopy (ICP-ES, Acme Analytical Laboratories LTD. - Vancouver, British Columbia) was utilized to determine the final composition of the glass, which was compared to the original batch composition. The glass samples were digested in a four acid solution (HNO_3, $HClO_4$, HF and HCl) at high temperature prior to analysis.

The viscosity of the SBW45 melt was measured using a rotating viscometer. A non-standard alumina spindle was constructed from a 10 cc straight wall crucible and calibrated using three standard viscosity oils (0.097, 0.099, and 0.965 Pa·s). Spindle speeds of 10, 20, and 50 rpm were used for each measurement. The estimated error for this procedure was less than ±5%. The melt was held at a selected temperature for 30 minutes to allow it to thermally equilibrate, at which time a preheated spindle was immersed in the melt. The viscosity was measured three times and then averaged. The

corrosion of the alumina spindle by the melt was negligible, determined by visual inspection.

The AC electrical conductivity of the molten SBW45 glass was measured at 1000 Hz by inserting 1 cm × 2 cm platinum electrodes 1.7 cm apart into the melt at temperatures ranging from 800°C to 1200°C. The temperature range chosen was based on the desire to know the response of iron phosphate glasses containing SBW not only at the melting temperature used in the present work, but also at temperatures where borosilicate wasteglasses are melted (~1150°C) for comparison.

The melt was heated to 1200°C where the first measurement was taken. The temperature was reduced by 50°C and the melt was held at this temperature for 30 minutes, after which the second measurement was taken; this process was repeated to 800°C. Once 800°C was reached, the temperature was increased in increments of 50°C, held for 30 minutes, and the AC conductivity remeasured to determine if the conductivity changed with time or thermal cycling.

The electrical resistivity of the melt was measured using an LCR meter connected to the platinum electrodes, and this resistance measurement was converted to electrical conductivity (σ) using the equation:

$$\sigma = \mathrm{K}\left(\frac{1}{\mathrm{R}} \bullet \frac{\mathrm{L}}{\mathrm{S}}\right) \tag{1}$$

where R is the electrical resistivity, L is the distance between the two electrodes, S is the surface area of the electrode immersed in the melt, and K is the cell constant that was determined to be 1.12 by calibrating the instrument using three different concentrations of KCl standard solution. The error was estimated to be ±5%.

To determine the valence and coordination number of iron in the glass, Mössbauer spectroscopy was employed. The Mössbauer spectra were measured at room temperature on a constant acceleration spectrometer (ASA600) using a 50 mCi rhodium matrix cobalt-57 source. Mössbauer absorbers of approximately 85 mg/cm^2 were prepared from 200 mesh powders.

2.4. Chemical durability

The chemical durability of the iron phosphate glasses was determined from the weight loss of bulk samples immersed in deionized water at 90°C and on powders (-100 to +200 mesh) according to the Product Consistency Test (PCT: ASTM C 1285-97) [25].

Bulk Dissolution Rate (DR) samples were cut from annealed glass bars using a diamond saw with kerosene as the cooling liquid and then polished to 600 grit. The dimensions of each sample were approximately 1 cm × 1 cm × 1 cm ±0.1 cm.

Some of the samples were deliberately crystallized by heating between 570 and 600°C for 24 hours. These heat-treated samples were used to determine the DR of the crystallized wasteform.

The glassy and crystallized cut monolith samples were rinsed with deionized water and acetone, dried at 90°C, cooled to room temperature and weighed (±0.01 mg). Each sample was suspended by a rayon thread in a 125 ml polyethylene bottle containing 100 ml of deionized water. A schematic of the DR setup is shown in Fig. 1. The bottles containing the wasteforms were placed in a 90°C oven and each sample was removed for measurement after 3, 7, 10, 14, 21, and 30 days. The samples were rinsed with deionized water, dried at 90°C, cooled and weighed (±0.01 mg). The pH of the solution was also measured each time using a Fisher Scientific Accumet® pH/ion meter model 25 (±0.1 units). The samples were replaced in the same bottle without changing the water and returned to the oven.

Samples of the Environmental Assessment (EA) glass obtained from the Savannah River Laboratory were measured under the same conditions and used as a reference for the DR values of the iron phosphate glasses.

The DR was calculated from the measured weight loss using the equation:

$$DR = \frac{\Delta W(g)}{A\,(cm^2) \cdot t\,(min)} \qquad (2)$$

where A is the geometrically determined surface area (cm^2) of the sample and t is the time (min) that the sample was immersed in the test solution at 90°C. The weight loss

(ΔW) is $W_i - W_t$, where W_i is the initial weight of the sample and W_t is the weight of the same sample after time t.

The chemical durability of the iron phosphate glass wasteforms was also measured by the PCT. The samples were mechanically crushed and sieved to isolate the -100 to +200 mesh fraction. The powders were washed thoroughly in water and ethyl alcohol in an ultrasonic bath to remove particles smaller than 200 mesh, which are known to reduce the accuracy of PCT measurements [26]. The washed powders were dried at 90°C overnight. The glass powder (1.5 grams ± 1mg) was weighed and placed into a Teflon vessel. Fifteen ml of deionized water was added to the powder. The vessel was sealed and placed in an oven at 90°C for seven days.

After completion of the PCT, the vessel was weighed to determine if any water had escaped. Leachate losses were less than 1% of the initial weight of the leachate. The pH of the water was measured before and after the test. The leachate was filtered through a Nalgene 0.45 μm filter, acidified with one volume percent 0.4 M Optima HNO_3 to ensure the cations remained in solution and the concentration of ions in the leachate was measured using ICP-ES (ACME Analytical Labs LTD. - Vancouver B.C.). All tests were conducted in duplicate and averaged. A blank was included in the measurement for control purposes.

The normalized elemental mass release, r, was calculated in two different units (g/L and g/m^2) from Equations 3 and 4, respectively, to provide easier comparison with other glasses:

$$r_i\left(g/L\right) = \frac{C_i}{f_i} \quad (3)$$

$$r_i\left(g/m^2\right) = \frac{C_i}{f_i\left(\frac{A}{V}\right)} \quad (4)$$

where C_i is the concentration of element i in the solution and f is the mass fraction of element i in the glass, calculated from the ICP-ES analyzed glass composition given in

Table 2. A/V is the ratio of the sample surface area to volume of leachate (m^{-1}). The elements used for the analysis of the release rate from the iron phosphate glass are aluminum, potassium, sodium and phosphorus. Three of the elements differ from those that are analyzed in borosilicate wasteforms (boron, lithium, sodium and silicon) due to the compositional differences of the glasses. Sodium is analyzed in both iron phosphate and borosilicate PCT studies.

3. Results

3.1. Glass formation

For waste loadings below 60 wt%, homogeneous glasses were black in color and free of crystals (determined by optical microscopy). Melts above 60 wt% wasteloading tended to crystallize quickly after pouring. A complete list of all compositions investigated in the present work is given in Appendix A along with the melting temperatures and DR in 90°C water.

3.1.1. Compositional analysis

During the melting of these glasses noticeable amounts of white smoke were given off, which were attributed to the volatilization of P_2O_5. Once the batch was fully melted, no more smoke was observed. The loss of P_2O_5 was compensated for by adding 5 wt% more P_2O_5 to the batch than was required for the target composition. The P_2O_5 content of the glass (Table 2) was 4 to 6 wt% higher in the analyzed composition than the batch composition in every case, which suggests that the 5% excess P_2O_5 added to compensate for volatilization was too large and that a 1 to 2% addition would be adequate.

Note that the ICP analysis (Table 2) showed the Al_2O_3 content was 1 to 2 wt% higher than the batch composition in every case, probably due to the corrosion of the alumina crucible, and incorporation of corrosion products into the melt. A typical example of the small amount of corrosion at the melt line is shown in Fig. 2 for the crucible in which SBW45 was melted for 2 hours at 1050°C. The depth of corrosion was estimated to be 100µm by optical microscopy. This amount of corrosion accounts for approximately 2 grams of alumina, or 1 wt% in the glass composition.

Several other components in the glasses vary between the batch and ICP analyzed compositions. It is unknown why the wt% of CaO, MnO or NiO are higher in the analyzed composition than expected from the batch composition, while Na_2O and K_2O are lower (Table 2). The small wt% (0.12 to 0.51 wt%) SiO_2 may have been introduced

into the glass when the melt was stirred using a silica rod. These elements are at relatively small concentrations and are not anticipated to have a significant effect on the measured properties in the present study.

3.1.2. Oxygen to phosphorus ratio

The molar ratio of oxygen to phosphorus (O/P) was calculated from the batch composition (assuming the oxides are in the form listed in Table 2) as well as from the analyzed composition (Table 2). The calculated O/P ratio from the batch and analyzed compositions for the SBW40 and SBW50 glasses were nearly the same (4.14 and 4.09 for SBW40, and 4.61 and 4.57 for SBW50 respectively). The largest change in O/P was for SBW45, which had a ratio of 4.36 from the batch composition and 4.06 from the analyzed composition.

These values are higher than the empirically known range of O/P values, which range from 3.4 to 3.7 for the best glass forming tendency and good chemical durability [23, 27]. To reduce this ratio the iron content would have to be lowered or the P_2O_5 content increased. These compositional changes were expected to lower the chemical durability, therefore it was decided to proceed, and use this higher oxygen to phosphorus ratio, knowing that higher iron contents have been shown to increase the durability of iron phosphate glasses [3, 28].

Another ratio that has been empirically shown to indicate the glass forming ability of iron phosphate glasses is the molar iron to phosphorus ratio (Fe/P) which for these SBW iron phosphate glasses is given in Table 2. It has been shown that an Fe/P ratio of 0.67 is favorable for good glass formation in iron phosphate glasses, while at a ratio below 0.33 the durability is significantly lower, and for a ratio >1.0, glass formation becomes difficult [10]. The Fe/P ratio for these SBW iron phosphate glasses are all ≤ 0.33, which would tend to indicate that these will not be durable, however, there has been work [7] which indicates that alumina in iron phosphate glasses can increase the durability in much the same way increased iron content does. To understand the extent to which alumina can aid in the glass forming properties of these glasses, the molar iron + aluminum to phosphorus ratio (Fe+Al)/P was also calculated. This ratio for all of the

SBW iron phosphate glasses in the present study was between 0.66 and 0.81, which is in the range of good glass formation indicated by the Fe/P ratio.

3.2. Physical properties

3.2.1. Density

The average density of each glass changed very little as the waste amount was increased, as Table 3 shows. Within the estimated error of ±0.05 g/cm^3, there was little change in the density of the samples; however, there appeared to be a small decrease in the density of the glass as the waste loading was increased.

3.2.2. Viscosity

The viscosity of the SBW45 glass is similar to that of other iron phosphate melts as shown in Fig. 3A. The curve labeled TFB20-40 is for an iron phosphate melt that contained 20 wt% of a waste [23] whose composition was the average of the waste from tank farm B (TFB) at Hanford, WA that contained 55% Na_2O. The curves labeled 40W10F50P and 48W10F42P are for iron phosphate melts containing 40 and 48 wt%, respectively, of the SBW at INEEL [29].

At the pouring temperature (1000°C), the viscosity of SBW45 iron phosphate melt is approximately 0.35 Pa·s which is approximately 30 times less viscous than the 11.55 Pa·s of the SBW-2-25 borosilicate waste glass (containing 25% SBW) at its pouring temperature (1150°C) [16]. The viscosity of the SBW45 melt is believed to be representative of the viscosity of the SBW40 and SBW50 melts in the present study.

The log viscosity plotted as a function of 1/T in Fig. 3B indicates that the viscosity of the SBW45 melt obeys the Arrhenius equation over the limited temperature range of the present study. The data plotted for comparison in Fig. 3B include the TFB waste from [23], as well as two glasses containing 40 and 48 wt% SBW from [30], and the F43 iron phosphate glass (43 wt% Fe_2O_3, 57 wt% P_2O_5). The activation energy for viscous flow was calculated from the slope of the regression line, and is given in Fig. 3B

for each melt. The activation energy for the SBW45 melt is 14.9 kcal/mol which falls into the same range as the activation energies for the comparison waste glasses 11.3 to 17.4 kcal/mol [30], but approximately half the activation energy for viscous flow (25.8 kcal/mol) in the alkali-free F43 glass.

3.2.3. AC electrical conductivity

The AC electrical conductivity of the SBW45 melt as a function of temperature is shown in Fig. 4A. The AC conductivity at the melting temperature of 1050°C is 105 $(\Omega m)^{-1}$ and is reproducible for heating and cooling. This melt temperature conductivity is ~2.5 times higher than the conductivity of the SBW-22-20 borosilicate glass containing 20% SBW at its melting temperature (42 $(\Omega m)^{-1}$ at 1150°C) [30] and is similar to results for iron phosphate glasses containing 40 and 48% SBW (~100 $(\Omega m)^{-1}$ at 1000°C) [30].

As shown in Fig. 4B, the AC conductivity of the SBW45 melt (6.4 kcal/mol) obeys the Arrhenius equation and is only about half that (13.5 kcal/mol) for the SBW-22-20 borosilicate and the IP40WG from [30].

3.2.4. Thermal properties

The thermal expansion, T_d and T_g in Table 3 are very similar for the SBW40 and SBW45 glasses. There was a much larger difference between the measurements for SBW45 and SBW50. The CTE ranged from 169×10^{-7} to 198×10^{-7} C^{-1} with SBW45 having the lowest measurement and SBW50 having the highest. SBW50 had the lowest values for Tg and Td (385°C and 440°C respectively) while SBW40 and SBW45 each had a Tg of 425°C, and Td measurements of 480°C and 475°C respectively. TGA indicated there was no weight change for any of the SBW glasses when heated to 800°C.

The DTA curves in Fig. 5 show a crystallization peak at 555°C for SBW40 and 560°C for SBW45. The lack of a distinct exothermic peak in the curve for the SBW50 glass is likely due to prior crystallization in this glass that most likely occurred during annealing.

3.2.5. XRD

The XRD patterns for the three annealed glasses that were studied in detail are shown in Fig. 6. The SBW40 and SBW45 samples had no detectable crystalline phases, while SBW50 contained a small amount of $Na_2Fe_2Al(PO_4)_3$ which possibly formed during annealing. The crystallized phases were small irregular shapes dispersed widely throughout the glass ranging in size from 10 to 50μm determined by optical microscopy at 400×. Due to the small size and the relatively large distance between the crystal phases, the amount of glass that crystallized is estimated to be ≤5%.

The most common crystalline phases found in the deliberately crystallized samples were $Na_3Fe_2(PO_4)_3$ and $Na_2Fe_2Al(PO_4)_3$, as shown in Fig. 7. The SBW45 melt that was cooled at the simulated CCC rate completely crystallized, and the crystal phases were nearly identical to the glass that was deliberately crystallized by reheating for 24 hours at 570°C.

Peaks which cannot be identified are denoted by "?" in Fig. 7, indicating that unidentified crystalline phases are present.

3.2.6. Mössbauer spectra

The results from the Mössbauer spectroscopy are given in Table 3 and typical spectra are plotted in Fig. 8. The SBW40 and SBW45 glasses contained about 10% Fe(II) which is about half the amount of Fe(II) reported previously in iron phosphate glasses [28, 31], where 20% Fe(II) was found on average. The lower Fe(II) percentage in the SBW40 and SBW45 glasses, however, agrees well with results for other iron phosphate glasses melted at temperatures below 1150°C [10] and for other iron phosphate glasses containing 40 wt% SBW [30]. The SBW50 had a high Fe(II) percentage (~63%) which likely caused the small amount of crystallization in this sample (see Fig. 6). It is unknown why the SBW50 sample had a significantly higher Fe(II) than the SBW45 sample.

3.3. Chemical durability

3.3.1. Bulk dissolution rate (DR)

3.3.1.1. Glass samples

The DR was measured on iron phosphate glasses containing from 25 to 50 wt% SBW using the procedure described above. As shown in Fig. 9, the glassy wasteforms (solid lines) had a DR ranging from a low of 2×10^{-9} to a high of 5×10^{-8} g/cm^2/min after 7 days in water at 90°C. The chemical durability of the iron phosphate glass wasteforms in the present study was as good as or better than that of the EA borosilicate glass in deionized water at 90°C, which had a DR of 5×10^{-8} g/cm^2/min after 7 days. There is a general tendency for the DR to decrease with time which suggests a chemically protective layer forms on the samples. Complete data are given in Appendix B, Table B1.

The increase in pH of the DI water that occurred during the DR measurements is shown in Fig. 10. Note that the increase in pH for the EA glass is larger than that for the iron phosphate glasses, due to the buffering action of the phosphate glasses [23, 28]. Note that the pH of the water used to test the iron phosphate glasses containing SBW did not exceeded 8. Complete data are given in Appendix B, Table B2.

3.3.1.2. Crystallized sample DR

The DR of the deliberately crystallized iron phosphate SBW wasteforms were also measured, and are shown by the dashed lines in Fig. 9. In general, the crystallized samples were not as durable as the corresponding glassy wasteform. Complete data are given in Appendix B, Table B3. The DR of the slowly cooled SBW45-CCC sample was 1.9×10^{-6} after 7 days. This sample was so fragile at 7 days that the test was discontinued.

3.3.2. Product consistency test - powder dissolution rate

The PCT results for the iron phosphate glass wasteforms and selected borosilicate glasses are given in Table 4. The quantity of ions (normalized elemental mass release) for Al, K, Na, and P released from the SBW40 and SBW45 glassy wasteforms was approximately 18 times smaller than the quantity of B, Li, Na, and Si released from the EA borosilicate glass [32]. The total quantity of ions released from the SBW40 and SBW45 iron phosphate glasses was about 3 times less than the quantity released from the borosilicate CVS-IS glass and was approximately equal to the total released from the LD6-54-12 borosilicate glass produced at the Pacific Northwest National Laboratory [33]. The chemical durability of the SBW50 glass was not as good as that of the SBW45 or SBW40 glass, but was approximately the same as the EA borosilicate glass.

The common element that is present in the PCT analysis for both the borosilicate glass and the iron phosphate glass is sodium. As Table 4 shows, sodium had the highest release in nearly every case for the borosilicate glasses as well as the iron phosphate glasses containing SBW. For the SBW50 the sodium release is 14.89 g/L compared to borosilicate EA release of 14.11 g/L. The sodium release for SBW45 (0.37 g/m^2) is approximately 4 times lower than that for CVS-IS borosilicate glass (1.3 g/m^2), and is approximately the same as that released from the LD6-54-12 borosilicate glass (0.38 g/m^2).

To compare the PCT results with the DR values described earlier, the dissolution rate of the powdered samples was determined from the total mass release of the powdered samples after a 7 day PCT using equation (2). A value of 30 cm^2 was estimated for the surface area of the powder using the equation in Appendix IX of ref [25]. As shown in Table 5, the dissolution rate calculated from PCT mass release is ~4 times larger than the DR measured for the bulk glass samples for SBW40 and SBW50, while it is ~2 times smaller for the SBW45. The higher pH values for the water from the PCT than the DR measurements for SBW40 and SBW50 may account for the higher calculated dissolution rate, indicating that more ions are in solution. The bulk DR values can be used in a general way to estimate the mass release of a sample in the PCT.

The absence of any visually noticeable corrosion of the iron phosphate glass particles during the PCT was confirmed by their morphology after testing. The appearance of uncorroded SBW50 glass particles is shown in Fig. 11A while the appearance of the particles of this less durable glass after the 7 day PCT is shown in Fig. 11B. The sharp corners and edges of the particles in Fig. 11B along with the absence of any detectable corrosion layer on the surface indicate that this glass is resistant to chemical attack by water. The SBW40 and SBW45 PCT particles also had nearly the same appearance with no noticeable corrosion.

4. Discussion

The present investigation of the iron phosphate glass wasteforms has identified several properties of iron phosphate glasses that are relevant to the vitrification of SBW at INEEL.

4.1. Glass properties

The iron phosphate melts containing SBW in the present study are fluid (<1 Pa·s) and can generally be melted at approximately 1000°C with good results. This fluidity reduces the necessary melting time substantially, so that homogeneous glasses are achieved after melting times of one to two hours.

Low melting temperatures and shorter melting times lead to less expensive and safer melting and mean that smaller furnaces can be used to achieve the same output. This translates into significant savings both in energy consumed to melt the glass (lower melting temperature) and into smaller amounts of glass due to the higher wasteloading potential of the iron phosphate glasses. The lower melting temperature also leads to less attack of the refractories allowing for longer furnace life.

An alternative technology for melting iron phosphate glasses is cold crucible induction melting (CCIM). The higher electrical conductivity (relative to borosilicate melts) of iron phosphate melts is beneficial for induction melting. The higher conductivity of the iron phosphate melt allows the melt to be more susceptible to the rf field of the melter. CCIM avoids potential problems with corrosion of refractories and electrodes since the glass serves as its own refractory and no metal electrodes are needed [36]. Iron phosphate glasses containing 40 to 48 wt% SBW have been successfully melted using CCIM technology [30]. Induction melting is still considered a backup technology due to the immaturity of the melters and power supplies, but it is a promising melter technology for iron phosphate waste glasses [29, 35, 36].

4.2. Chemical durability

4.2.1. Composition

The PCT results indicate that the total quantity of all ions leached from the SBW45 iron phosphate wasteform (1.25 g/L for SBW45) is ~35 times smaller than the total quantity of ions leached from the EA glass (46 g/L). The SBW50 glass had a chemical durability similar to that of the EA glass in both the DR and PCT tests. The iron phosphate SBW45 glass had a total mass release below the 1g/m^2 conservative constraint that has been quoted for acceptable durability [16, 24]. Another study [29] of iron phosphate glasses containing SBW found similar chemical durability results, where a DR of 2×10^{-9} g/cm^2/min at 16 days in 90°C water was reported for an iron phosphate glass containing 40 wt% SBW.

The durability of the iron phosphate wasteform decreased as the amount of SBW in the glass increased, probably due to the increasing soda content. A soda content of 22 to 24 wt% appears to be the limit for acceptable durability in these SBW iron phosphate glass wasteforms. This maximum soda content is consistent with work performed at Hanford, WA where iron phosphate glasses containing up to 24 wt% alkali (21 wt% Na_2O and 3 wt% K_2O) were found to have good durability (PCT total mass release <2 g/m^2) [34].

The O/P ratio has been shown to be important to the chemical durability of iron phosphate glasses [23]. An O/P ratio of 3.5, which corresponds to the P_2O_7 pyrophosphate composition, seems to provide the best chemical durability [23, 37]. An increase in the O/P ratio toward the orthophosphate composition (O/P = 4.0) or a decrease in the O/P ratio toward the metaphosphate composition (O/P = 3.0) leads to a decrease in the chemical durability [23, 37]. The reduction in chemical durability is more significant when the O/P decreased from 3.5 than when it increases, indicating that orthophosphate compositions are more chemically durable than metaphosphate compositions [37].

The DR (14 days in 90°C DI water) is plotted in Fig. 12 as a function of molar O/P ratio for iron phosphate glasses containing SBW as well as 20 to 40 wt% TFB waste

(which contains 55 wt% Na_2O compared to the 58 wt% Na_2O and K_2O in the SBW) [23], as well as NKFP and NCFP [37] which contain (20 mol% alkali, 20 to 32 mol% Fe_2O_3 and 48 to 60 mol% P_2O_5), F40M [37] (containing 40wt% Fe_2O_3 and 60 wt% P_2O_5) and FCs17 [38] (which contains 29 wt% Fe_2O_3, 38 wt% P_2O_5, and 33 wt% Cs_2O). The general trend toward lower durability at O/P ratios above and below 3.5 is shown by the "V" shape of the shaded area in Fig. 12.

The dependence of DR on the O/P ratio for the SBW glasses in Fig. 12 follows the same trend as previous data: as the O/P ratio increases, the durability decreases. However the durability for the SBW glasses is usually better than for the glasses containing TFB for any given O/P value. This can be attributed to the SBW's higher alumina content (27 wt% for SBW compared to 1.3 wt% for TFB), which has been shown to improve the durability of iron phosphate glasses [7].

4.2.2. Effect of crystallization

The iron phosphate SBW glasses in the present study crystallized on slow cooling from the melt temperature causing the dissolution rate of the wasteform to increase by ~10 times. The DR of the crystallized samples exceeds that of the glassy samples and the DR of the EA glass as shown in Fig. 9. The higher DR of the crystallized samples is possibly a result of the reduced chemical durability of the remaining glass after the crystalline phase forms. Iron is the limiting element for all of the crystal phases that formed, therefore the glass that remains after crystallization will contain a majority of sodium and phosphorus which is more susceptible to chemical attack by water.

An increase in DR with crystallization has been noted in other iron phosphate glasses containing between 11 and 25 wt% of Na_2O [23, 29, 37]. The DR increase in these previous studies was smaller than that found for the SBW samples in the present study. These previous studies generally had less than a 10 times increase in DR upon crystallization; there have been iron phosphate waste containing glasses which show almost no change or even decrease in DR with crystallization [38].

The general glass forming tendency for the iron phosphate glasses containing SBW, as indicated by the XRD patterns for the glass samples after annealing in Fig. 6,

appears to be good with the exception of the SBW50 sample glass, which contained $Na_2Fe_2Al(PO_4)_3$) crystals in its structure. The Mössbauer analysis of these samples indicated that SBW50 contained 63% Fe(II), which explains why $Na_2Fe_2Al(PO_4)_3$) (Fe(II) compound) crystallized from the glass.

The crystallized compounds (determined by XRD, given in Fig. 7) that formed when the SBW iron phosphate glasses were deliberately crystallized correlate with the Mössbauer results. The SBW40 and SBW45 samples that were low in Fe(II) did not form appreciable amounts of $Na_2Fe_2Al(PO_4)_3$, but instead formed a majority of $Na_3Fe_2(PO_4)_3$ which is a Fe(III) compound. The maximum amount of each crystal phase that could form from the glass is in the same proportion as the amount of iron in the correct valence found by Mössbauer. Therefore, it would be expected that SBW50 would form a majority $Na_2Fe_2Al(PO_4)_3$) while the SBW40 and SBW45 glasses would form approximately 90% $Na_3Fe_2(PO_4)_3$.

The unusual structure of the slowly cooled sample (SBW45-CCC) contained more internal voids than the sample heat-treated at 570°C for 24 hours (SBW45x) as shown by the SEM images of SBW45 crystallized samples in Fig. 13. Analysis by XRD did not reveal any major difference between the crystal phases in these samples, but the structural difference is a possible reason for the higher DR of the CCC sample. It is possible that the voids in the CCC sample provided more surface area for chemical attack by the water.

4.3. Iron phosphate glass for the vitrification of SBW

Based on the properties of the iron phosphate glasses that were measured in the present study (waste loading, chemical durability, melting temperature, and electrical conductivity), it appears that iron phosphate glasses are good potential host materials for SBW.

The wasteloading for SBW in borosilicate glasses is limited to 20% by its sulfate concentration [21] which forms a sulfate layer on the surface of the melt. It appears that the limiting factor for vitrification of SBW in iron phosphate glasses is the amount of soda in the waste composition. As mentioned previously, once the waste loading reached ~23 wt% Na_2O in the glass, the durability decreased substantially.

If iron phosphate glasses are chosen for the vitrification of this waste, the waste loading could be more than doubled compared to waste loadings in a borosilicate glass. Or, in other words, there would be 50% less waste glass when the project is completed. The lower viscosity of the iron phosphate glasses than borosilicate glasses may provide for shorter melting times than currently used. This shorter melt time would allow for smaller melters to be used to achieve the same wasteform output.

The cost savings would be realized not only in the lower energy requirements for vitrification of the iron phosphate glass itself, but also in the transportation of the waste glass and in the construction of the final repository for the glass. Considering that there are 1.3 million gallons of liquid waste at INEEL [16-19], it is estimated that more than 1200 canisters (of the type used at the Savannah River Site) would be required if borosilicate glass were to be used at a waste loading of 20% [13]. The iron phosphate glass with a waste loading of 45% would require 550 of the same canisters. The elimination of 650 containers at an approximate cost of $250,000 each [4] would allow for a savings of $160 million in disposal alone. A smaller repository could be constructed to contain the waste because there would be <50% less glass to dispose of.

The production of the borosilicate wasteform would incur larger costs in terms of raw materials due to the greater amount that would be required to vitrify a given amount of waste. There is a possibility that a majority of the raw materials needed to form iron phosphate waste glass could come from industrial metal phosphating waste where iron phosphate is a by-product, currently being put in landfills.

5. Conclusions

The results of the present study indicate that the SBW at INEEL can be vitrified in an iron phosphate glass at 1000°C at waste loadings of up to 45 wt% with a chemical durability (PCT) that satisfies current DOE requirements, <1 g/m^2. The limiting factor in the waste is the high sodium content, as the iron phosphates studied here were limited to 23 wt% Na_2O before the durability became unsatisfactory. Preliminary studies indicate, however, that alkali contents below 23 wt% do not seem to have a detrimental affect on the durability of the glass. The relatively large amount of alumina (27 wt%) in the waste was an advantage in that it appeared to increase the durability of the glass beyond what would have been expected based solely on the O/P ratio.

The iron phosphate glasses in the present study tended to crystallize on slow cooling from the melt temperature and the crystallized wasteform had a greater dissolution rate than the corresponding glass. Crystallization of the wasteform must be avoided to ensure the highest possible chemical durability. Two possible ways of avoiding crystallization are to change the composition to reduce the rate of crystallization, or to cool the melt rapidly after melting.

The higher electrical conductivity of iron phosphate melts than borosilicate melts may allow for alternative melting technologies such as CCIM, which could be utilized to melt the glass without the need for electrodes in the glass melt, or refractories lining the melt tank.

Because of their low viscosity and rapid homogenization, melting times need only be approximately two hours. The high wasteloadings that are possible for iron phosphate glasses allow for smaller amounts of final wasteform that need to be disposed of, which can translate into significant cost savings and smaller repository size.

References

[1] B.C. Sales, L.A. Boatner, Lead-iron phosphate glass, in: W. Lutze, R.C. Ewing (Eds.), Radioactive Waste Forms for the Future, Elsevier Science Publisher, North-Holland, Amsterdam, 1988.

[2] B.C. Sales, L.A. Boatner, J. Non-Cryst. Solids 79 (1986) 83.

[3] C.M. Jantzen, J. Non-Cryst. Solids 84 (1986) 215.

[4] J.M. Perez, D.F. Bickford, D.E. Day, D.S. Kim, S.L. Lambert, S.L. Marra, D.K. Peeler, D.M. Strachan, M.B. Triplett, J.D. Vienna, R.S. Wittman, High-level Waste Melter Study Report, PNNL-13582, DOE, 2001.

[5] B.C. Sales, L.A. Boatner, Science 226(4670) (1984) 45.

[6] D.J. Wronkiewicz, Personal Communication, 2002.

[7] M.G. Mesko, D.E. Day, J. Nucl. Mater. 273 (1999) 27.

[8] A. Mogus-Milankovic, B. Pivac, K. Furic, D.E. Day, Phys. Chem. Glasses 38 (1997) 74.

[9] G.K. Marasinghe, M. Karabulut, C.S. Ray, D.E. Day, C.H. Booth, P.G. Allen, D.K. Shuh, Redox Characteristics and Structural Properties of Iron Phosphate Glasses: A Potential Host Matrix for Vitrifying High Level Nuclear Waste, in Environmental Issues and Waste Management Technologies III, The American Ceramic Society, Cincinnati, OH, 1998.

[10] C.S. Ray, X. Fang, M. Karabulut, G.K. Marasinghe, D.E. Day, J. Non-Cryst. Solids 249 (1999) 1.

[11] M. Karabulut, E. Melnik, R. Stefan, G.K. Marasinghe, C.S. Ray, C.R. Kurkjian, D.E. Day, J. Non-Cryst. Solids 288 (2001) 8.

[12] M.G. Mesko, D.E. Day, B.C. Bunker, Waste Management 20 (2000) 271.

[13] J. Ahearne, J.A. Gentilucci, D. Pye, E.T. Webber, F.E. Woolley, High-level Waste Melter Review Report, TFA-0108, DOE, 2001.

[14] J. J. M. Perez, D.F. Bickford, D.E. Day, D.S. Kim, S.L. Lambert, S.L. Marra, D.K. Peeler, D.M. Strachan, M.B. Triplett, J.D. Vienna, R.S. Wittman, High-level waste melter study report, DOE, 2001.

[15] S.N. Crichton, T.J. Barbieri, M. Tomozawa, Solubility Limits for Troublesome Components in a Simulated Low Level Nuclear Waste Glass, in Environmental Issues and Waste Management in the Ceramic and Nuclear Industries, The American Ceramic Society, Cincinnati, OH, 1995.

[16] D.K. Peeler, T.B. Edwards, I.A. Reamer, R.J. Workman, J.D. Vienna, J.V. Crum, M.J. Schweiger, Glass Formulation Development for INEEL Sodium-Bearing Waste (FY2001 WM-180), Savannah River Technology Center, 2001.

[17] R.W. Goles, J.A.D. Debbio, R.J. Kirkham, B.D. MacIsaac, J.A. McCray, D.D. Siemer, N.R. Soelberg, Sodium-bearing Waste Vitrification Demonstration RSM-01-2, PNNL-13522, Pacific Northwest National Laboratory, 2002.

[18] K.J. Perry, R.R. Kimmitt, N.R. Soelberg, R.D. Tillotson, A.N. Olson, Test Results From SBW-FY01-PS-01 Vitrification Demonstration of Sodium Bearing Waste Simulant Using WM-180 Surrogate, Report INEEL/EXT-01-01073, Idaho National Engineering and Environmental Laboratory, 2001.

[19] J.G. Darab, D.D. Graham, B.D. MacIssac, R.L. Russell, H.D. Smith, J.D. Vienna, D.K. Peeler, Sulfur Partitioning During Vitrification of INEEL Sodium Bearing Waste: Status Report, PNNL, 2001.

[20] D.O.E., The INEEL Spent Nuclear Fuel and Environmental Restoration and Waste Management Programs Environmental Impact Statement. DOE/EIS-0203-F, 1995.
[21] D. Gombert, J. Richardson, A. Aloy, D. Day, Cold Crucible Design Parameters for Next Generation HLW Melters, WM'02 Conference, Tucson, AZ, 2002.
[22] D. Peeler, J.D. Vienna, INEEL Glass Formulation Activities, INEEL, 2001.
[23] D.E. Day, Z. Wu, C.S. Ray, P. Hrma, J. Non-Cryst. Solids 241 (1998) 1.
[24] J.V. Crum, J.D. Vienna, D.K. Peeler, I.A. Reamer, Formulation Efforts for Direct Vitrification of INEEL Blend Calcine Waste Simulate: Fiscal Year 2000, PNNL-13483, Pacific Northwest National Laboratory, 2001.
[25] ASTM, Standard test methods for determining chemical durability of nuclear waste glasses: The Product Consistency Test (PCT), in, ASTM Standards, Vol. C 1285-94, 1998.
[26] W.L. Ebert, N.L. Dietz, M.A. Lewis, P.L. Johnson, B.S. Tani, Long-term and Accelerated Testing of Hanford Low-activity Waste Glasses: Data Report for Fiscal Year 2001, ANL FY2001 Annual Letter Report, Argonne National Laboratory, 2001.
[27] A. Mogus-Milankovic, A. Gajovic, A. Santic, D.E. Day, J. Non-Cryst. Solids 289 (2001) 204.
[28] X. Yu, D.E. Day, G.J. Long, R.K. Brow, J. Non-Cryst. Solids 215 (1997) 21.
[29] C.W. Kim, D. Zhu, D.E. Day, D. Gombert, Ceramic Transactions (in press)
[30] C.W. Kim, D.E. Day, C.S. Ray, D. Zhu, D. Gombert, A. Aloy, A. Mogus-Milankovic, M. Karabulut, Journal of Nuclear Materials (submitted for publication)
[31] G.K. Marasinghe, M. Karabulut, C.S. Ray, D.E. Day, M.G. Shumsky, W.B. Yelon, C.H. Booth, P.G. Allen, D.K. Shuh, J. Non-Cryst. Solids 222 (1997) 144.
[32] C.M. Jantzen, N.E. Bibler, D.C. Beam, C.I. Crawford, M.A. Pickett, Characterization of the Defense Waste Processing Facility (DWPF) Environmental Assessment (EA) Glass Standard Reference Material (U), WSRC-TR-92-346, Westinghouse Savannah River Company, 1993.
[33] P.R. Hrma, G.F. Piepel, M.J. Schweiger, D.E. Smith, D.S. Kim, P.E. Redgate, J.D. Vienna, C.A. LoPresti, D.B. Simpson, D.K. Peeler, M.H. Langowski, Property Composition Relationships for Hanford High-Level Waste Glasses Melting at 1150C, PNL-10359, Pacific Northwest Laboratory, 1994.
[34] D.S. Kim, J.D. Vienna, P. Hrma, N.J. Cassingham, Phosphate glasses for vitrification of wastes with high sulfur content, 2002.
[35] A. Jouan, Waste Vitrification: A Contribution to Safeguarding the Earth, International Congress on Glass, Edinburgh, Scotland, 2001.
[36] E.T. Webber, R.B. Calmus, C.N. Wilson, Vitrification Technology for Hanford Site Tank Waste CONF-950401-35, Westinghouse Hanford Company, 1995.
[37] X. Fang, C.S. Ray, G.K. Marasinghe, D.E. Day, J. Non-Cryst. Solids 263&264 (2000) 293.
[38] M.G. Mesko, D.E. Day, B.C. Bunker, Immobilization of High-level Radioactive Sludges in Iron Phosphate Glass, in The American Chemical Society Symposium on Science and Technology for Disposal of Radioactive Tank Wastes, Plenum Press, Las Vegas, NV, 1998.

Table 1
Sodium bearing waste composition; original composition from INEEL [16, 22] and the simplified composition and raw materials used.

	Original Wt%	Simplified Wt%	Raw Materials	Weight* (g)
Al_2O_3	27.34%	27.47%	Al_2O_3	27.50
B_2O_3	0.65%	0.65%	H_3BO_3	1.25
CaO	2.23%	2.24%	$Ca(NO_3)_2*4H_2O$	5.34
Cl	1.04%	1.05%	NaCl	1.65
Cr_2O_3	0.25%	0.50%	Cr_2O_3	0.50
Fe_2O_3	1.55%	1.56%	$Fe(NO_3)_2*9H_2O$	6.85
F	0.98%	0.98%	CaF_2	2.05
I	0.02%	---		---
K_2O	7.91%	7.96%	KNO_3	17.17
MgO	0.05%	---		---
MnO	0.78%	0.78%	$Mn(NO_3)_2*6H_2O$	3.24
MoO_3	0.13%	---		---
Na_2O	50.05%	50.30%	$NaNO_3$	130.34
NiO	0.55%	0.55%	$Ni(NO_3)_2*6H_2O$	2.34
P_2O_5	1.19%	1.20%	$(NH_4)H_2PO_4$	2.76
PbO	0.31%	---		---
RuO_2	0.04%	---		---
SO_3	3.73%	3.75%	Na_2SO_4	6.57
SiO_2	0.18%	---		---
SnO	0.02%	---		---
ZrO_2	1.00%	1.00%	ZrO_2	1.00
Total	100.00%	100.00%	Total	208.55

* Batch yielding 100 grams of waste

Table 2
Batch and analyzed (as determined by ICP-ES labeled as ICP) compositions of the three iron phosphate glasses studied in detail. Molar oxygen to phosphorus ratio, iron to phosphorus ratio, and iron + aluminum to phosphorus ratio given for each composition.

	SBW40		SBW45		SBW50	
	Batch	ICP	Batch	ICP	Batch	ICP
Al_2O_3	10.9%	12.0%	12.3%	13.6%	13.7%	15.9%
B_2O_3	0.3%	---	0.3%	---	0.3%	---
CaO*	0.9%	1.2%	1.0%	1.3%	1.1%	1.6%
Cl	0.4%	---	0.5%	---	0.5%	---
Cr_2O_3	0.2%	0.2%	0.2%	0.2%	0.3%	0.2%
Fe_2O_3	16.6%	15.7%	14.7%	13.8%	12.8%	11.8%
F	0.4%	---	0.4%	---	0.5%	---
K_2O	3.2%	2.7%	3.6%	3.0%	3.9%	3.6%
MgO	---	0.1%	---	0.1%	---	0.1%
MnO	0.3%	0.5%	0.4%	0.5%	0.4%	0.6%
Na_2O	20.0%	19.6%	22.5%	18.4%	25.0%	23.4%
NiO	0.2%	0.3%	0.3%	0.3%	0.3%	0.3%
P_2O_5	44.5%	46.8%	41.5%	47.4%	38.6%	40.5%
SO_3	1.5%	---	1.7%	---	1.9%	---
SiO_2	---	0.1%	---	0.2%	---	0.5%
ZrO_2	0.4%	0.2%	0.5%	0.3%	0.5%	0.3%
Total	99.8%	99.5%	99.8%	99.0%	99.8%	98.7%
O/P Ratio	4.14	4.09	4.36	4.06	4.61	4.57
Fe/P Ratio	0.33	0.30	0.31	0.26	0.29	0.26
(Fe+Al)/P Ratio	0.67	0.66	0.73	0.66	0.79	0.81

* The calcium from the calcium fluoride is included as calcium oxide value measured by ICP-ES.

Table 3
Properties of iron phosphate glasses containing 40, 45, and 50 wt% SBW.

Property		**SBW40**	**SBW45**	**SBW50**
Density ±0.05 g/cm^3		2.92	2.87	2.81
Average CTE (Ave from 100 to 375°C)C^{-1}		169×10^{-7}	161×10^{-7}	198×10^{-7}
Dilatometric and DTA Transformation Temp (T_g, °C) ±5°C		425 (440)*	425 (450)*	385 (410)*
Dilatometric Softening Point (T_d, °C) ±5°C		480	475	440
DTA Crystallization (T_x, °C) ±5°C		555	565	---
Melting Temperature (°C) ±10°C		1050	1050	1050
Annealing Temperature (°C) ±5°C		400	400	400
Mössbauer Hyperfine Parameters				
Isomer Shifts, δ (±0.05 mm/s)	Fe(II)	1.09	1.04	0.91
	Fe(III)	0.42	0.42	0.41
Quadrupole Splitting, ΔE_Q (±0.05 mm/s)	Fe(II)	2.11	2.28	2.26
	Fe(III)	0.86	0.86	0.89
% Fe(II)		9%	11%	63%

*(DTA value)

Table 4
Normalized mass release (PCT) from glassy iron phosphate wasteforms containing 40, 45 and 50 wt% SBW.

Iron phosphate glasses containing SBW				Borosilicate Glasses	
Normalized mass release (g/L)	SBW40	SBW45	SBW50	Normalized mass release (g/L)	EA*
r_{Al}	0.18	0.10	1.33	r_B	17.38
r_K	0.93	0.31	19.31	r_{Li}	10.18
r_{Na}	1.11	0.69	14.89	r_{Na}	14.11
r_P	0.28	0.15	3.18	r_{Si}	4.29
r_{total}	2.50	1.25	38.71	r_{total}	45.96
Initial pH (±0.1)	6.1	5.6	6.1	Initial pH	5.7
Final pH (±0.1)	9.2	8.7	10.1	Final pH	11.9

Normalized mass release (g/m^2)	SBW40	SBW45	SBW50	Normalized mass release (g/m^2)	CVS-IS**	LD6-54-12**
r_{Al}	0.10	0.05	0.69	r_B	1.7	0.11
r_K	0.50	0.17	10.04	r_{Li}	1.4	---
r_{Na}	0.60	0.37	7.74	r_{Na}	1.3	0.38
r_P	0.15	0.08	1.65	r_{Si}	0.4	0.10
r_{total}	1.35	0.67	20.12	r_{total}	4.8	0.59
Initial pH (±0.1)	6.1	5.6	6.1	Initial pH	5.9	5.7
Final pH (±0.1)	9.2	8.7	10.1	Final pH	10.3	11.4

*Average data for EA glasses produced at the Savannah River Site [32].

**CVS-IS and LD6-54-12 are standard borosilicate glasses made by PNNL [33].

Table 5
Dissolution rate measured on bulk glass and crystallized samples and calculated from the PCT total mass release.

Dissolution rate ($g/cm^2/min$)*	SBW-40	SBW-45	SBW-50
Calculated from PCT, glass powder	1.2×10^{-8}	6.2×10^{-9}	1.9×10^{-7}
Measured, Bulk Glass	2.9×10^{-9}	1.3×10^{-8}	5.2×10^{-8}
Measured, Bulk Crystallized	3.4×10^{-7}	6.9×10^{-7}	1.7×10^{-6}
Measured, Bulk CCC	-----	1.9×10^{-6}	-----

* 7 days in DI water @ 90°C

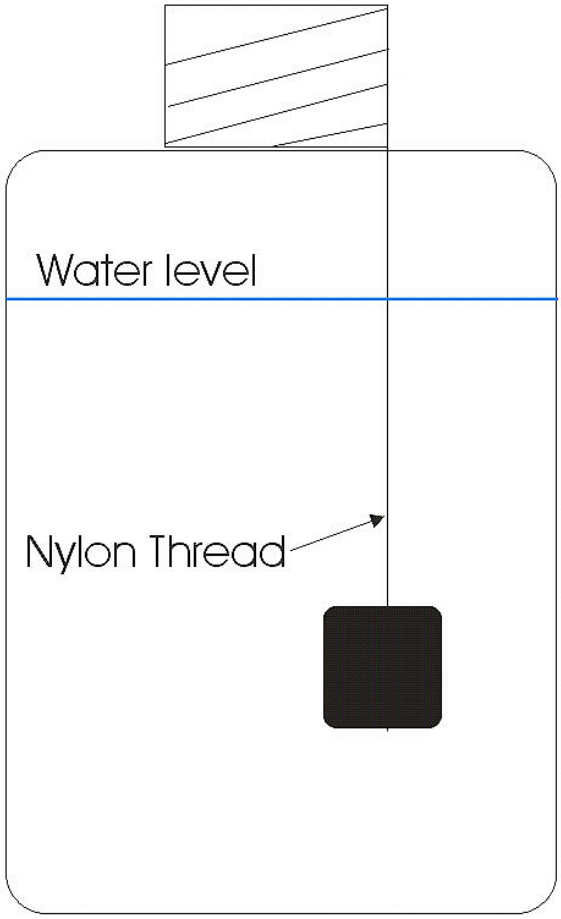

Fig. 1. Schematic of bulk durability device.

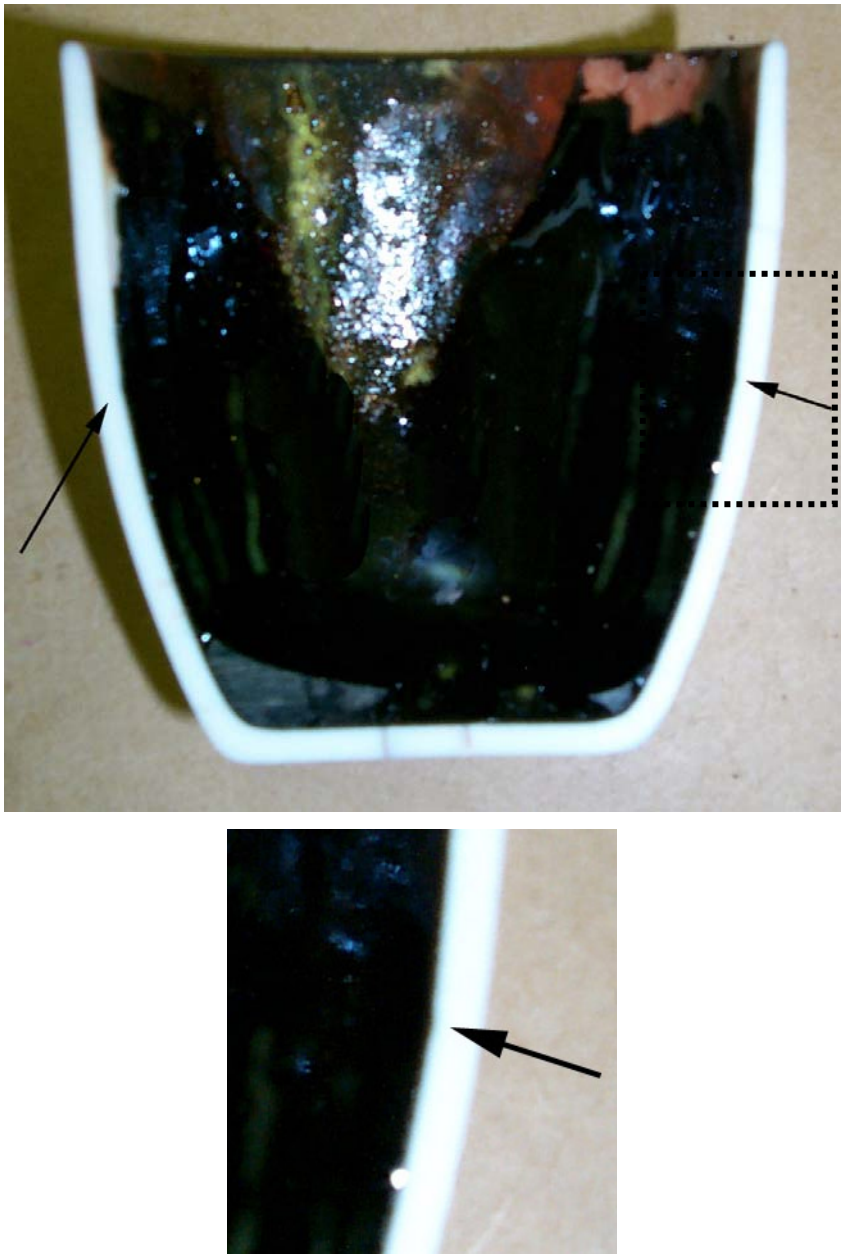

Fig. 2. Appearance of the cross section of a dense alumina crucible used to melt iron phosphate SBW45 for 2 hours at 1050°C. The corrosion at the melt-line (indicated by the arrows) was approximately 100μm deep (optical microscopy). Lower picture is an increased magnification of boxed area in the upper picture.

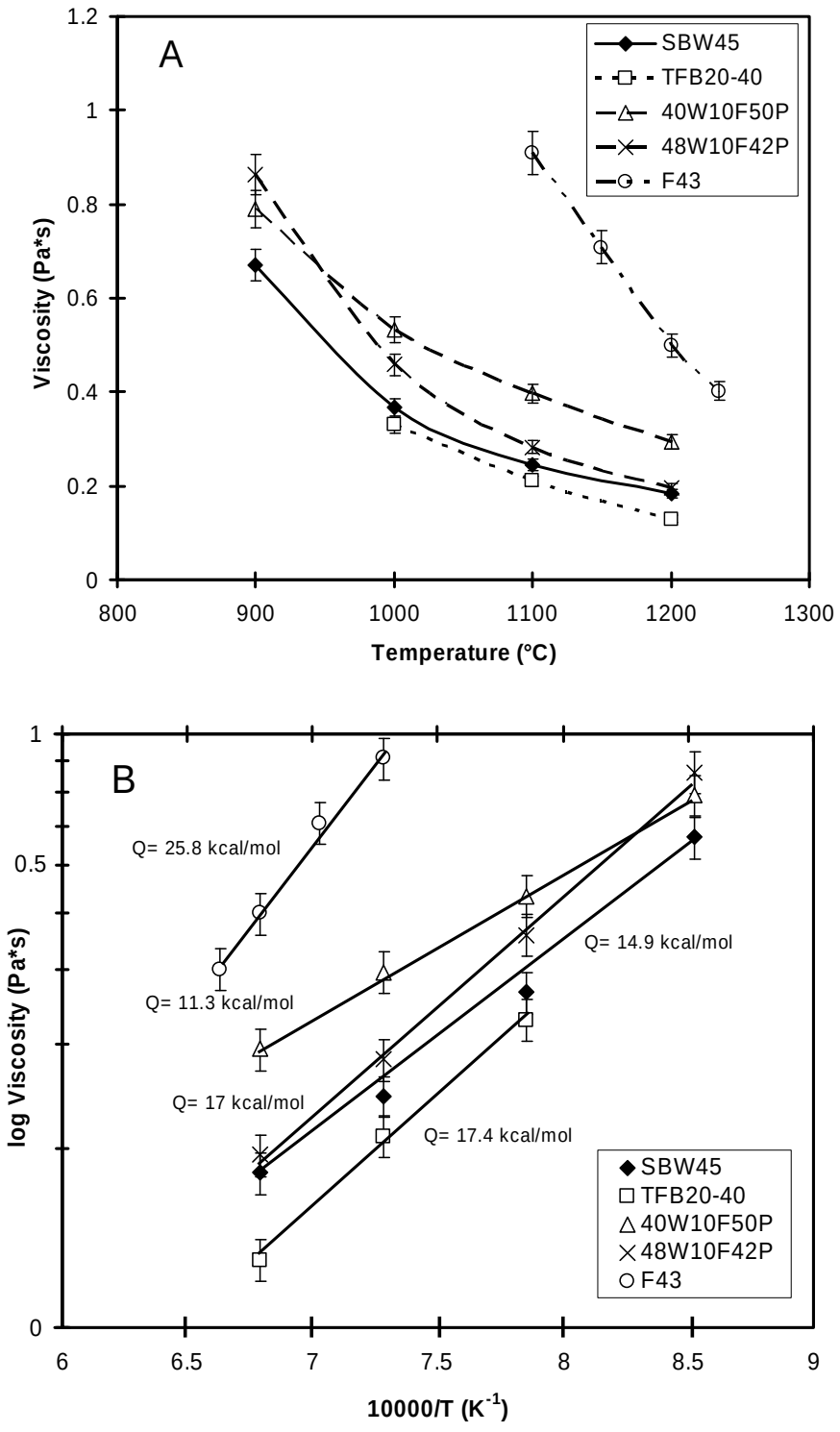

Fig. 3. A) Viscosity vs temperature for an SBW45 melt and iron phosphate melts from refs [23, 29]. The comparison iron phosphate melts contained from 12 to 26 wt% Na_2O, except for the alkali-free F43 which contained 43 wt% Fe_2O_3 and 57 P_2O_5.

B) log viscosity as a function of 10000/T (K^{-1}). The activation energy for viscous flow is given for each composition.

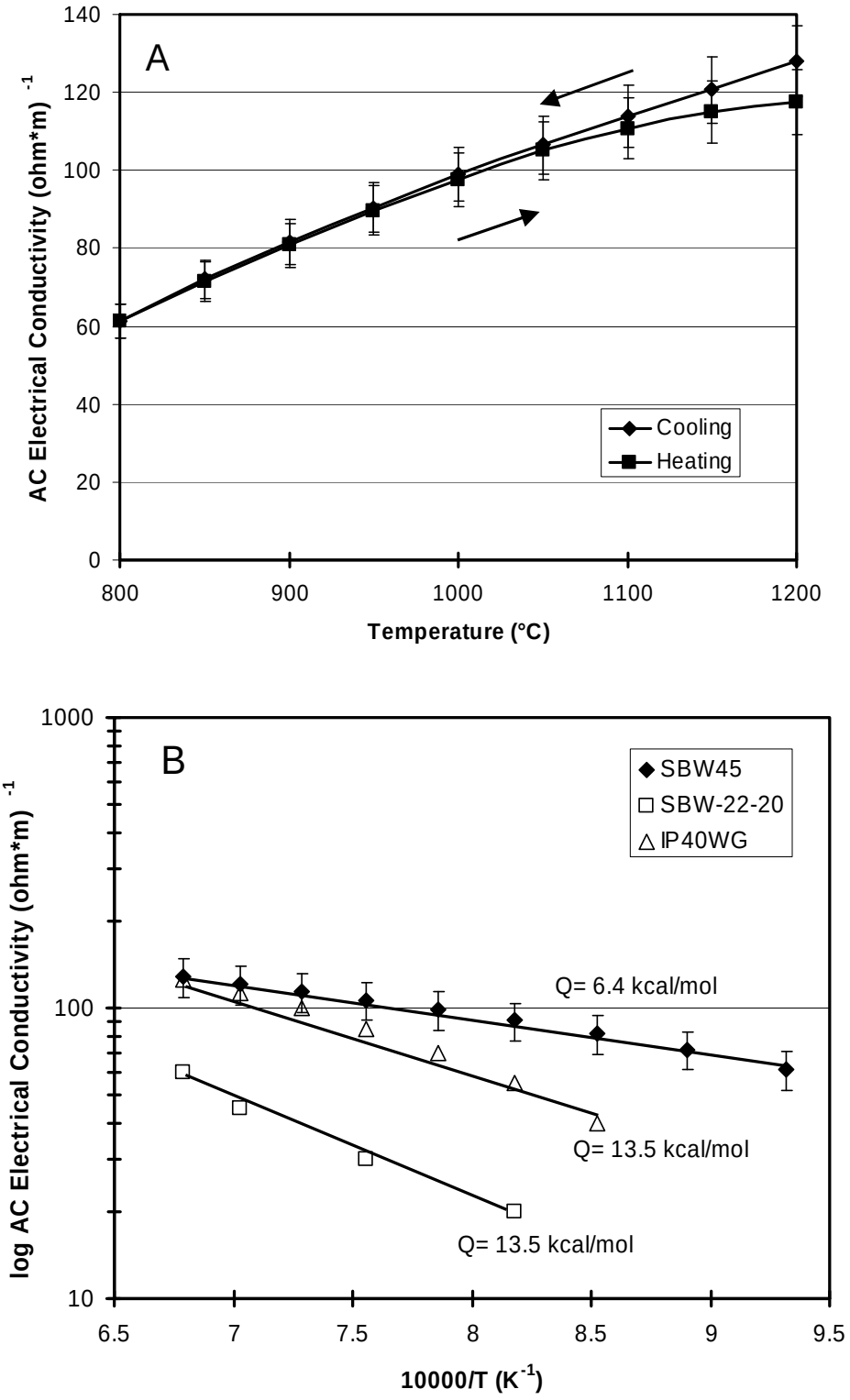

Fig. 4. A) AC electrical conductivity as a function of temperature for the iron phosphate SBW45 melt on heating and cooling.

B) Plot of log AC electrical conductivity vs 10000/T for SBW45 compared with IP40WG iron phosphate glass and borosilicate glass SBW22-20 [23, 29].

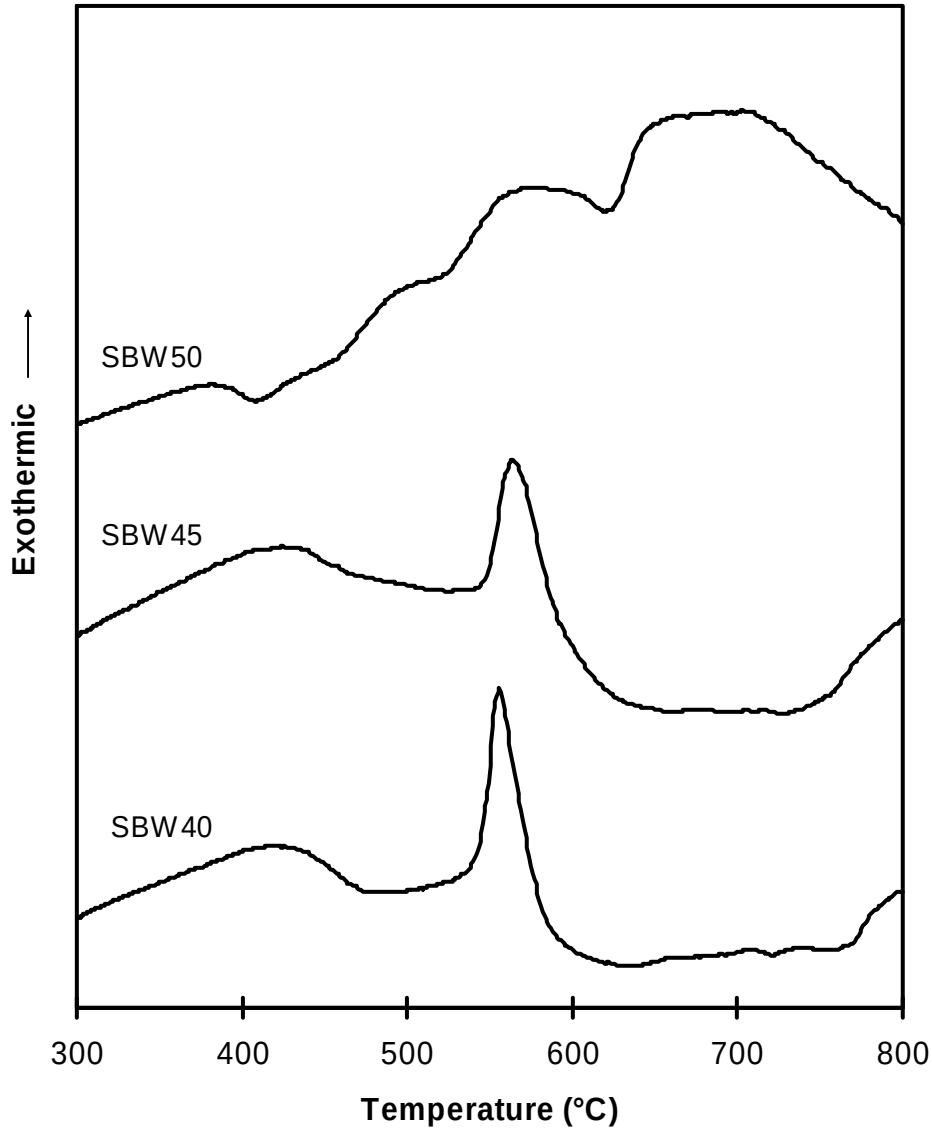

Fig. 5. Differential Thermal Analysis (DTA) of the SBW glasses measured at a heating rate of 10°C/min in air atmosphere.

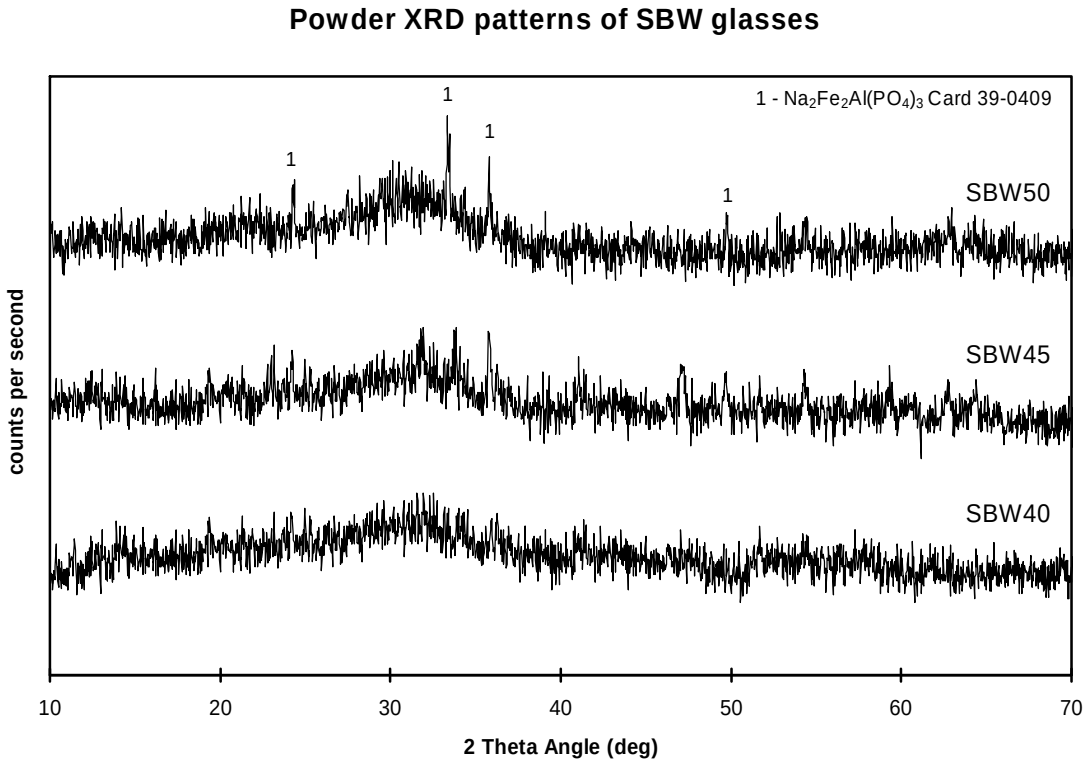

Fig. 6. Powder XRD patterns for iron phosphate glasses after annealing at 400°C.

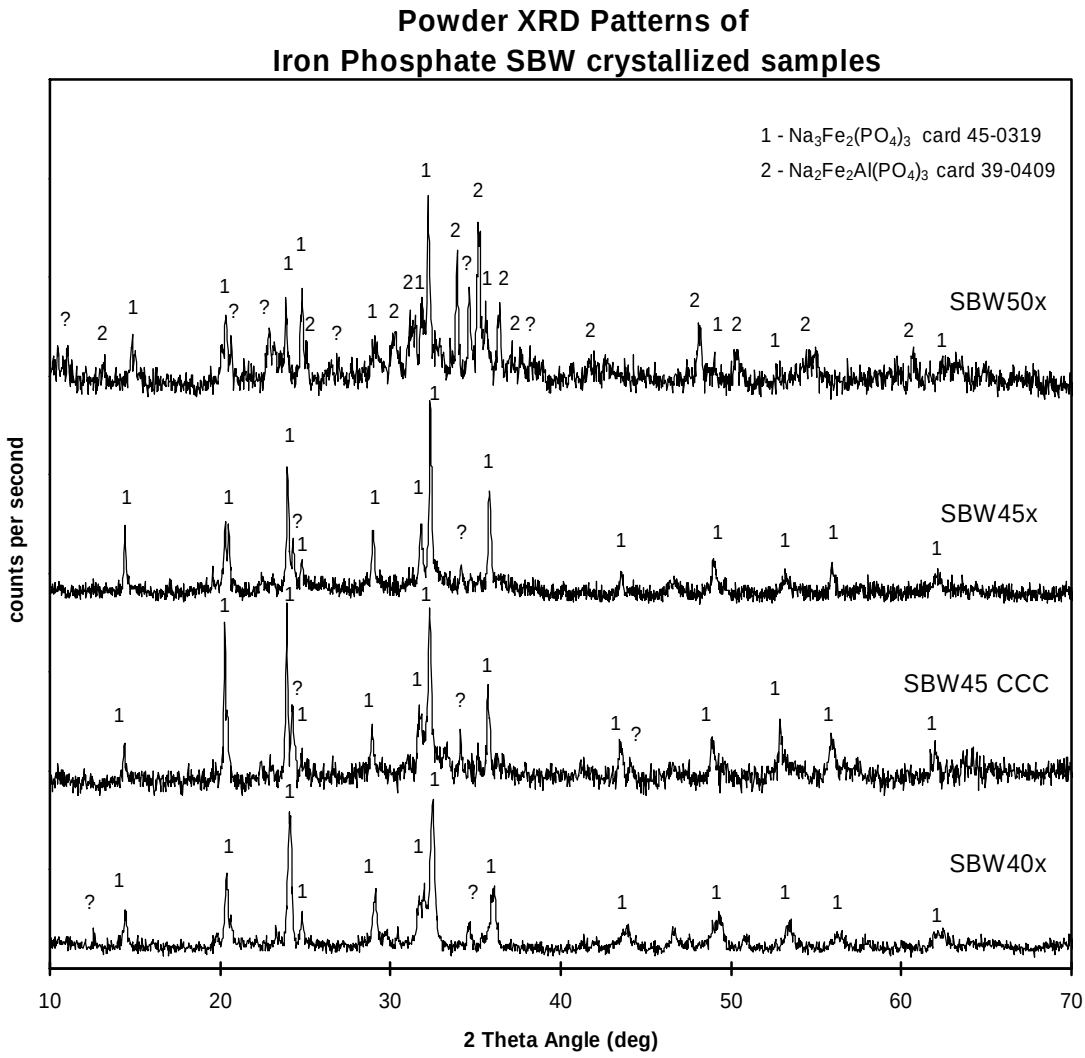

Fig. 7. Powder XRD patterns for the deliberately crystallized SBW40x, SBW45x and SBW50x waste forms and for the SBW45 melt that was slowly cooled from its melting temperature of 1050°C (SBW45-CCC).

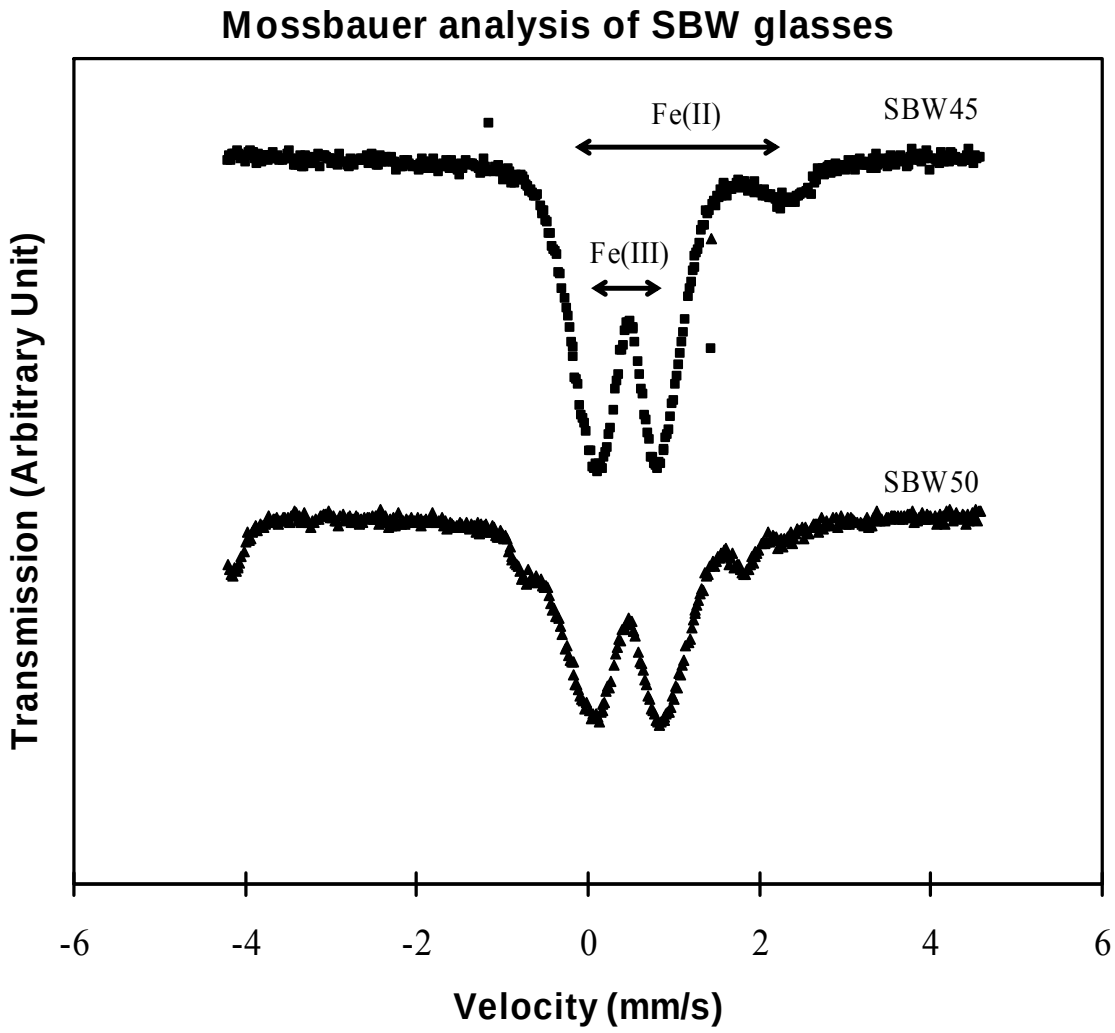

Fig. 8. Mössbauer spectra obtained at 23°C for SBW45 and SBW50 iron phosphate glasses. The SBW40 spectra was nearly identical to the SBW45 and is not shown here.

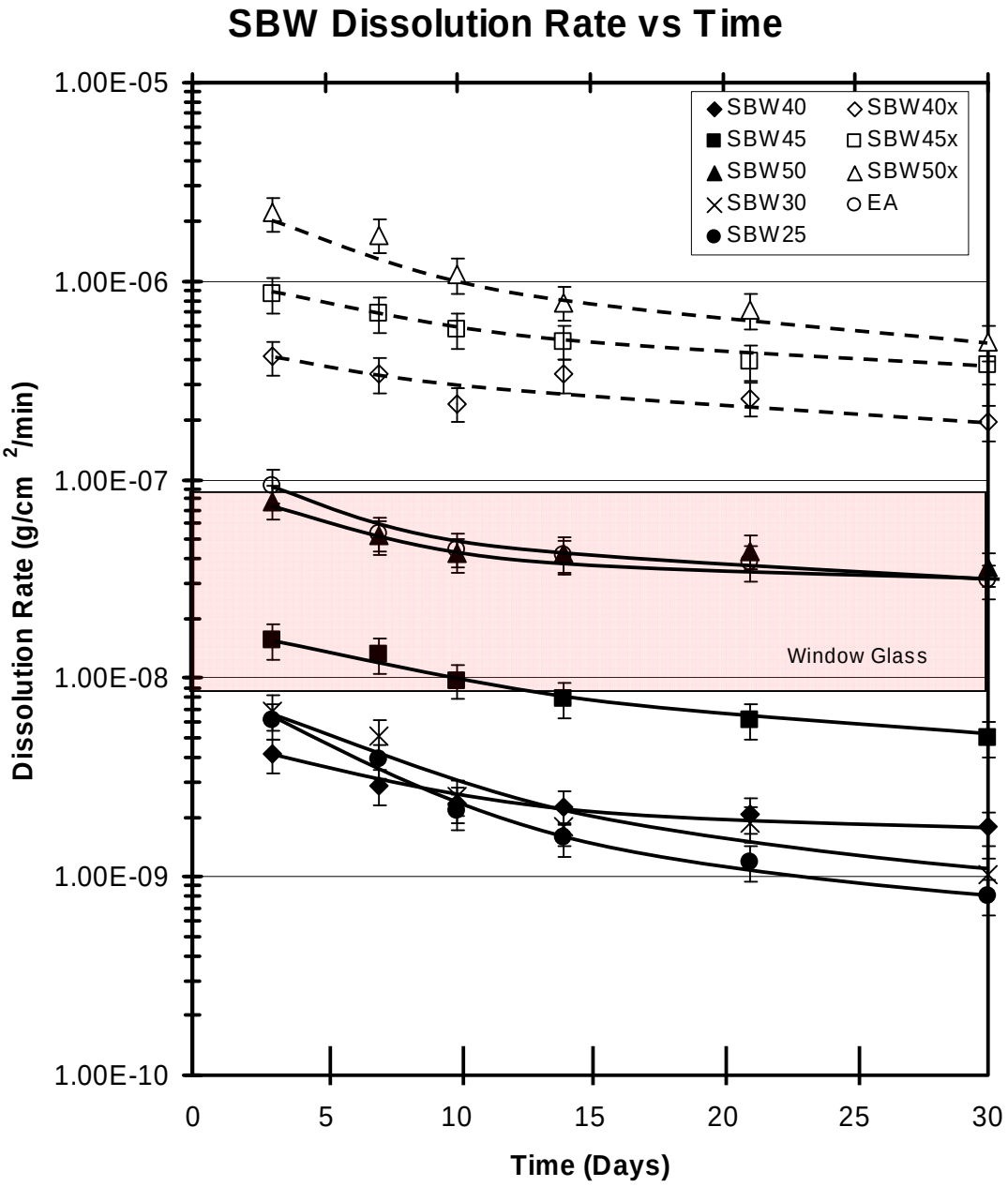

Fig. 9. Glass and crystallized sample dissolution rate as a function of time in 90°C DI water. Solid lines are for glassy samples, dashed lines are for crystallized samples. EA glass is included for comparison as well as the range for window glass (shaded area). DR data for glasses containing 25 (SBW25) and 30 (SBW30) wt% SBW are also given for comparison. Lines are drawn as guides for the eye.

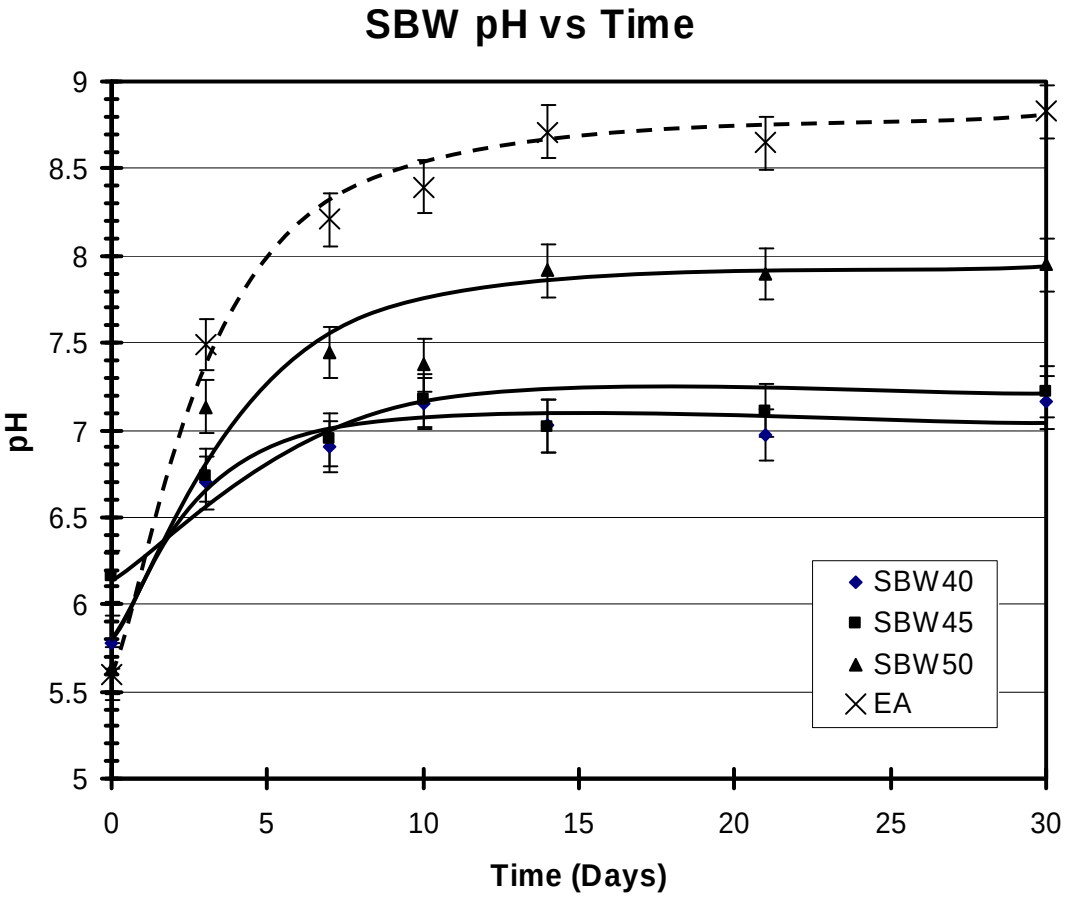

Fig. 10. Change in the pH of the DI water during dissolution rate measurements for the iron phosphate SBW glasses (solid lines) as well as EA borosilicate glass (dashed line). Lines are drawn as guides for the eye.

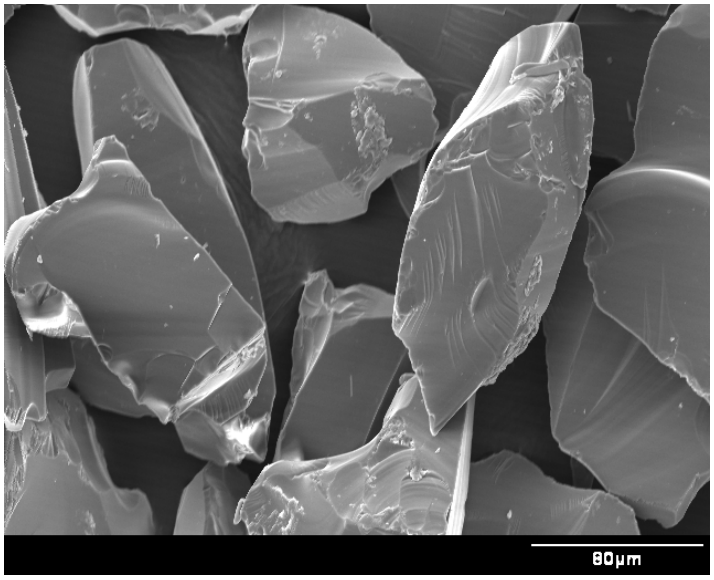

A

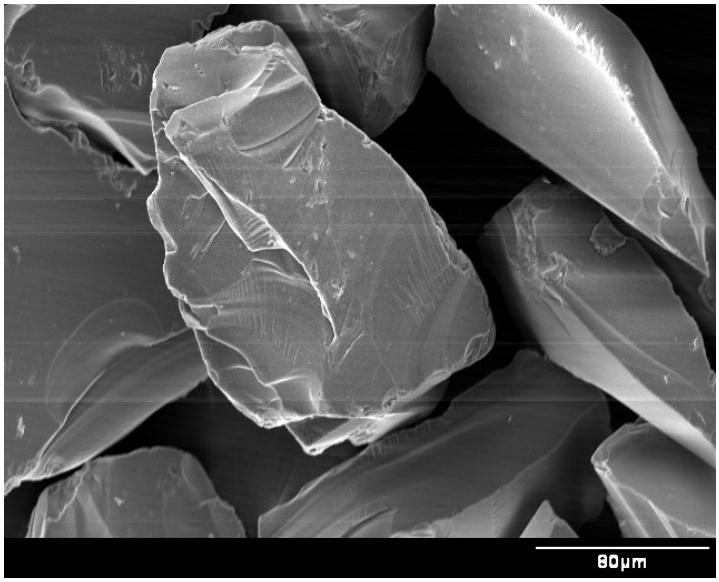

B

Fig. 11. A) SEM micrograph of uncorroded SBW50 glass particles at 500x.
B) SBW50 glass particles after immersion in deionized water at 90°C for seven days (PCT).

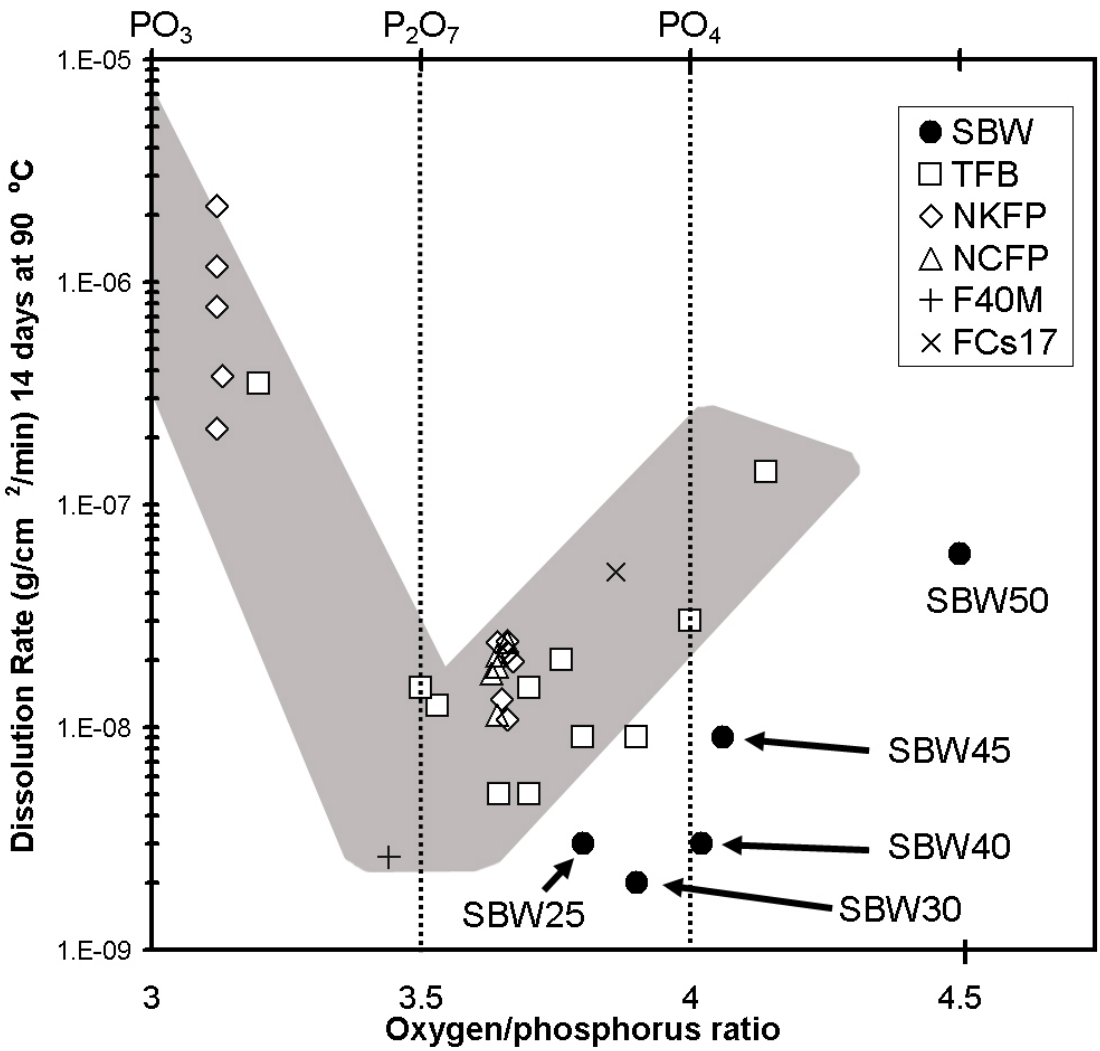

Fig. 12. Dissolution rate as a function of O/P ratio for iron phosphate glasses containing SBW. Data for iron phosphate glass containing (20 to 40 wt%) TFB waste from ref. [23]. NKFP and NCFP [37] which contain (20 mol% alkali, 20 to 32 mol% Fe_2O_3 and 48 to 60 mol% P_2O_5), F40M [37] (containing 40wt% Fe_2O_3 and 60 wt% P_2O_5) and FCs17 [38] (which contains 29 wt% Fe_2O_3, 38 wt% P_2O_5, and 33 wt% Cs_2O). Shaded area denotes general trend in DR with O/P ratio reported previously [23, 37].

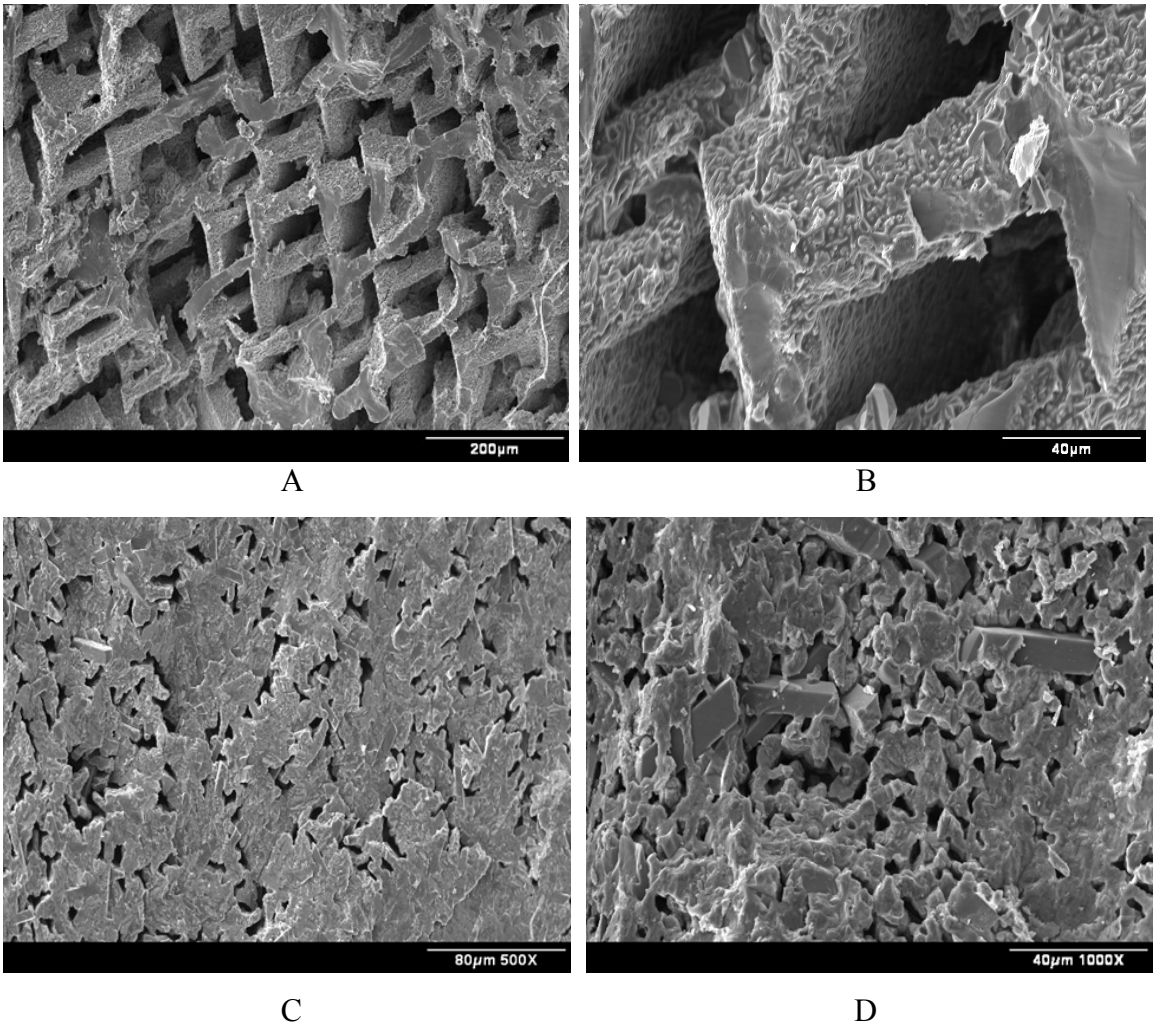

Fig. 13. SEM images of fracture surfaces:
A and B) SBW45-CCC.
C and D) SBW45 deliberately crystallized at 560°C for 24 hours.

APPENDIX A

COMPLETE LIST OF IRON PHOSPHATE SBW GLASSES MELTED

Table A1
Compositions of Iron phosphate glasses containing SBW that were melted.

Name	Composition	O/P	T (°C)	Anneal (°C)	DR*	Note
Trial Melts:	W=SBW waste, F=Fe_2O_3, P=P_2O_5, U=UO_2, M=2%Bi2O3, 2%CaF2, 2%CaO, 2%PbO, 2%ZnO					
SBW25	25W, 25F, 50P	3.9	1100	450	3.2-09	good glass
SBW30	30W, 23F, 47P	4.1	1050	475	2.8E-09	fluid at 1000 partially crystallized
SBW30 (2)	30W, 23F, 47P	4.1	1100	475	1.7E-09	melted longer than previous
SBW30B	30W, 20F, 50P.	3.9	1100	475	3.5E-09	good glass
SBW30n	30W, 20F, 50P.	3.9	1100	450	3.5E-09	good glass
SBW40	40W, 14F, 46P.	4.1	1050	425	4.9E-09	melted well, good glass
SBW45	45W, 12F, 43P.	4.4	1050	425	6.8-09	good glass
SBW50	50W, 10F, 40P.	4.6	1050	425	2.1E-08	good glass
SBW40b	40W, 16F, 44P.	4.3	1050	425	8.9E-09	melted well, exterior of bar crystallized after annealing.
SBW45b	45W, 14F, 41P.	4.5	1050	425	6.7E-09	good glass
SBW50b	50W, 12F, 38P.	4.8	1050	425	2.1E-08	good glass, significant amt of residue in crucible
SBW50 (2)	50W, 12F, 38P.	4.8	1100	425	2.0E-07	good glass, stirred more, less residue in crucible
SBW50B	50W, 15F, 35P.	5.1	1100	400	4.6-07	good glass, brown
SBW55	55W, 10F, 35P.	4.9	1100	400	5.0E-06	Partially crystallized
SBW60	60W, 10F, 30P.	5.8	1100	400	9.3E-06	crystallized
SBW60 (2)	60W, 10F, 30P.	5.8	1300	-	6.8-06	crystallized
SBW60B	60W, 40P.	4.6	1100	400	1.8-06	good glass small crystals
SBW60C	60W, 5F, 35P.	5.1	1100	400	6.4E-06	crystallized
SBW70	70W, 30P	5.8	1300	400	Fell apart	partially crystallized
SBW75	75% waste 25% F40 frit	8.9	1100	-	-	didn't melt at 1100
SBW75A	75% waste 25% F40 glass	8.9	1350	-	-	didn't melt
SBW45M	45W 10F 35P 10M	4.9	1100	400	1.9-07	brown Glass
SBW45U	45W 10F 35P 6U	4.1	950	400	8.9E-07	green glass, residue in crucible
Final Melts:						
SBW40	40W, 14F, 46P.	4.0	1050	400	1.7E-09	good glass 5 Samples for DR
SBW45	45W, 12F, 43P.	4.4	1050	400	6.9E-09	good glass 5 Samples for DR
SBW50	50W, 10F, 40P.	4.6	1050	400	5.0E-08	good glass 5 Samples for DR
SBW40x	40W, 14F, 46P.	4.0	1050	400	4.2E-07	Crystallized 590C 24 hrs 5 samples for DR
SBW45x	45W, 12F, 43P.	4.4	1050	400	3.4E-07	Crystallized 580C 24 hrs 5 samples for DR
SBW50x	50W, 10F, 40P.	4.6	1050	400	1.6-07	Crystallized 550C 24 hrs 5 samples for DR
SBW45-CCC	45W, 12F, 43P.	4.4	1050	---	1.9E-06	Cooled 40°C/hr to RT.

* $g/cm^2/min$ @ seven days in DI water at 90°C.

APPENDIX B.

COMPLETE DR DATA FOR IRON PHOSPHATE GLASSES CONTAINING SBW

Table B1

DR data for iron phosphate glasses containing SBW measured from 3 to 30 days. Bold average values used in Fig. 9.

	Dissolution Rate g/cm^2/min					
	3 days	**7 days**	**10 days**	**14 days**	**21 days**	**30 days**
SBW40-1	3.4E-09	2.3E-09	2.2E-09	2.2E-09	2.1E-09	2.1E-09
SBW40-2	2.3E-09	1.8E-09	1.6E-09	1.6E-09	1.5E-09	1.3E-09
SBW40-3	4.5E-09	3.9E-09	3.4E-09	3.1E-09	2.2E-09	2.9E-09
SBW40-4	4.7E-09	3.3E-09	2.0E-09	2.3E-09	2.4E-09	2.9E-10
SBW40-5	5.8E-09	3.0E-09	2.5E-09	2.1E-09	2.1E-09	2.2E-09
SBW40 Avg	**4.1E-09**	**2.9E-09**	**2.3E-09**	**2.3E-09**	**2.1E-09**	**1.8E-09**
SBW45-1	2.1E-08	2.0E-08	1.4E-08	1.2E-08	5.1E-09	5.0E-09
SBW45-2	1.5E-08	1.1E-08	8.1E-09	6.2E-09	6.6E-09	4.5E-09
SBW45-3	1.4E-08	1.4E-08	1.0E-08	8.9E-09	6.2E-09	5.8E-09
SBW45-4	1.4E-08	1.2E-08	8.4E-09	6.3E-09	6.6E-09	4.7E-09
SBW45-5	1.4E-08	9.5E-09	8.0E-09	6.0E-09	6.0E-09	5.2E-09
SBW45 Avg	**1.6E-08**	**1.3E-08**	**9.8E-09**	**7.8E-09**	**6.1E-09**	**5.0E-09**
SBW50-1	8.4E-08	5.2E-08	3.9E-08	3.7E-08	3.5E-08	3.5E-08
SBW50-2	1.1E-07	7.8E-08	6.5E-08	7.0E-08	7.4E-08	5.3E-08
SBW50-3	5.4E-08	2.8E-08	1.9E-08	1.4E-08	1.4E-08	1.5E-08
SBW50-4	5.7E-08	3.6E-08	2.6E-08	2.2E-08	2.1E-08	2.1E-08
SBW50-5	8.7E-08	6.5E-08	6.2E-08	6.9E-08	7.5E-08	5.5E-08
SBW50 Avg	**7.8E-08**	**5.2E-08**	**4.2E-08**	**4.3E-08**	**4.4E-08**	**3.6E-08**

Table B2
pH values of water used in dissolution rate measurements for iron phosphate glasses containing SBW. Bold average values used in Fig. 10.

	Initial	**3 days**	**7 days**	**10 days**	**14 days**	**21 days**	**30 days**
SBW40-1	5.78	5.89	6.63	7.10	6.63	6.96	7.13
SBW40-2	5.78	6.75	6.95	7.18	7.05	7.15	7.25
SBW40-3	5.78	6.99	6.90	7.09	6.98	6.96	7.06
SBW40-4	5.78	6.84	6.93	7.13	7.14	6.90	7.17
SBW40-5	5.78	7.02	7.12	7.27	7.32	6.88	7.14
SBW40 Avg	**5.78**	**6.70**	**6.91**	**7.15**	**7.02**	**6.97**	**7.15**
SBW45-1	6.16	6.63	6.85	7.17	6.80	7.03	7.05
SBW45-2	6.16	6.86	6.99	7.15	6.96	7.21	7.24
SBW45-3	6.16	6.75	7.05	7.16	7.14	7.28	7.37
SBW45-4	6.16	6.76	6.98	7.17	7.14	7.14	7.25
SBW45-5	6.16	6.70	6.86	7.20	7.07	6.90	7.19
SBW45 Avg	**6.16**	**6.74**	**6.95**	**7.17**	**7.02**	**7.11**	**7.22**
SBW50-1	5.63	7.81	7.93	7.80	8.13	8.26	8.36
SBW50-2	5.63	7.89	8.16	7.86	8.59	8.35	8.42
SBW50-3	5.63	4.71	5.40	5.51	6.39	6.27	6.43
SBW50-4	5.63	7.37	7.63	7.58	7.91	8.11	8.16
SBW50-5	5.63	7.89	8.10	8.11	8.56	8.49	8.41
SBW50 Avg	**5.63**	**7.13**	**7.44**	**7.37**	**7.92**	**7.90**	**7.96**

Table B3
DR data for iron phosphate glasses containing SBW that were deliberately crystallized (by heat treatment at 550 to 590°C for 24 hours) measured from 7 to 35 days. Bold average values used in Fig. 9

	Dissolution Rate g/cm^2/min					
	3 days	**7 days**	**10 days**	**14 days**	**21 days**	**30 days**
SBW40x-1	4.0E-07	3.2E-07	1.8E-07	2.9E-07	2.3E-07	1.5E-07
SBW40x-2	4.1E-07	3.6E-07	2.4E-07	3.4E-07	3.1E-07	2.4E-07
SBW40x-3	4.4E-07	3.4E-07	2.8E-07	3.8E-07	2.5E-07	2.0E-07
SBW40x Avg	**4.2E-07**	**3.4E-07**	**2.4E-07**	**3.4E-07**	**2.6E-07**	**2.0E-07**
SBW45x-1	8.3E-07	7.4E-07	5.6E-07	4.9E-07	3.6E-07	3.3E-07
SBW45x-2	9.0E-07	7.2E-07	6.8E-07	5.1E-07	3.2E-07	3.2E-07
SBW45x-3	8.6E-07	6.2E-07	4.7E-07	5.0E-07	5.0E-07	4.9E-07
SBW45x Avg	**8.6E-07**	**6.9E-07**	**5.7E-07**	**5.0E-07**	**3.9E-07**	**3.8E-07**
SBW50x-1	1.6E-06	9.9E-07	9.5E-07	7.5E-07	7.8E-07	5.5E-07
SBW50x-2	3.0E-06	2.6E-06	1.4E-06	9.4E-07	8.1E-07	5.4E-07
SBW50x-3	1.9E-06	1.6E-06	9.3E-07	6.6E-07	5.5E-07	4.0E-07
SBW50x Avg	**2.2E-06**	**1.7E-06**	**1.1E-06**	**7.8E-07**	**7.1E-07**	**4.9E-07**

Iron phosphate glass for the vitrification of Hanford low activity waste with high sulfur content

R.D. Leerssen, D.E. Day*

Ceramic Engineering Department and Graduate Center for Materials Research, University of Missouri-Rolla, MO 65409

Abstract

The Low Activity Waste (LAW) streams at the Hanford, WA site contain from 7.42 to 11.50 wt% sulfate content, making them ill-suited for vitrification in borosilicate glass at high wasteloadings. Iron phosphate glasses melted at 950°C with wasteloadings of up to 30 wt% had dissolution rates below 6×10^{-9} g/cm^2/min after 14 days in 90°C water and Product Consistency Test (PCT) total normalized mass release of less than 1 g/m^2 in 90°C water for 7 days. The high soda content of the LAW (75 wt% Na_2O) limited the wasteloading to 30% (22.6 wt% Na_2O) for a chemically durable waste-glass. These iron phosphate glasses crystallized upon cooling at <1 °C/min from the melting temperature (950°C) and when heat-treated at 580°C for 24 hours. The crystallized wasteforms had dissolution rates that were ten times higher than their glassy form. Sulfate content of up to 4.5 wt% was found for iron phosphate wasteglasses with no evidence of a sulfate layer on the melt surface or sulfate segregation within the glass. The retention of sulfate decreased with increasing time and temperature. For melting temperatures up to 950°C and times less than 2 hours, more than 50 wt% of the sulfate in the waste was retained in the glass. The durability of the glass appeared to decrease somewhat with increasing sulfate content, however, processing conditions varied.

PACS codes: 28.41.Kw

Key words: iron phosphate glass; low activity waste; chemical durability, sulfur retention

---

*Corresponding Author: Delbert E. Day, Graduate Center for Materials Research, University of Missouri – Rolla, 1870 Miner Circle, Rolla, MO 65401, email: day@umr.edu

1. Introduction

Thousands of nuclear warheads were produced in the United States during the arms race with the former Soviet Union. In the U.S., a large nuclear complex (16 major facilities) was developed to research, manufacture, assemble, and test nuclear materials and bombs [1]. The largest of the production facilities is the Department of Energy's (formerly Department of Defense) Hanford Site in Washington State, where the largest amount of defense waste in North America is located [2]. This site is where a majority of the plutonium processing for the nuclear arms race took place. This processing included nine nuclear reactors used to convert uranium-238 to plutonium that was then reprocessed in one of five chemical plants.

These plants produced more than 55 million gallons of radioactive waste, which is stored in 177 underground storage tanks. The majority (149) of the tanks are single-shell tanks (single carbon steel shell surrounded by concrete) ranging in size from 55,000 gallons to 1 million gallons. These tanks were designed with a life expectancy between 10 and 20 years [1], but many are over 50 years old (built between 1943 and 1964). The remaining 28 tanks are newer double-shell tanks (two carbon steel shells surrounded by concrete) with capacities of 1.0 to 1.1 million gallons and were designed to last between 25 and 50 years [1] and currently range in age from 20 to 32 years old. Although none of the double-shell tanks have leaked, over a million gallons from the single-shell tanks are estimated to have leaked into the ground [2].

The waste in the tanks consists of a settled sludge layer containing heavy metals, transuranics and phosphates, and a liquid layer containing sodium, nitrates, phosphates and sulfates. The liquid layer will be pumped from the tanks and prepared for vitrification as a low activity waste feed. The majority of the radiation in these tanks is in the sludge layer, therefore, it will be vitrified as high level waste [3]. The amount of waste in the liquid fraction is by far the largest [3], and it has been estimated that the vitrification of this waste will create nearly 500,000 tons of waste glass to be stored in vaults at the Hanford, WA site [4].

One complication for the vitrification of these wastes is the fact that there are more than 40 different waste compositions being stored in the waste tanks. This waste diversity stems from the three different separation techniques used for the isolation of plutonium through the years, as well as additives such as NaOH to neutralize the acidic waste stream (reduce corrosion of the tanks) as well as additions of ferrocyanide to the tank to precipitate radioactive cesium thus allowing the water with very little radioactivity to be decanted and transferred to storage ponds, reducing the volume of liquid in the tanks [1].

One of the concerns with this waste is its high sulfate content, which has proven to be problematic in borosilicate glasses due to a sulfate layer that forms on the surface of the melt and is extremely corrosive to the refractory lining in the melter [5, 6]. There is also a tendency for silicate melts with more than 5 wt% sulfate to form a foam [7] that can interfere with the melting. A limit of 1 wt% sulfate has been placed on borosilicate glasses to avoid these problems [6, 8-14]. Other wastes that have proven to be problematic for vitrification in borosilicate glass are those that are high in sodium, phosphorus, chromium or heavy metals [8, 15].

Currently, there are two methods of dealing with the high sulfate containing waste streams: (1) blend the high sulfate waste streams with others that are low in sulfate, or (2) dilute the waste using an extremely low wasteloading (8-10wt%) [3]. Neither of these choices are particularly attractive, one involves too much handling of this dangerous waste, and the other will create an undesirably large amount of final wasteform for disposal. A possible alternative that would allow direct vitrification of these high sulfate wastes is to have another approved wasteform which has a higher tolerance for components that limit the wasteloading in borosilicates.

Research to identify a glass which can contain higher concentrations of the wastes that are not well suited for vitrification in the current borosilicate glass has been undertaken [16-18]. Iron phosphate glasses have attracted attention as a possible candidate in this regard. Iron phosphate glasses containing 5% sulfate have been made without difficulty [19] due to a higher solubility limit for sulfur in phosphate glasses [20].

There have been numerous publications on the effectiveness of iron phosphate glasses as nuclear waste vitrification host glasses [21-24]. Iron phosphates have many of

the same attributes that led to the approval of borosilicate glass as the vitrification standard: (1) good chemical durability [25, 26], (2) processing temperatures below 1100°C [25, 27] and (3) resistance to crystallization [21], with the added benefit (4) of high solubility for phosphorus and sulfur [20].

In the present work, the average composition for the Low Activity Waste (LAW) at Hanford WA was studied for vitrification in iron phosphate glass [28]. This waste is hereafter called Hanford High Sulfate (HHS) waste. Sixty-eight iron phosphate glasses containing from 20 to 50 wt% HHS waste have been prepared from which selected compositions were chosen for closer investigation.

The objectives of the present work were: (1) determine the maximum amount of HHS that can be vitrified in iron phosphate glass, (2) determine the chemical durability of iron phosphate wasteforms as a function of composition, (3) identify compositions of iron phosphate glassy wasteforms with the maximum wasteloading and acceptable durability, (4) evaluate the chemical durability of glassy and deliberately crystallized iron phosphate wasteforms, and (5) determine sulfate retention in the wasteform.

2. Experimental Procedure

2.1. Simulated waste formulation

The composition of the Hanford High Sulfate (HHS) for the present research is a modified version of the average composition of the LAW at Hanford [28]. Table 1 gives the original composition as well as the slightly simplified version that was used. The original waste composition was simplified by ignoring several minor components whose concentrations were below 0.5 weight percent and increasing the remaining components accordingly. The slight compositional difference is not expected to affect the overall properties of the wasteform, nor the results reported herein.

Due to the high nitrate content of the HHS waste at Hanford, the majority of the Na_2O (75.3 wt% of the waste) was added as $NaNO_3$. Table 1 lists the raw materials used for the simulated HHS composition. This supply of simulated waste was mixed by tumbling in a plastic container and stored in a sealed container until used. The calculated weight loss on ignition for the HHS was 53.9%.

2.2. Glass preparation

Batches that produced 100g of glass were prepared by mixing reagent grade Fe_2O_3 and P_2O_5 dry crystalline powders with varying amounts of HHS. The simulated HHS and additives were dry mixed and melted in a high purity alumina crucible (CoorsTek 65505) in an electric furnace. These glasses were melted in an uncovered crucible at the lowest temperature possible (generally between 900 and 1000°C) for 2 hours in an air atmosphere.

The batch was placed into the crucible in several small amounts at temperatures ranging from 400 to 900°C, adding more as the batch melted. To ensure that the melt was homogeneous, each liquid was stirred three times during melting (at approximately 60 minutes, 90 minutes and 10 minutes prior to pouring the melt) using a silica rod. The melt was poured into steel molds to form 1 cm × 1 cm × 10 cm rectangular bars, which were annealed at 400°C for approximately 2 hours and then cooled overnight to room

temperature in the annealing furnace. The resulting glasses were black in color and opaque.

Since P_2O_5 was used as a raw material, the amount used in the batch included an additional 5 wt% of the required amount to compensate for potential volatilization losses of P_2O_5 during melting. Other chemicals such as $(NH_4)H_2PO_4$, or phosphoric acid (including industrial waste from metal phosphating) can be used instead of P_2O_5 to avoid the hygroscopic nature of this raw material [29].

Using ammonium phosphate as the source of P_2O_5 causes the batch to be more reducing during melting. A reducing melt affects the sulfur retention by reducing the SO_3 to SO_2, causing it to volatilize from the melt faster [30]. Adding sugar to the batch had a similar effect on the retention of sulfur.

Several additives have been shown to have a positive impact on the durability of iron phosphate wasteforms. These include calcium fluoride, calcium oxide and manganese oxide which seem to decrease the tendency for crystallization [21], and lead oxide and alumina which increase the chemical durability of the glass [31].

After the initial glasses were melted and preliminary durability testing performed, four of the promising glass compositions, given in Table 2, were chosen for more comprehensive study. These include three glasses containing 30 wt% HHS and one containing 25 wt% HHS. The three compositions at 30 wt% HHS included one with 20% Fe_2O_3 and 50% P_2O_5 (HHS30), and two other glasses that included several additives. In an attempt to reduce the crystallization tendency and to increase the durability of the glasses, 2 wt% each of Bi_2O_3, CaF_2, CaO, PbO and ZnO were substituted for P_2O_5 in HHS30M, and 5% each of calcium fluoride and alumina were substituted for Fe_2O_3 in HHS30CA. The composition with a waste loading of 25% (HHS25) did not include any additives.

2.3. Property measurements

Samples for property measurements were cut from the annealed glass bars. The density of the glasses was measured by the Archimedes method using kerosene as the suspension liquid. The average linear thermal expansion coefficient, α, and dilatometric

softening temperature, T_d, were measured using an Orton model 1600 auto-recording dilatometer. T_d was determined as the peak of the expansion curve, and α was calculated from the slope of the expansion curve, using the most linear region of the curve between 100 and 375°C.

Some of the annealed glass was deliberately crystallized by heat treatment between 540 and 590ºC for 24 hours. Some of the crystallized samples were ground to -200 mesh powder and the crystal phases were determined from X-Ray Diffraction (XRD) patterns that were collected over a 2θ range from 10 to 90 degrees, at a scan rate of 1º/min using a Scintag PADX x-ray diffractometer using copper *K*α radiation with a wavelength of 1.5418Å.

One HHS30 melt was cooled over a 24 hour period to simulate the Canister Centerline Cooling rate (CCC) at the center of the current wasteform containers used at the Defense Waste Processing Facility (DWPF) in Aiken, SC. The cooling rate chosen was approximately 40°C/hr from the melt temperature of 950°C to room temperature. This rate is approximately twice the rate used previously for an iron phosphate glass [26] and twenty times faster than the actual CCC rate of about 2°C/hr [32], but the higher rate was considered acceptable for the purposes of the present study. The objective of this cooling experiment was to determine if there was a difference in the phases that crystallized from the slowly cooled melt as compared to the phases crystallizing when the same glass was reheated from room temperature to 570°C where crystallization occurs.

A Netzsch (Simultaneous Thermal Analysis STA 409) Differential Thermal Analysis/Thermal Gravimetric Analysis instrument (DTA/TGA) was used to determine the crystallization temperature as well as note any weight change that occurred in the sample. Approximately 40 mg of glass was heated in an alumina crucible to 800ºC at a rate of 10ºC/min in air.

A JEOL T330A Scanning Electron Microscope (SEM) was used to examine the surface of glassy, crystallized and chemically corroded samples. The samples were affixed onto the SEM mounts with carbon tape and sputter coated with gold/palladium to form a conductive layer.

Inductively Coupled Plasma – Emission Spectroscopy (ICP-ES, Acme Analytical Laboratories LTD. - Vancouver, British Columbia) was utilized to determine the final

composition of the glass, which was compared to the original batch composition. The glass samples were digested in a four acid solution (HNO_3, $HClO_4$, HF and HCl) at high temperature prior to analysis. The analysis package used was the "whole rock analysis" which does not include detection of the Bi_2O_3, PbO, SO_3 and ZnO found in the HHS30M glass.

The viscosity of the HHS30 melt was measured using a rotating viscometer. A non-standard alumina spindle was constructed from a 10 cc straight wall crucible and calibrated using three standard viscosity oils (0.097, 0.099, and 0.965 Pa·s). Spindle speeds of 10, 20, and 50 rpm were used for each measurement. The estimated error for this procedure was less than ±5%. The melt was held at a selected temperature for 30 minutes to allow it to thermally equilibrate, at which time a preheated spindle was immersed in the melt. The viscosity was measured three times and then averaged. The corrosion of the alumina spindle by the melt was negligible, determined by visual inspection.

The AC Electrical conductivity of the molten HHS30 glass was measured at 1000 Hz by inserting 1 cm × 2 cm platinum electrodes 1.7 cm apart into the melt at temperatures ranging from 800°C to 1200°C. The temperature range chosen was based on the desire to know the response of iron phosphate glasses containing HHS not only at the melting temperature used in the present work, but also at temperatures where borosilicate wasteglasses are melted (~1150°C) for comparison.

The melt was heated to 1200°C where the first measurement was taken. The temperature was reduced by 50°C and the melt was held at this temperature for 30 minutes after which the second measurement was taken; this process was repeated to 800°C. Once 800°C was reached the temperature was increased in increments of 50°C, held for 30 minutes and the AC conductivity remeasured to determine if the conductivity changed with time or thermal cycling.

The electrical resistivity of the melt was measured using an LCR meter connected to the platinum electrodes, and this resistance measurement was converted to electrical conductivity (σ) using the equation:

$$\sigma = K\left(\frac{1}{R} \bullet \frac{L}{S}\right) \quad (1)$$

where R is the electrical resistivity, L is the distance between the two electrodes, S is the surface area of the electrode immersed in the melt, and K is the cell constant that was determined to be 1.12 by calibrating the instrument using three different concentrations of KCl standard solution. The error was estimated to be ±5%.

To determine the valence and coordination number of iron in the glass, Mössbauer spectroscopy was employed. The Mössbauer spectra were measured at room temperature on a constant acceleration spectrometer (ASA600) using a 50 mCi rhodium matrix cobalt-57 source. Mössbauer absorbers of approximately 85 mg/cm^2 were prepared from 200 mesh powders.

2.4. Chemical durability

The chemical durability of the iron phosphate glasses was determined from the weight loss of bulk samples immersed in deionized water at 90°C and on powders (-100 to +200 mesh) according to the Product Consistency Test (PCT, ASTM C 1285-97) [33].

The bulk Dissolution Rate (DR) samples were cut from annealed glass bars using a diamond saw with kerosene as the cooling liquid and then polished to 600 grit. The dimensions of each sample were approximately 1 cm × 1 cm × 1 cm (±0.1cm). The DR for each glass was measured on three samples and averaged.

Some of the samples were deliberately crystallized by heat-treating between 550 and 590°C for 24 hours. These heat-treated samples were used to determine the DR of the crystallized wasteform.

The glassy and crystallized samples were rinsed with deionized water and acetone, dried at 90°C, cooled to room temperature and weighed (±0.01 mg). Each sample was suspended by a rayon thread in a 125 ml polyethylene bottle containing 100 ml of deionized water. A schematic of this setup is given in Fig. 1. The bottles containing the wasteforms were placed in a 90°C oven and each sample was removed for measurement after 7, 14, 21, 28, and 35 days. The samples were rinsed with deionized water, dried at 90°C, cooled and weighed (±0.01 mg). The pH of the solution was measured each time using a Fisher Scientific Accumet® pH/ion meter model 25 (±0.1

units). The samples were replaced in the same bottle without changing the water and returned to the oven.

Samples of the Environmental Assessment (EA) glass obtained from the Savannah River Laboratory were measured under the same conditions and used as a reference for the DR values of the iron phosphate glasses.

The DR was calculated from the measured weight loss using the equation:

$$DR = \frac{\Delta W(g)}{A\,(cm^2) \cdot t\,(min)} \tag{2}$$

where A is the geometrically determined surface area (cm^2) of the sample and t is the time (min) that the sample was immersed in DI water at 90°C. The weight loss (ΔW) is $W_i - W_t$, where W_i is the initial weight of the sample and W_t is the weight of the same sample after time t.

The chemical durability of the iron phosphate glass wasteforms was also measured by the PCT. The samples were mechanically crushed and sieved to isolate the -100 to +200 mesh fraction. The powders were washed thoroughly in water and ethyl alcohol in an ultrasonic bath to remove particles smaller than 200 mesh, which are known to reduce the accuracy of PCT measurements [34]. The washed powders were dried at 90°C overnight. The glass powder (1.5 grams ± 0.5mg) was weighed and placed into a Teflon vessel. Fifteen ml of deionized water was added to the powder. The vessel was sealed and then placed in an oven at 90°C for seven days.

After completion of the PCT, the vessel was weighed and compared to the original weight to determine if any water had escaped. Leachate losses were less than 1% of the initial weight of the leachate. The pH of the water was measured before and after the test. The leachate was filtered through a Nalgene 0.45 μm filter, acidified with one volume percent 0.4 M Optima HNO_3 to ensure the cations remained in solution and the concentration of ions in the leachate was measured using ICP-ES (ACME Analytical Labs LTD. - Vancouver B.C.). All tests were conducted in duplicate and averaged. A blank was included in the analysis for control purposes.

The normalized elemental mass release, r, was calculated in two different units (g/L and g/m^2) from Equations 3 and 4, respectively, to provide easier comparison with other glasses:

$$r_i\left(\frac{g}{L}\right) = \frac{C_i}{f_i} \tag{3}$$

$$r_i\left(\frac{g}{m^2}\right) = \frac{C_i}{f_i\left(\frac{A}{V}\right)} \tag{4}$$

where C_i is the concentration of element i in the solution and f is the mass fraction of element i in the glass (unitless). The ICP-ES analyzed glass composition given in Table 2 was used to calculate f. A/V is the ratio of the sample surface area to volume of leachate (m^{-1}). The elements used for the analysis of the release rate from the iron phosphate glass are aluminum, potassium, sodium and phosphorus. These elements differ from those that are analyzed in borosilicate wasteforms (boron, lithium, sodium and silicon) due to the compositional differences of the glasses.

2.5. Sulfur retention

Several experiments were conducted to find effects of the melting time and temperature on the retention of sulfur by these iron phosphate glasses. The first experiments included melting several small batches of HHS30 (containing 2.85 wt% SO_3) at temperatures ranging from 900 to 1150°C, in increments of 50°C, for one hour at each temperature. To study sulfur retention in HHS30 as a function of melting time, a 200g melt was held at 900°C and small sample bars (~25g) were poured at time intervals ranging from 1 to 24 hours. These glasses were analyzed for sulfur content by both X-ray Fluorescence (XRF) and by the Leco method (Acme Analytical Laboratory LTD – Vancouver, British Columbia). The wt% sulfur in the glass was then converted to SO_3. Other glass compositions tested for retention of sulfate were HHS40 (containing 3.8 wt% SO_3) and HHS50 (containing 4.75 wt% SO_3).

To determine the effect that the sulfate percentage had on the chemical durability of the glass, the dissolution rate was measured for the HHS30 samples produced for the studies of sulfate retention as a function of temperature and time.

3. Results

3.1. Glass formation

For waste loadings below 40 wt%, the glasses were black in color and free of crystals. Melts containing between 40 and 50 wt% wasteloading formed a green glass (possibly due to iron valence change), while melts above 50% wasteloading tended to crystallize quickly after pouring. A complete list of all compositions investigated in the present study along with the melting temperature and dissolution rate in water at 90°C is given in Appendix A.

3.1.1. Compositional analysis

During the initial melting of these glasses noticeable amounts of white smoke were given off, which was attributed to the volatilization of P_2O_5. Once the batch was fully melted, no more smoke was observed. The loss of P_2O_5 was compensated for by adding 5% more P_2O_5 to the batch than was required for the composition. The ICP analysis of the composition in Table 2 shows that the addition of excess P_2O_5 overcompensated for the volatilization losses, as the analyzed amount of P_2O_5 was typically higher than the batch composition in all but the HHS30CA glass.

Several other components of the glasses vary between the batch and ICP analyzed compositions. It is unknown why trace amounts of K_2O, MgO and MnO were reported in the analyzed compositions. Perhaps some of the raw materials used in making the batch were contaminated, but this is unlikely. The MgO and MnO amounts are small <0.1 wt%, but the amount of K_2O was large enough to cause an increase in the PCT normalized release rate (discussed later).

The Al_2O_3 content was 1 to 4 wt% higher than was expected in all of the glasses, most likely as a result of dissolution from the crucible and the incorporation of corrosion products into the melt (Table 2). However, very little corrosion or chemical attack of the alumina crucible by the iron phosphate melts below 30 wt% HHS was observed. A typical example of the crucible corrosion at the melt line is shown in Fig. 2 for a crucible

in which HHS30 was melted for 2 hours at 950°C. The depth of corrosion was estimated to be 220 μm by optical microscopy. This amount of corrosion accounts for approximately 4 grams of alumina added to the melt, or 2 wt% in the glass composition. In melts containing >40 wt% waste (~30 wt% Na_2O), the high soda content tends to attack crucibles. Some of the initial batches containing 40 to 60 wt% HHS leached through porous fireclay crucibles in an hour at 1000°C. Below 30% wasteloading, however, these glasses can be melted in fireclay crucibles for several hours without problems.

3.1.2. Oxygen to phosphorus ratio

The molar ratio of oxygen to phosphorus (O/P) was calculated from the batch composition (assuming the oxides are in the form listed in Table 2) as well as from the analyzed composition, and the results are reported in Table 2. For the glass compositions with no additives (HHS30 and HHS25) the O/P ratios from the analyzed compositions were lower than the ones calculated from the batch composition (3.57 vs. 3.71 and 3.63 vs. 3.73, respectively), but for the glasses containing 10 wt% additives (HHS30CA and HHS30M) the opposite is true (3.93 vs. 3.58 and 3.87 vs. 3.68, respectively). This difference in the HHS30M can be attributed to the large wt% of elements not detected by the ICP analysis of this sample (Bi_2O_3, PbO, SO_3 and ZnO were not detected in the chosen analysis of these samples, therefore ~9 wt% of the HHS30M batch composition was not detected by ICP), making the wt % of the detected elements artificially high. The cause for the low P_2O_5 concentration in the HHS30CA sample is unknown.

These glasses have ratios that fall into the empirically known range of O/P values for good durability, from 3.4 to 3.7. Generally the glasses that fall in this range have the best glass forming tendency and good chemical durability [26, 35].

Another ratio that has been empirically shown to indicate the glass forming ability of iron phosphate glasses is the molar iron to phosphorus ratio (Fe/P) which for these HHS iron phosphate glasses is given in Table 2. It has been shown in previous studies [24, 36] that an Fe/P ratio of 0.67 is favorable for good glass formation, while at a ratio below 0.33 the durability is significantly lower, and a ratio >1.0 glass formation becomes

difficult. The HHS30CA sample has a Fe/P ratio of 0.17 in the batch composition (0.24 from the analyzed composition) which is significantly below the desired ratio of 0.33. This low Fe/P ratio may account for the lower chemical durability of the HHS30CA glass.

3.2. Physical properties

3.2.1. Density

The density of the HHS glasses, provided in Table 3, as measured on five samples of each glass, ranged from a low of 2.75 g/cm^3 for HHS30CA (possibly due to lower Fe_2O_3 content) to 3.14 g/cm^3 for HHS30M (possibly due to replacing P_2O_5 with heavier elements such as PbO and Bi_2O_3). The estimated error was ±0.05 g/cm^3.

3.2.2. Viscosity

Because of the high soda content (75.3 wt%) and lack of other major components in the HHS waste composition, the viscosity of the iron phosphate glasses containing HHS was low enough that they could be melted and poured at temperatures between 900°C and 950°C. The HHS iron phosphate melts are more fluid at these temperatures than other iron phosphate melts as indicated by the viscosity curve for HHS30 compared with other waste containing iron phosphate glasses shown in Fig. 3A. The curve labeled TFB20-40 is for an iron phosphate melt containing 20 wt% of a simulated waste [26] whose composition was the average of the tank farm B (TFB) waste at Hanford, WA that contained 55% Na_2O. The glasses labeled 40W10F50P and 48W10F42P are for iron phosphate melts containing 40 and 48 wt%, respectively, of the Sodium Bearing Waste (SBW) at the Idaho National Engineering and Environmental Laboratory (INEEL) which contains 52.3 wt% Na_2O [37]. F43 is an alkali-free iron phosphate glass composed of 43 wt % Fe_2O_3 and 57 wt % P_2O_5.

At the pouring temperature (950°C), the viscosity of the HHS30 iron phosphate melt is approximately 0.26 Pa·s; about 40 times less viscous than the 11.55 Pa·s of the

SBW-2-25 borosilicate waste glass from INEEL, containing 25 wt% SBW (~13 wt% Na_2O), at its pouring temperature of 1150°C [15]. The viscosity of the HHS30 melt is believed to be representative of the viscosity of the other iron phosphate HHS melts in the present study.

The log viscosity plotted as a function of 1/T in Fig. 3B indicates that the viscosity of the HHS30 melt obeys the Arrhenius equation over the limited temperature range of the present study. The data plotted for comparison in Fig. 3B include the TFB waste from Hanford [26], as well as two glasses containing 40 and 48 wt% SBW waste [27], and the F43 iron phosphate glass (43 wt% Fe_2O_3, 57 wt% P_2O_5). The activation energy for viscous flow was calculated from the slope of the regression line, and is given in Fig. 3B for each melt. The activation energy for the HHS30 melt is 9.3 kcal/mol which is similar to the activation energy calculated for the 40W10F50P (11.3 kcal/mol) [27], but significantly lower than the activation energy for viscous flow in the alkali-free F43 glass (25.8 kcal/mol). The HHS30 melt is less viscous and also has the lowest activation energy most likely due to the high soda content of the waste, and lack of other major components.

To find the general trend in viscosity with respect to Na_2O content in iron phosphate melts, the data from previous studies [26, 27] are plotted in Fig. 4, where the viscosity is plotted as a function of wt% Na_2O in the melt. There is a general trend indicating that as the Na_2O content increases, the viscosity decreases and reaches a minimum between 15 and 20 wt% Na_2O and commences to increase with increasing soda. It is emphasized that the curves in Fig. 4 are intended to indicate the general trend in viscosity with soda content only since there are other significant compositional differences between these melts. For example, TFB20-40 contains 33.7 wt% Fe_2O_3 compared to 20 wt% in HHS30, and the SBW45, 40W10F50P and 48W1042P melts contain between 12.9 and 13.6 wt% Al_2O_3 compared to only 3.43 wt% in HHS30.

3.2.3. AC electrical conductivity

The AC electrical conductivity of the HHS30 melt as a function of temperature is shown in Fig. 5A. The AC conductivity at the melting temperature of 950°C is 100

$(\Omega m)^{-1}$ and is reproducible for heating and cooling. This melt conductivity at 950°C is ~2.5 times greater than the conductivity (42 $(\Omega m)^{-1}$) of the SBW-22-20 borosilicate melt (which contains 20% SBW) at its melting temperature of 1150°C [27] and is essentially the same as the conductivity (~100 $(\Omega m)^{-1}$ at 1000°C) [27] of the iron phosphate glasses containing 40 and 48% SBW.

As shown in Fig. 5B, the AC conductivity of the HHS30 melt obeys the Arrhenius equation and has an activation energy of 6.3 kcal/mol which is about half that for the SBW-22-20 borosilicate and the IP40WG (13.5 kcal/mol) from [27].

3.2.4. Thermal properties

The compositions of the HHS iron phosphate glasses in the present study are similar in composition and, therefore, it was expected that the thermal properties of these glasses would be similar. The thermal expansion coefficient for these iron phosphate glasses ranges from 144×10^{-7} °C^{-1} to 203×10^{-7} °C^{-1}, while the dilatometric softening point (T_d) ranges from 500 to 515°C and the transformation temperature (T_g) ranges from 450 to 475°C. Complete data are given in Table 3. TGA showed no weight change for any of the HHS glasses when heated to 800°C.

The DTA curves in Fig. 6 show the crystallization peaks are between 558 and 600°C for these glasses while T_g was between 460 and 472°C, which agrees well the T_g from the dilatometry measurements given in Table 3. All of the DTA samples were run in an identical fashion in an air atmosphere. It is unclear why the DTA curves are nearly identical for the HHS30 and HHS30CA, although the high sodium content may have overshadowed the change that substituting Al_2O_3 and CaF_2 for Fe_2O_3 would have on the melt. The HHS30M glass crystallized at a lower temperature and had a much broader exothermic peak. The HHS25 glass had a lower Na_2O content and therefore crystallized and melted at a slightly higher temperature, but the composition was very similar to the HHS30, therefore no large difference was expected.

3.2.5. XRD

The four annealed glasses that were studied in detail did not contain any detectable crystalline phases after annealing as shown by their XRD patterns in Fig. 7.

The XRD curves shown in Fig. 8 indicate that the most common phases found in the deliberately crystallized (heat-treated) samples were $NaFe(P_2O_7)$ and $Na_3Fe_2(PO_4)_3$ in the HHS30 and HHS25 samples, $Na_2Fe_2Al(PO_4)_3$ and $Na_3Fe_2(PO_4)_3$ in the HHS30M sample and $Al(PO_3)_3$ and $NaFe(P_2O_7)$ in the HHS30CA sample. With the exception of $Al(PO_3)_3$, all of the identified crystalline phases in these samples are either orthophosphates or pyrophosphates which have been noted as having good chemical durability in previous work [36].

By a simple calculation using the molar ratio of Na_2O, Fe_2O_3, Al_2O_3, and P_2O_5 in the iron phosphate HHS glasses a general indication of the amount of each identified crystalline phase in each sample was estimated. HHS30 could contain approximately 75 mol% $NaFe(P_2O_7)$ and 25 mol% $Na_3Fe_2(PO_4)_3$, however, approximately 50 mol% of the Na_2O is unaccounted for after the iron oxide is exhausted. HHS25 could contain approximately 50 mol% $NaFe(P_2O_7)$ and 50 mol% $Na_3Fe_2(PO_4)_3$ which leaves approximately 25 mol% of the Na_2O unaccounted for. HHS30M could contain 25 mol% $Na_2Fe_2Al(PO_4)_3$ and 75 mol% $Na_3Fe_2(PO_4)_3$ which accounts for all of the oxides in the calculation with the exception of 35 mol% of the Na_2O. HHS30CA could contain 50 mol% $Al(PO_3)_3$ and 50% $NaFe(P_2O_7)$ which leaves 50 mol% of the Na_2O unaccounted for.

Peaks which cannot be identified are denoted by "?" on Fig. 8, indicating that unidentified crystalline phases are present..

The HHS30-CCC sample (slow cooled at the simulated CCC rate) appeared to be completely crystallized, by visual inspection (optical microscope) of the sample. The crystallization was confirmed using SEM where it can be seen in Figs. 9 A and B that there are regions of large crystals as well as porosity in the sample. Other locations within the sample appeared similar; therefore the images shown are considered representative of the whole sample.

Micrographs for the heat-treated HHS30x sample are given in Figs. 9 C and D (at a higher magnification to show the structure) for comparison. The XRD patterns for these samples did not indicate any significant differences in the crystal phases present in the two samples. The HHS30-CCC pattern is shown in Fig. 8 to compare with the XRD patterns for the deliberately crystallized samples. A possible cause for the lower durability for the slow cooled (CCC) sample is that the voids that are evident in the SEM images may have created a larger surface area for chemical attack.

3.2.6. Mössbauer spectra

The results from the Mössbauer spectroscopy are given in Table 3 and typical spectra are plotted in Fig. 10. Compared to other iron phosphate glasses melted in air which usually contain 20% Fe(II) [24, 38, 39], there seems to be a low amount of Fe(II) in the iron phosphate glasses containing HHS (from 5 to 9% Fe(II)). The lower Fe(II) percentage in these glasses, however, is reasonable when compared with results for other iron phosphate glasses melted at temperatures below 1150°C (12% Fe(II)) [24] and for other iron phosphate glasses containing 40 wt% SBW (11% Fe(II)) [27]. The lower percentage of Fe(II) in the present glasses is attributed to the lower melting temperature used in the present study since lower melting temperatures are known [24] to favor Fe(III).

3.3. Chemical durability

3.3.1. Bulk dissolution rate (DR)

3.3.1.1. Glass samples

As shown in Fig. 11, the glassy wasteforms (solid lines) had a DR ranging from a low of 8.6×10^{-9} (HHS25) to a high of 5.1×10^{-8} g/cm^2/min (HHS30CA) after 7 days in water at 90°C. The chemical durability of the iron phosphate glass wasteforms in the

present study was as good as or better than that of EA glass, which had a DR of approximately 5.2×10^{-8} g/cm^2/min after 7 days in deionized water at 90°C. There is a general tendency for the DR to decrease with time which suggests a chemically protective layer forms on the samples. Complete data are given in Appendix B, Table B1.

The increase in pH of the DI water that occurred during the DR measurements is shown in Fig. 12. The pH change from the EA glass is given as a comparison. Note that the increase in pH for the iron phosphate glasses is smaller than that for the EA borosilicate glass, due to the buffering action of the phosphate glasses [26, 38]. Note that the pH of the water used to test the iron phosphate glasses did not exceeded 7.5. Complete data are given in Appendix B, Table B2.

3.3.1.2. Crystalline samples

The DR of the deliberately crystallized iron phosphate HHS wasteforms were also measured, and are shown by the dashed lines in Fig. 11. In general, the crystallized samples were not as durable as the corresponding glassy wasteform, the DR ranged from a low of 5.2×10^{-8} for HHS25x to a high of 6.3×10^{-7} g/cm^2/min for HHS30CAx after 7 days in water at 90°C. Complete data are given in Appendix B, Table B3. The DR of the slowly cooled HHS30-CCC sample was 1.5×10^{-5} after 7 days. This sample was so fragile at 7 days that the test was discontinued.

3.3.2. Product consistency test - powder dissolution rate

The PCT results for the iron phosphate glass wasteforms and selected borosilicate glass wasteforms are given in Table 4. The quantity of ions (normalized elemental mass release) such as Al, K, Na, and P released from the glassy wasteform was about 10 times less than the quantity (B, Li, Na, and Si) released from the EA borosilicate glass [40]. The total quantity of ions released from the iron phosphate glasses was less than the quantity released from the CVS-IS borosilicate glass, but ~2 times higher than the release

from the LD6-54-12 borosilicate glass produced at the Pacific Northwest National Laboratory [41]. All of the HHS glasses had normalized mass releases below 1g/m^2.

The common element that is present in the PCT analysis for both the borosilicate glass and the iron phosphate glass is sodium. As Table 4 shows, sodium had the highest release in every case for the iron phosphate glasses containing HHS as well as the borosilicate glasses. All of the HHS iron phosphate glasses had a sodium release of ≤1.04 g/L compared to the borosilicate EA release of 14.11 g/L. The sodium release for HHS30CA (0.41 g/m^2) is approximately 3 times lower than that for CVS-IS borosilicate glass (1.3 g/m^2), and is approximately the same as that released from the LD6-54-12 borosilicate glass (0.38 g/m^2).

It is unknown why the amount of K_2O released is as large as reported. A small amount of K found in the leachate from PCT and divided by the small percentage in the analyzed composition leads to an inflated normalized mass release number. Because the wt% of K_2O in the analyzed composition is below 1% it should be ignored in the analysis of these glasses [33], there is an improvement in the total mass release for the iron phosphate HHS glasses when the K release is omitted, see r_{total}-r_K in Table 4.

To compare the PCT results with the DR values described earlier, the dissolution rate of the powdered samples was determined from the total mass release (ΔW) of the powdered samples after a 7 day PCT using equation (2). A value of 30 cm^2 was estimated for the surface area of the powder using the equation in Appendix IX of ref [33]. As shown in Table 5, the dissolution rate calculated from PCT mass release is 2 to 8 times larger than the DR measured for the bulk glass samples. The higher pH values for the water from the PCT than from the DR measurement may account for the higher calculated dissolution rate, indicating that more ions are in solution. The bulk DR values can be used in a general way to estimate the mass release of a sample in the PCT.

The absence of any significant corrosion of the iron phosphate glass particles during the PCT was confirmed by SEM examination of their morphology. The appearance of uncorroded HHS30 particles is shown in Fig. 13A while the appearance of the HHS30 particles after the 7 day PCT is shown in Fig. 13B. There is no discernible difference in their appearance and the sharp corners and edges of the particles in Fig. 13B and the absence of any detectable corrosion layer on the surface indicate that this glass is

resistant to chemical attack by water. The HHS30M, HHS30CA and HHS25 PCT powders also appeared virtually identical with no noticeable corrosion.

3.4. Sulfur retention

Visual inspection of the melts each time they were stirred yielded no observable sulfate layer on the surface of any of the iron phosphate melts. Similarly, no sulfate droplets were detected in the glass, either by optical microscopy or SEM. Iron phosphate glasses were formed which contained >4.5wt% SO_3 after melting at 900°C for one hour. This was determined for a 50wt% HHS glass that had a SO_3 content of 4.75wt% in the batch. The measurement was performed by XRF using standards containing known amounts of sulfur. This SO_3 content agrees with previous work [19], where it was found that 5 wt% SO_3 was retained in iron phosphate glasses.

As shown in Fig. 14, sulfur has a tendency to volatilize from the melt as the melting temperature is increased. These glasses were heated at the specified temperature in an open crucible for 1 hour in air. Volatilization of sulfur from the melt is also seen in the HHS30 glass when it was held at a constant temperature (900°C) in air for up to 24 hours, see Fig. 15. Based on data Figs. 14 and 15, it is estimated that for melting temperatures of up to 950°C, the glass should retain ~50% of the SO_3 in the batch for a melting time of 2 hours.

The addition of 1 wt% sugar to make the batch more reducing caused a lower retention of sulfate, as shown by the open triangles in Figs. 14 and 15.

The DR (at 14 days in 90°C water) as a function of wt% sulfate in the glass is plotted in Fig. 16 for the HHS30 glasses melted at various temperatures and time (from Figs 14 and 15). These data suggest that the DR increases slightly with increasing sulfate content. However, the differences in melting conditions, especially at the higher temperature (1100°C) and longer melting times (20 to 24 hours) may also cause some change in DR. Nevertheless, the data are concluded to indicate that the DR probably depends upon the sulfate content of the glass. Complete data are given in Appendix C, Table C1.

4. Discussion

The present investigation of the iron phosphate glass wasteforms has identified several properties of iron phosphate glasses that are relevant to the vitrification of HHS at Hanford, WA.

4.1. Glass properties

The iron phosphate melts in the present study which contain HHS are fluid (<1 Pa·s) and can generally be melted at approximately 950°C with good results. This fluidity reduces the necessary melting time substantially, so that homogeneous glasses are achieved after melting times of one to two hours.

Low melting temperatures and shorter melting times lead to less expensive and safer melting and mean that smaller furnaces can be used to achieve the same output. This translates into significant savings both in energy consumed to melt the glass (lower melting temperature) and by smaller amounts of glass due to the higher wasteloading potential of the iron phosphate glasses. The lower melting temperature also leads to less attack of the refractories, allowing for longer furnace life.

An alternative technology for melting iron phosphate glasses is cold crucible induction melting (CCIM). The higher electrical conductivity (relative to borosilicate melts) of iron phosphate melts is beneficial for induction melting. The higher conductivity of the iron phosphate melt allows the melt to be more susceptible to the rf field of the melter. CCIM avoids potential problems with corrosion of refractories and electrodes because the glass serves as its own refractory and no metal electrodes are needed [3]. Iron phosphate glasses containing 40 to 48 wt% SBW have been successfully melted using CCIM technology [27]. Induction melting is still considered a backup technology due to the immaturity of the melters and power supplies, but it is a promising melter technology for iron phosphate waste glasses [3, 37].

4.2. Chemical durability

4.2.1. Composition

The PCT results indicate that the total quantity of all ions leached from the iron phosphate wasteforms (0.9 g/L for HHS30M) is ~50 times smaller than the total quantity of ions leached from the EA glass (46 g/L). All of the HHS30 glasses had mass releases below the conservative constraint of 1g/m^2 that has been quoted for good PCT durability [15, 32]. The DR for the iron phosphate glasses in the present study is slightly higher than the DR reported [37] for iron phosphate glasses containing the SBW (which contains 52.3 wt% soda) where a DR of 2×10^{-9} g/cm^2/min (16 days in 90°C water) was reported for a composition that had similar soda content (23 wt%) to the glasses in the present study.

The additives used in the HHS30M (2 wt% each of Bi_2O_3, CaF_2, CaO, PbO and ZnO) and HHS30CA (5% each of CaF_2 and Al_2O_3) did not have a large effect on the durability as measured by either DR or PCT. These additives lowered the PCT mass release (Table 4) and changed the phases that crystallized from the glass (Fig.8). The HHS30M glass had a lower DR than HHS30 glass in both its glassy and crystallized forms; however, the DR for the HHS30CA glass was higher in both cases (Fig. 11).

The durability of the iron phosphate glasses containing HHS decreased as the amount of waste in the glass increased, most likely due to the increasing soda content. A soda content of 22 to 24 wt% appears to be the limit for acceptable durability in these HHS iron phosphate glass wasteforms. This soda content agrees with work performed at Hanford, WA where iron phosphate glasses containing up to 24 wt% alkali (21 wt% Na_2O and 3 wt% K_2O) were found to have good durability (total PCT mass release of <2 g/m^2) [19].

The O/P ratio has been shown to be important to the chemical durability of iron phosphate glasses [26]. An O/P ratio of 3.5, which corresponds to the P_2O_7 pyrophosphate composition, seems to provide the best chemical durability [26, 36]. An increase in the O/P ratio toward the orthophosphate composition (O/P = 4.0) or a decrease in the O/P ratio toward the metaphosphate composition (O/P = 3.0) leads to an

increase in DR [26, 36]. The reduction in chemical durability is more significant when the O/P decreases from 3.5 than when it increases, indicating that orthophosphate compositions are more chemically durable than metaphosphate compositions [36].

The DR (14 days in 90°C DI water) is plotted in Fig. 17 as a function of the molar O/P ratio for iron phosphate glasses containing HHS. Results from previous studies are also given, these previous results include 20 to 40 wt% TFB waste (which contains 55 wt% Na_2O) [26], as well as NKFP and NCFP [37] (which contain 20 mol% alkali, 20 to 32 mol% Fe_2O_3 and 48 to 60 mol% P_2O_5), F40M [37] (containing 40wt% Fe_2O_3 and 60 wt% P_2O_5) and FCs17 [38] (which contains 29 wt% Fe_2O_3, 38 wt% P_2O_5, and 33 wt% Cs_2O). The general trend toward lower durability at O/P ratios above and below 3.5 is shown by the "V" shape of the shaded area in Fig. 17. It can be seen that the DR for HHS glasses in Fig. 17 falls in the same range as the DR for previous iron phosphate glasses with similar O/P ratios.

4.2.2. Effect of crystallization

The iron phosphate HHS glasses in the present study crystallized on slow cooling (<1°C/min) from the melt temperature causing the dissolution rate of the wasteform to increase by ~10 times. The DR of the crystallized samples exceeded that of the glassy samples and the DR of the EA glass as shown in Fig.11.

A decrease in durability with crystallization has been noted in other iron phosphate glasses containing between 11 and 25 wt% of Na_2O [26, 36, 37]. The durability decrease in these previous studies was smaller than that found for the HHS samples in the present study. The difference in durability noted in these previous studies was generally less than the 10 times increase in DR upon crystallization; there have been iron phosphate waste containing glasses which show almost no change or even decrease in DR with crystallization [31]. It is possible that the durability of the crystalline phases that formed from these glasses is lower than the phases that formed in previous studies.

In general, all of the compositions in Table 2 were good glass formers, as illustrated by the XRD patterns in Fig. 7, where no crystalline phases were detectable in the annealed samples.

The compounds that crystallized from the glasses, shown in Fig. 8, correlate well with the Mössbauer results, which indicate that all of the glasses containing 30 wt% HHS in the present study contain from 5 to 9% Fe(II). Iron is in the Fe(III) state in $NaFe(P_2O_7)$ and $Na_3Fe_2(PO_4)_3$, which are the major phases found in the HHS30 and HHS25 samples. HHS30M has some $Na_2Fe_2Al(PO_4)_3$ where the iron is present as Fe(II), but from previous calculations this appears to be the lower concentration compound while $Na_3Fe_2(PO_4)_3$ is at a higher percentage in the HHS30M sample. The crystalline phase containing iron that crystallized from the HHS30CA glass was $NaFe(P_2O_7)$, also confirmed by Mössbauer.

The higher DR of the crystallized samples is possibly a result of the reduced chemical durability of the remaining glass after the crystalline phase forms. Iron is the limiting element for most of the crystal phases that formed, therefore the glass that remains in the samples after crystallization will contain a majority of sodium and phosphorus which is more susceptible to chemical attack by water.

There is a difference between the structures of the samples that were heat-treated at 570°C and the one that was cooled using the simulated CCC rate. The HHS30-CCC sample appeared to contain more internal voids in its structure compared to the heat-treated sample (HHS30x). This structural difference is a possible reason for the lower chemical durability of the CCC sample, because these voids could provide a larger surface area for chemical attack by the water. Analysis by XRD did not reveal any major difference between the crystalline phases present in these samples; however, the peak intensity differences indicate that the phases are present in different concentrations.

4.3. Sulfate retention

Iron phosphate glasses (containing 50 wt% HHS) were made that contained >4.5 wt% SO_3. This glass was melted at 900°C for 1 hour, and retained approximately 90% of the SO_3 in the batch. The high sulfate solubility of phosphate glasses is related to the P_2O_5 content of the glass. It has been reported that increasing the P_2O_5 content in a silicate glass increases the solubility of sulfur [11, 13, 42].

The fact that iron phosphate glasses containing SBW can be melted at only 950°C is beneficial for retaining the sulfate in the melt. The sulfate retention of the glass is reduced as the melting temperature is increased. Below 1000°C and 2 hour melting time, more than 50% of the sulfate is retained on average; when melted at 1100°C for 1 hour, less than 10% of the sulfate remains in the glass on average. The retention at 1100°C agrees with previous results where it was reported that no sulfate was retained in an iron phosphate glass melted at 1106°C for 10 hours [10]. Under these conditions only a small fraction of the sulfate would be expected to be retained, as the solubility of sulfate decreases with increasing temperature [43].

4.4. Iron phosphate glass for vitrifying HHS

Based on the properties of the iron phosphate glasses that were measured in the present study (waste loading, chemical durability, melting temperature, and electrical conductivity), it appears that iron phosphate glasses are good potential host materials for HHS. The iron phosphate glasses in the present study had no observable sulfur layer at the surface of the melt, as has been noted to be a problem in borosilicate melts that contain large amounts of sulfur.

It appears that the amount of soda in the waste composition is the limiting factor for vitrification of HHS in iron phosphate glasses. As mentioned previously, once the waste loading reached ~23 wt% Na_2O in the glass, the durability decreased substantially.

Based on the solubility limits for SO_3 and P_2O_5 in borosilicate glass (1 wt% each [6, 8-14]), and the sulfur and phosphorus content of the HHS waste (9.5 wt% SO_3, and 7.7 wt% P_2O_5), a wasteloading of approximately 10% is expected for borosilicate glasses without preprocessing of the waste to lower these concentrations. Assuming that the waste will not be processed before vitrification, then the iron phosphate glasses studied here provide a three-fold increase in vitrified waste per unit of glass. Or, in other words, there would be only one third as much waste glass when vitrification is completed if iron phosphate glasses are used.

Assuming a 25% wasteloading for the iron phosphate glasses, there would only be 200,000 tons of wasteform as opposed to the estimated 500,000 tons of borosilicate

wasteform [3, 4]. In terms of volume, the iron phosphate wasteform would occupy 60,000 m^3 based on a density of 2.9 g/cm^3, whereas the borosilicate waste form would occupy 170,000 m^3 based on a 2.7 g/cm^3 density. Assuming the cost of disposal of this low level waste glass containing HHS is $5,000 per m^3 [44], then there is a potential for savings of $550 million in disposal costs alone due to the smaller volume of waste glass. A smaller volume of waste glass would contribute to lower transportation costs as well as lower construction costs for the waste repository.

5. Conclusions

The HHS waste from Hanford can be vitrified in an iron phosphate glass at wasteloadings up to 30% with a PCT chemical durability that meets DOE requirements, <1 g/m^2 mass release. Because of their low viscosity and rapid homogenization, melting times need only be approximately two hours.

The wasteloading in iron phosphate glasses was limited by the amount of soda in the waste stream, as opposed to the high sulfur content which limits the waste loading in borosilicate glasses. The soda content does not have a negative impact on the durability of the glass until the glass contains about 23 wt% soda.

The vitrification of high sulfate wastes in iron phosphate glasses offers an attractive alternative to either reducing the level of sulfate by chemical pretreatment of the waste or diluting the waste to acceptable levels for a borosilicate glass wasteform, creating large additional volumes of waste that must be stored. No evidence was found which indicated solubility or phase separation problems with high sulfate contents. There is a possibility, however, that increasing levels of sulfate may reduce the durability of the iron phosphate glass.

The iron phosphate glasses in the present study tended to crystallize on slow cooling from the melt temperature and the crystallized wasteform had a lower chemical durability than the glass wasteform. Crystallization must be avoided to ensure highest possible chemical durability. Two possible ways of avoiding crystallization is to change the composition to reduce the rate of crystallization or to cool the melt rapidly after melting.

Alternative melting technologies such as cold crucible induction melting (CCIM) could be utilized which could melt the glass without the need for electrodes in the glass melt, or refractories lining the melt tank.

More work is needed to determine additives that will reduce the crystallization tendency in slowly cooled iron phosphate glasses containing HHS. From the present study it appears that adding a variety of components to the batch in order to complicate the structure increases the chemical durability, but more work to determine a more optimized additive group should be undertaken. Further investigation of CCIM as a

potential melt technology for iron phosphate waste glasses should also be a priority. More testing is necessary to determine the effect of increasing sulfate content on the chemical durability of iron phosphate glasses.

References

[1] R.E. Gephart, R.E. Lundgren, Hanford Tank Clean Up: A Guide to Understanding the Technical Issues PNL-10773, Pacific Northwest Laboratory, 1996.

[2] R.L. Murray, Understanding Radioactive Waste, 4th ed., Battelle Press, Columbus, OH, 1994.

[3] E.T. Webber, R.B. Calmus, C.N. Wilson, Vitrification Technology for Hanford Site Tank Waste CONF-950401-35, Westinghouse Hanford Company, 1995.

[4] F.M. Mann, R.J. Puigh, E.J. Freeman, S.H. Finfrock, D.H. Bacon, M.P. Bergeron, B.P. McGrail, S.K. Wurstner, White Paper Updating Conclusions of 1998 ILAW Performance Assessment, DOE/ORP-2000-07 Rev. 0, PNNL, Fluor Federal Services, 2000.

[5] F. Chen, D.E. Day, Corrosion of Selected Refractories by Iron Phosphate Melts, The American Ceramic Society, Cincinnati, OH, 1999.

[6] H. Li, M.H. Langowski, P. Hrma, Segregation of Sulfate and Phosphate in the Vitrification of High-level Wastes, in Environmental Issues and Waste Management in the Ceramic and Nuclear Industries, The American Ceramic Society, Cincinnati, OH, 1995.

[7] S.S. Fu, K.S. Matlack, R.K. Mohr, W. Luo, E. Wang, M. Leontiev, H. Hojaji, M. Brandys, I.L. Pegg, P.B. Macedo, Minimelter Runs of Mixed Wastes High in Lead, Barium, Phosphorus, and Sulfur, in Environmental Issues and Waste Management Technologies II, The American Ceramic Society, Indianapolis, IN, 1996.

[8] S.N. Crichton, T.J. Barbieri, M. Tomozawa, Solubility Limits for Troublesome Components in a Simulated Low Level Nuclear Waste Glass, in Environmental Issues and Waste Management in the Ceramic and Nuclear Industries, The American Ceramic Society, Cincinnati, OH, 1995.

[9] X. Feng, M.J. Schweiger, H. Li, M. Gong, Retention of sulfur, phosphorus, chlorine, and fluorine in Hanford Phase II vendor LLW glasses, in Proceedings of the International Topical Meeting on Nuclear and Hazardous Waste Management, American Nuclear Society, Seattle, WA, 1996.

[10] W.K. Kot, H. Gan, I.L. Pegg, Sulfur Incorporations in Waste Glass Melts of Various Compositions, in Environmental Issues and Waste Management Technologies V, The American Ceramic Society, St. Louis, MO, 1999.

[11] H. Li, P. Hrma, J.D. Vienna, Sulfate Retention and Segregation in Simulated Radioactive Waste Borosilicate Glasses, in Environmental Issues and Waste Management Technologies VI, The American Ceramic Society, St. Louis, MO, 2001.

[12] H.D. Schreiber, C.W. Schreiber, E.D. Sisk, S.J. Kozak, Sulfur Systematics in Model Glass Compositions from West Valley, in Environmental and Waste Management Issues in the Ceramic Industry II, The American Ceramic Society, Indianapolis, IN, 1994.

[13] G.K. Sullivan, Sulfate Segregation in Vitrification of Simulated Hanford Nuclear Waste, The American Ceramic Society, in Environmental Issues and Waste Management Technologies in the Ceramic and Nuclear Industries, Cincinnati, OH, 1995.

[14] F.V. Tooley, The Handbook of Glass Manufacture, Ashlee Publishing, New York, 1984.

[15] D.K. Peeler, T.B. Edwards, I.A. Reamer, R.J. Workman, J.D. Vienna, J.V. Crum, M.J. Schweiger, Glass Formulation Development for INEEL Sodium-Bearing Waste (FY2001 WM-180), Savannah River Technology Center, 2001.
[16] J. Ahearne, J.A. Gentilucci, D. Pye, E.T. Webber, F.E. Woolley, High-level Waste Melter Review Report, TFA-0108, DOE, 2001.
[17] C.M. Jantzen, J. Non-Cryst. Solids 84 (1986) 215.
[18] J. J. M. Perez, D.F. Bickford, D.E. Day, D.S. Kim, S.L. Lambert, S.L. Marra, D.K. Peeler, D.M. Strachan, M.B. Triplett, J.D. Vienna, R.S. Wittman, High-level waste melter study report, DOE, 2001.
[19] D.S. Kim, J.D. Vienna, P. Hrma, N.J. Cassingham Phosphate glasses for vitrification of wastes with high sulfur content, 2002.
[20] B.C. Sales, L.A. Boatner, Lead-iron phosphate glass, in: W. Lutze, R.C. Ewing (Eds.), Radioactive Waste Forms for the Future, Elsevier Science Publisher, North-Holland, Amsterdam, 1988.
[21] M.G. Mesko, D.E. Day, J. Nucl. Mater. 273 (1999) 27.
[22] A. Mogus-Milankovic, B. Pivac, K. Furic, D.E. Day, Phys. Chem. Glasses 38 (1997) 74.
[23] G.K. Marasinghe, M. Karabulut, C.S. Ray, D.E. Day, C.H. Booth, P.G. Allen, D.K. Shuh, Redox Characteristics and Structural Properties of Iron Phosphate Glasses: A Potential Host Matrix for Vitrifying High Level Nuclear Waste, in Environmental Issues and Waste Management Technologies III, The American Ceramic Society, Cincinnati, OH, 1998.
[24] C.S. Ray, X. Fang, M. Karabulut, G.K. Marasinghe, D.E. Day, J. Non-Cryst. Solids 249 (1999) 1.
[25] M.G. Mesko, D.E. Day, B.C. Bunker, Waste Management 20 (2000) 271.
[26] D.E. Day, Z. Wu, C.S. Ray, P. Hrma, J. Non-Cryst. Solids 241 (1998) 1.
[27] C.W. Kim, D.E. Day, C.S. Ray, D. Zhu, D. Gombert, A. Aloy, A. Mogus-Milankovic, M. Karabulut, J. Nucl. Mater. (to be published)
[28] J.D. Vienna, Hanford LAW Composition, Edited by D.E. Day, 2001.
[29] D.E. Day, Iron Phosphate Glasses: An Alternative for Vitrifying Certain Nuclear Wastes, University of Missouri - Rolla, 2000.
[30] J.E. Shelby, Introduction to Glass Science and Technology, 1st ed., The Royal Society of Chemistry, Cambridge, UK, 1997.
[31] M.G. Mesko, D.E. Day, B.C. Bunker, Immobilization of High-level Radioactive Sludges in Iron Phosphate Glass, in The American Chemical Society Symposium on Science and Technology for Disposal of Radioactive Tank Wastes, Plenum Press, Las Vegas, NV, 1998.
[32] J.V. Crum, J.D. Vienna, D.K. Peeler, I.A. Reamer, Formulation Efforts for Direct Vitrification of INEEL Blend Calcine Waste Simulate: Fiscal Year 2000, PNNL-13483, Pacific Northwest National Laboratory, 2001.
[33] ASTM, Standard test methods for determining chemical durability of nuclear waste glasses: The Product Consistency Test (PCT), in, ASTM Standards, Vol. C 1285-94, 1998.
[34] W.L. Ebert, N.L. Dietz, M.A. Lewis, P.L. Johnson, B.S. Tani, Long-term and Accelerated Testing of Hanford Low-activity Waste Glasses: Data Report for Fiscal

Year 2001, ANL FY2001 Annual Letter Report, Argonne National Laboratory, 2001.
[35] A. Mogus-Milankovic, A. Gajovic, A. Santic, D.E. Day, J. Non-Cryst. Solids 289 (2001) 204.
[36] X. Fang, C.S. Ray, G.K. Marasinghe, D.E. Day, J. Non-Cryst. Solids 263&264 (2000) 293.
[37] C.W. Kim, D. Zhu, D.E. Day, D. Gombert, Ceramic Transactions (in press)
[38] X. Yu, D.E. Day, G.J. Long, R.K. Brow, J. Non-Cryst. Solids 215 (1997) 21.
[39] G.K. Marasinghe, M. Karabulut, C.S. Ray, D.E. Day, M.G. Shumsky, W.B. Yelon, C.H. Booth, P.G. Allen, D.K. Shuh, J. Non-Cryst. Solids 222 (1997) 144.
[40] C.M. Jantzen, N.E. Bibler, D.C. Beam, C.I. Crawford, M.A. Pickett, Characterization of the Defense Waste Processing Facility (DWPF) Environmental Assessment (EA) Glass Standard Reference Material (U), WSRC-TR-92-346, Westinghouse Savannah River Company, 1993.
[41] P.R. Hrma, G.F. Piepel, M.J. Schweiger, D.E. Smith, D.S. Kim, P.E. Redgate, J.D. Vienna, C.A. LoPresti, D.B. Simpson, D.K. Peeler, M.H. Langowski, Property Composition Relationships for Hanford High-Level Waste Glasses Melting at 1150C, PNL-10359, Pacific Northwest Laboratory, 1994.
[42] H. Gan, I. Muller, L. Goloski, I. Pegg, Sulfate Solubility in Glasses for Hanford Low Activity Wastes, International Congress on Glass, Edinburgh, Scotland, 2001.
[43] M. Ooura, T. Hanada, Glass Tech. 39(2) (1998) 68.
[44] C.A. Judd, Statement of Charles A. Judd President, Envirocare of Utah, Inc. before the subcommittee on strategic forces committee on armed services United States Senate. http://www.senate.gov/~armed_services/statemnt/980903cj.htm, 1998.

Table 1
Hanford high sulfate waste composition, simplified composition and raw materials used.

Oxide	Original Wt%	Simplified Wt%	Raw Materials	Weight* (g)
Al_2O_3	4.39	4.4	Al_2O_3	4.4
Bi_2O_3	0.02	---	---	---
CaO	0.09	---	---	---
Cl	0.59	0.6	NaCl	1.0
Cr_2O_3	0.29	0.4	Cr_2O_3	0.4
F	1.59	1.6	NaF	3.5
Fe_2O_3	0.08	---	---	---
K_2O	0.49	---	---	---
Na_2O	74.80	75.3	$NaNO_3$	177.7
NiO	0.01	---	---	---
P_2O_5	7.68	7.7	$NH_4H_2PO_4$	12.5
PbO	0.01	---	---	---
SeO_2	0.01	---	---	---
SiO_2	0.50	0.5	SiO_2	0.5
SO_3	9.45	9.5	Na_2SO_4	16.9
Total	100	100	Total	216.9

* Batch yielding 100 grams of waste

Table 2
Batch and analyzed compositions, in weight percent, of four iron phosphate glasses that were studied in detail. The analyzed compositions were determined by ICP-ES.

	HHS30		**HHS30CA**		**HHS30M**		**HHS25**	
	Batch	ICP	Batch	ICP	Batch	ICP	Batch	ICP
Al_2O_3	1.32	3.43	6.32	10.16	1.32	4.33	1.10	1.97
Bi_2O_3	---	---	---	---	2.00	**	---	---
CaO	---	0.01	---	3.14	2.00	3.64	---	0.03
CaF_2*	---	---	5.00	---	2.00	---	---	---
Cl	0.18	---	0.18	---	0.18	---	0.15	---
Cr_2O_3	0.12	0.10	0.12	0.10	0.12	0.09	0.10	0.10
F	0.48	---	0.48	---	0.48	---	0.40	---
Fe_2O_3	20.00	19.01	10.00	13.60	20.00	21.40	25.00	24.16
K_2O	---	0.23	---	0.15	---	0.21	---	0.37
MgO	---	0.04	---	0.04	---	0.06	---	0.05
MnO	---	0.04	---	0.03	---	0.05	---	0.04
Na_2O	22.59	21.23	22.59	21.87	22.59	21.98	18.83	18.4
P_2O_5	52.31	55.26	52.31	49.98	42.31	46.29	51.91	53.52
PbO	---	---	---	---	2.00	**	---	---
SiO_2	0.15	0.18	0.15	0.34	0.15	0.18	0.13	0.83
SO_3	2.85	**	2.85	**	2.85	**	2.38	**
ZnO	---	---	---	---	2.00	**	---	---
Total	100	99.6	100	99.4	100	98.3	100	99.5
O/P Ratio	3.71	3.57	3.58	3.93	3.68	3.87	3.73	3.63
Fe/P Ratio	0.34	0.31	0.17	0.24	0.42	0.41	0.43	0.40

* The calcium from the calcium fluoride is included in the calcium oxide value measured by ICP-ES.
** Not detected by ICP-ES method used.

Table 3
Properties of iron phosphate glasses containing HHS waste.

Property		HHS30	HHS30CA	HHS30M	HHS25
Density ±0.05 g/cm^3		2.85	2.75	3.14	2.90
Average CTE (100-375°C) C^{-1}		157×10^{-7}	159×10^{-7}	203×10^{-7}	144×10^{-7}
Dilatometric and DTA Transformation Temp (T_g, °C) ±5°C		475 (455)*	450 (460)*	460 (470)*	470 (472)*
Dilatometric Softening Point (T_d, °C) ±5°C		515	500	505	513
DTA Crystallization (T_x, °C) ±5°C		583	584	558	598
Melting Temperature (°C) ±10°C		950	950	950	950
Annealing Temperature (°C) ±5°C		400	400	400	400
Mössbauer Hyperfine Parameters					
Isomer Shifts, δ (±0.05 mm/s)	Fe(II)	1.07	1.13	1.10	NM**
	Fe(III)	0.43	0.43	0.42	NM**
Quadrupole Splitting, ΔE_Q (±0.05 mm/s)	Fe(II)	2.34	2.18	2.39	NM**
	Fe(III)	0.79	0.78	0.81	NM**
% Fe(II)		9%	5%	5%	NM**

*(DTA value)
**NM = not measured

Table 4
Normalized mass release (PCT) from glassy iron phosphate wasteforms containing 25 and 30 wt% HHS.

Iron Phosphate Glasses Containing HHS

Normalized mass release (g/L)	HHS25	HHS30	HHS30CA	HHS30M
r_{Al}	0.04	0.09	0.23	0.09
r_K	0.35	0.07	0.05	0.07
r_{Na}	1.04	0.97	0.76	0.80
r_P	0.37	0.29	0.24	0.13
r_{total}	1.80	1.42	1.28	1.09
r_{total}-r_K	1.45	1.35	1.05	1.02
Normalized mass release (g/m^2)	HHS25	HHS30	HHS30CA	HHS30M
r_{Al}	0.02	0.05	0.12	0.05
r_K	0.03	0.03	0.02	0.04
r_{Na}	0.55	0.51	0.41	0.42
r_P	0.19	0.15	0.13	0.08
r_{total}	0.89	0.74	0.68	0.59
r_{total}-r_K	0.86	0.71	0.66	0.55
Initial pH (±0.1)	6.1	5.6	6.1	5.6
Final pH (±0.1)	7.4	7.6	9.1	8.7

Borosilicate Glasses

Normalized mass release (g/m^2)	CVS-IS*	LD6-54-12*	Normalized mass release (g/L)	EA**
r_B	1.7	0.11	r_B	17.38
r_{Li}	1.4	-----	r_{Li}	10.18
r_{Na}	1.3	0.38	r_{Na}	14.11
r_{Si}	0.4	0.10	r_{Si}	4.29
r_{total}	4.8	0.59	r_{total}	45.96
Initial pH	5.9	5.7	Initial pH	5.7
Final pH	10.3	11.4	Final pH	11.9

*CVS-IS and LD6-54-12 are borosilicate glasses made by PNNL [41].
**Average data for EA glasses produced at the Savannah River Site [40].

Table 5
Dissolution rate measured on bulk glass and crystallized samples and calculated from the PCT total mass release.

Dissolution rate ($g/cm^2/min$)*	HHS25	HHS30	HHS30CA	HHS30M
Calculated from PCT, glass powder	7.2×10^{-8}	6.7×10^{-8}	5.4×10^{-8}	5.2×10^{-8}
Measured, Bulk - Glass	8.6×10^{-9}	1.6×10^{-8}	5.1×10^{-8}	1.1×10^{-8}
Measured, Bulk - Crystallized	5.0×10^{-8}	6.2×10^{-7}	2.3×10^{-7}	2.0×10^{-7}
Measured, bulk CCC	-----	1.5×10^{-5}	-----	-----

* 7 days in DI water @ 90°C

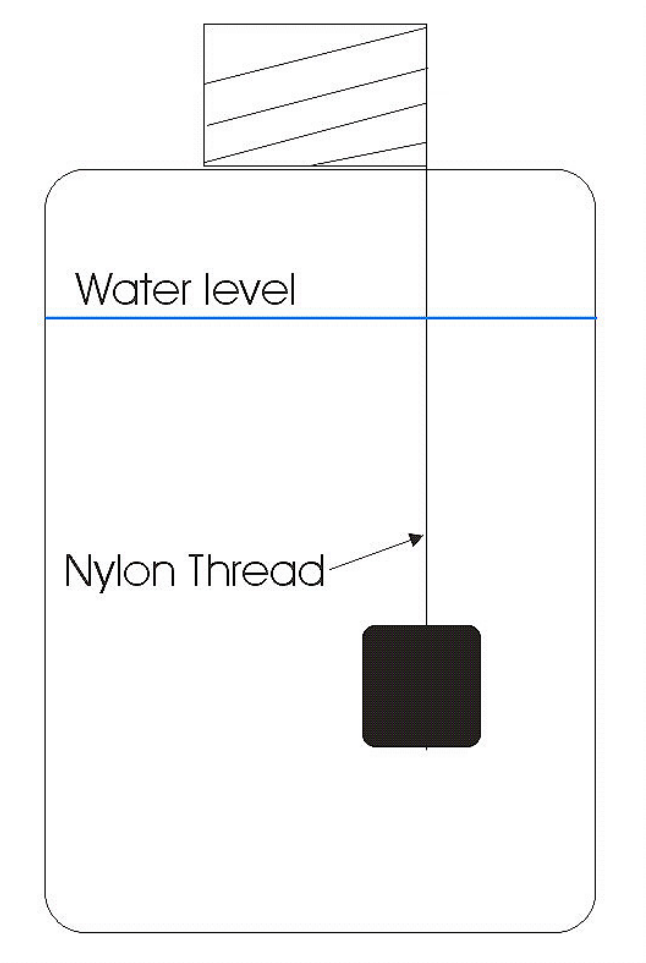

Fig. 1. Schematic of bulk durability device.

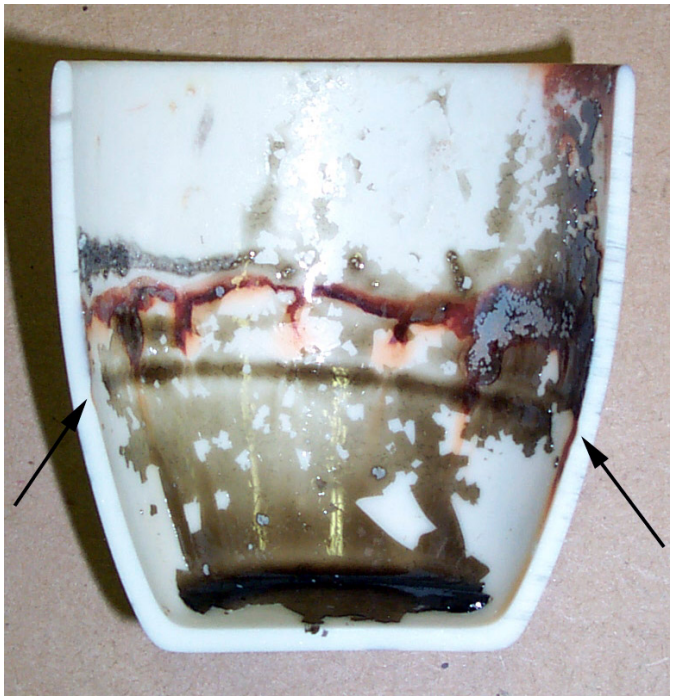

Fig. 2. Appearance of the cross section of a dense alumina crucible used to melt iron phosphate HHS30 for 2 hours at 950°C. The corrosion at the melt-line (indicated by the arrows) was approximately 220μm deep (optical microscopy).

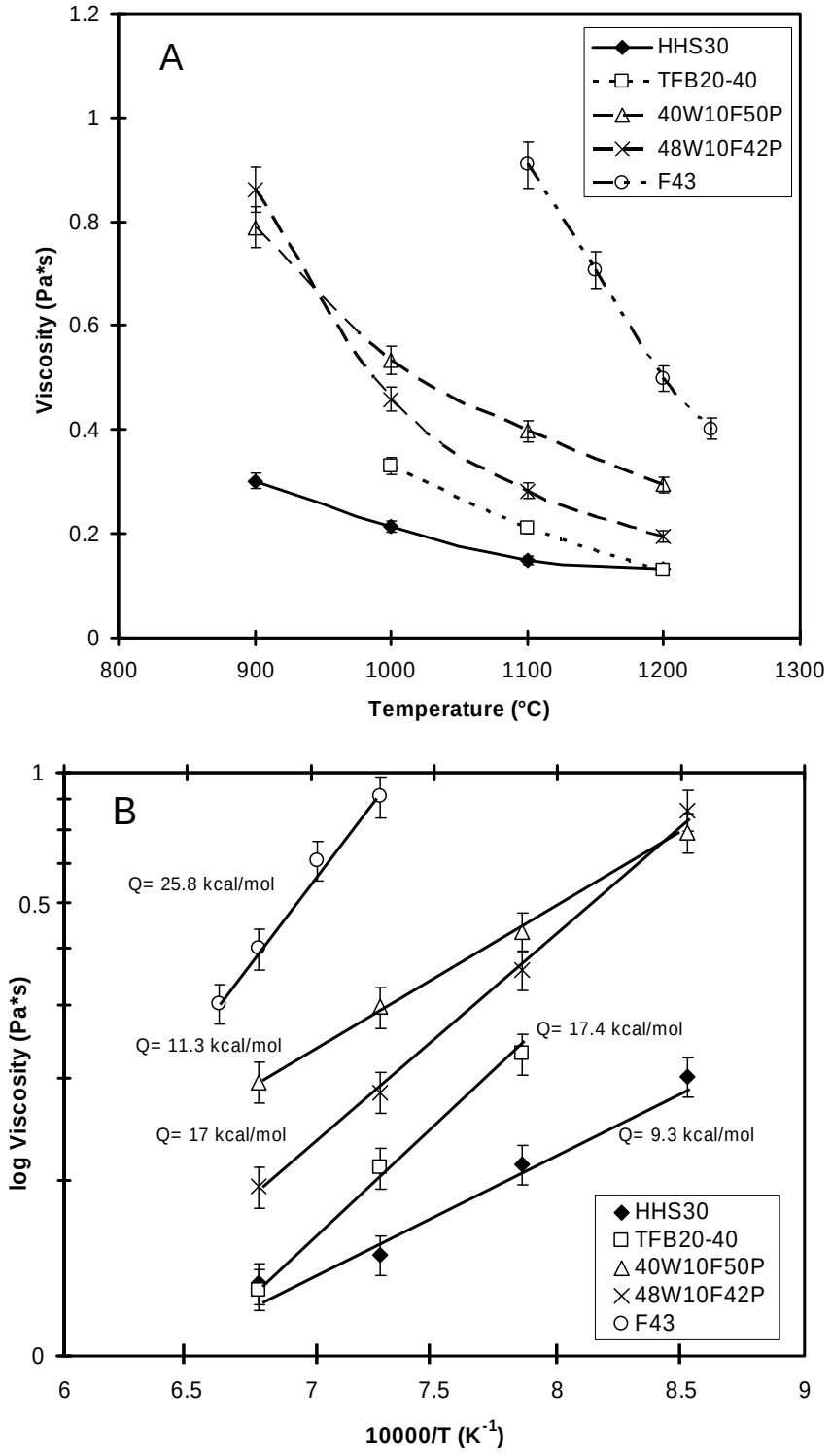

Fig. 3. A) Viscosity vs temperature for HHS30 melts compared with iron phosphate melts from refs [26, 37]. The comparison iron phosphate melts contained from 12 to 26 wt% Na_2O, except for the alkali-free F43 which contained 43 wt% Fe_2O_3 and 57 wt% P_2O_5.

B) log viscosity as a function of 10000/T. The activation energy for viscous flow is given for each composition.

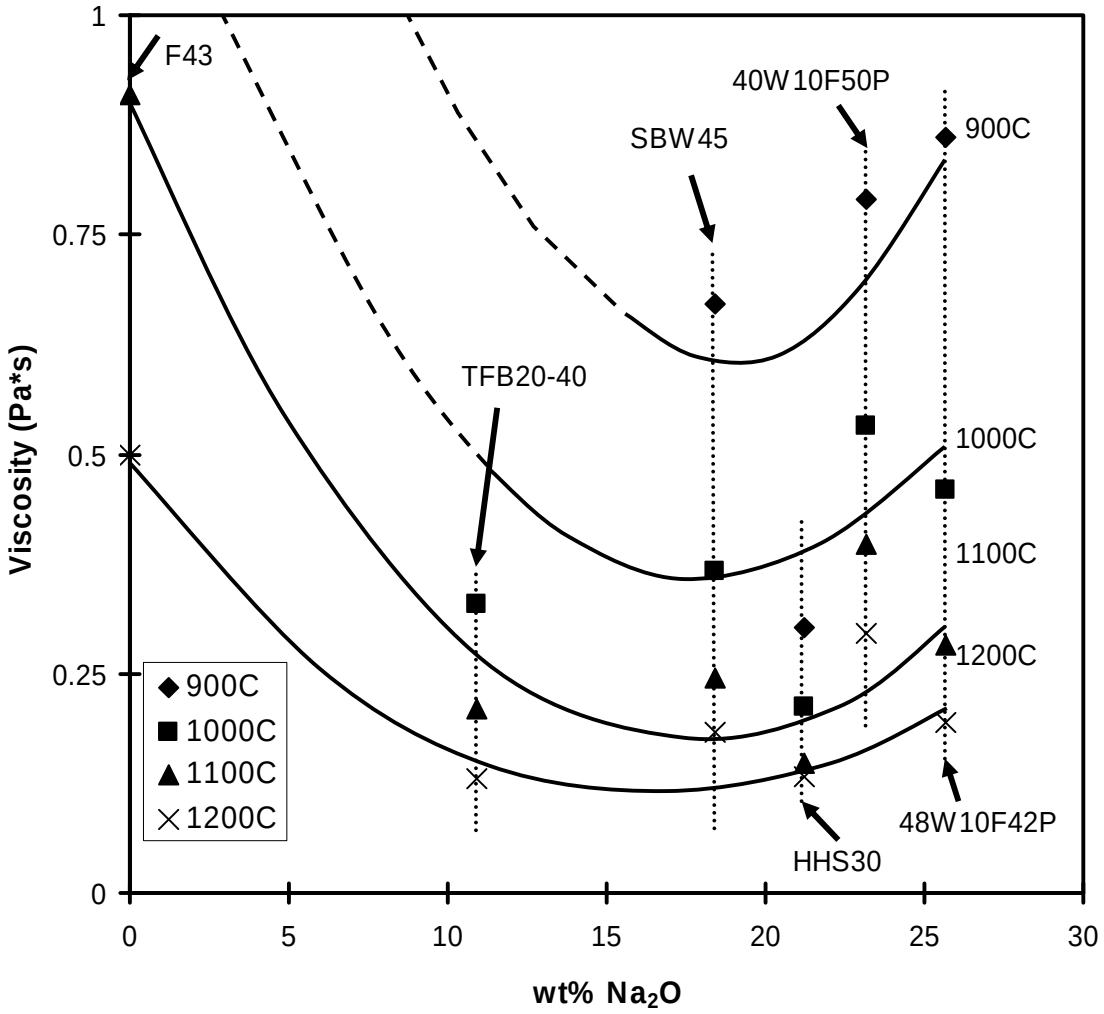

Fig. 4. Melt viscosity as a function of wt% Na_2O in iron phosphate glasses. No data was available for 900°C for TFB20-40 or 900°C and 1000°C for F43, therefore, the dashed lines are estimates only.

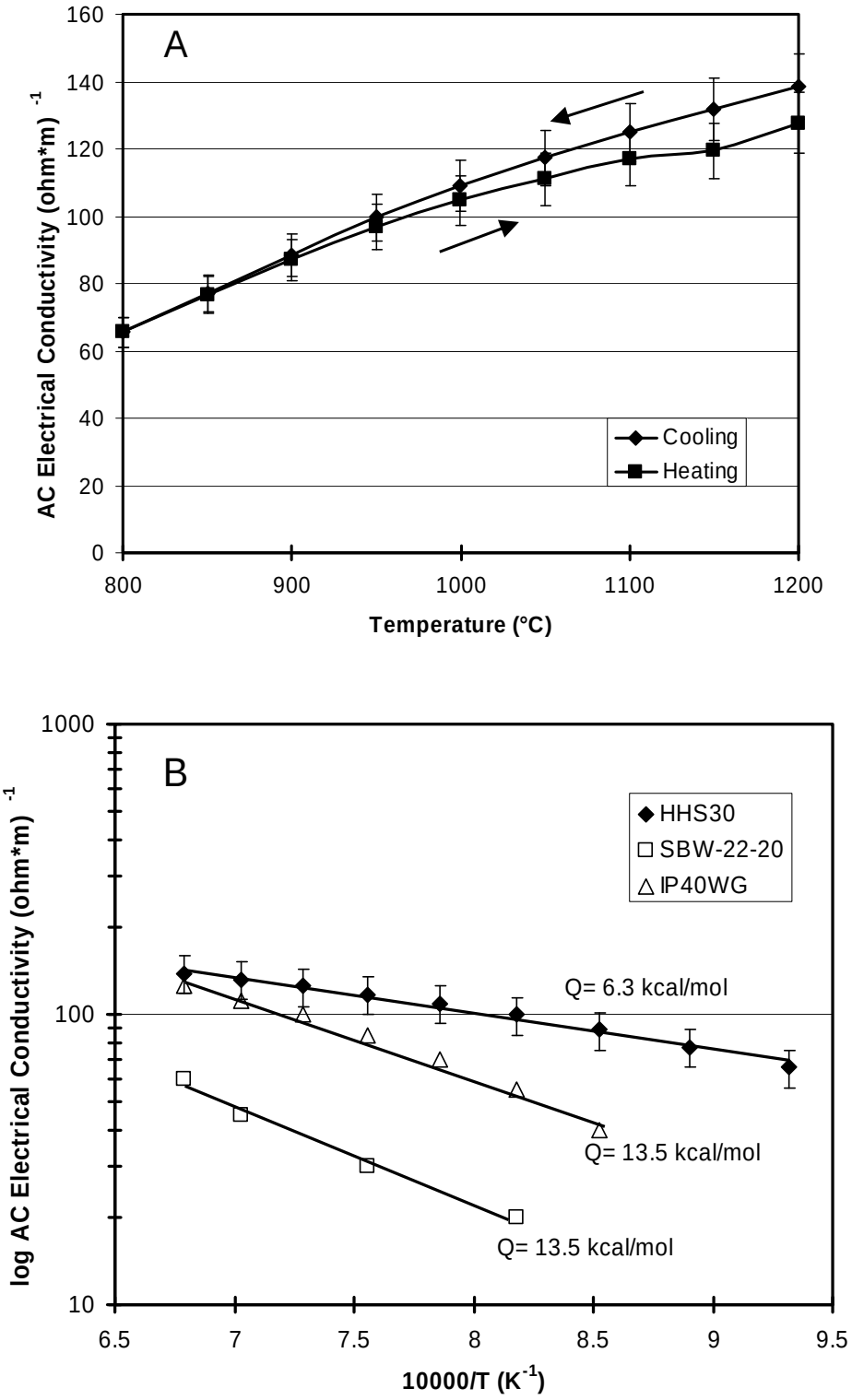

Fig. 5. A) AC electrical conductivity as a function of temperature for the iron phosphate HHS30 melt on heating and cooling.

B) Plot of log AC electrical conductivity vs 10000/T for HHS30 compared with IP40WG iron phosphate glass and borosilicate glass SBW22-20 [26, 37].

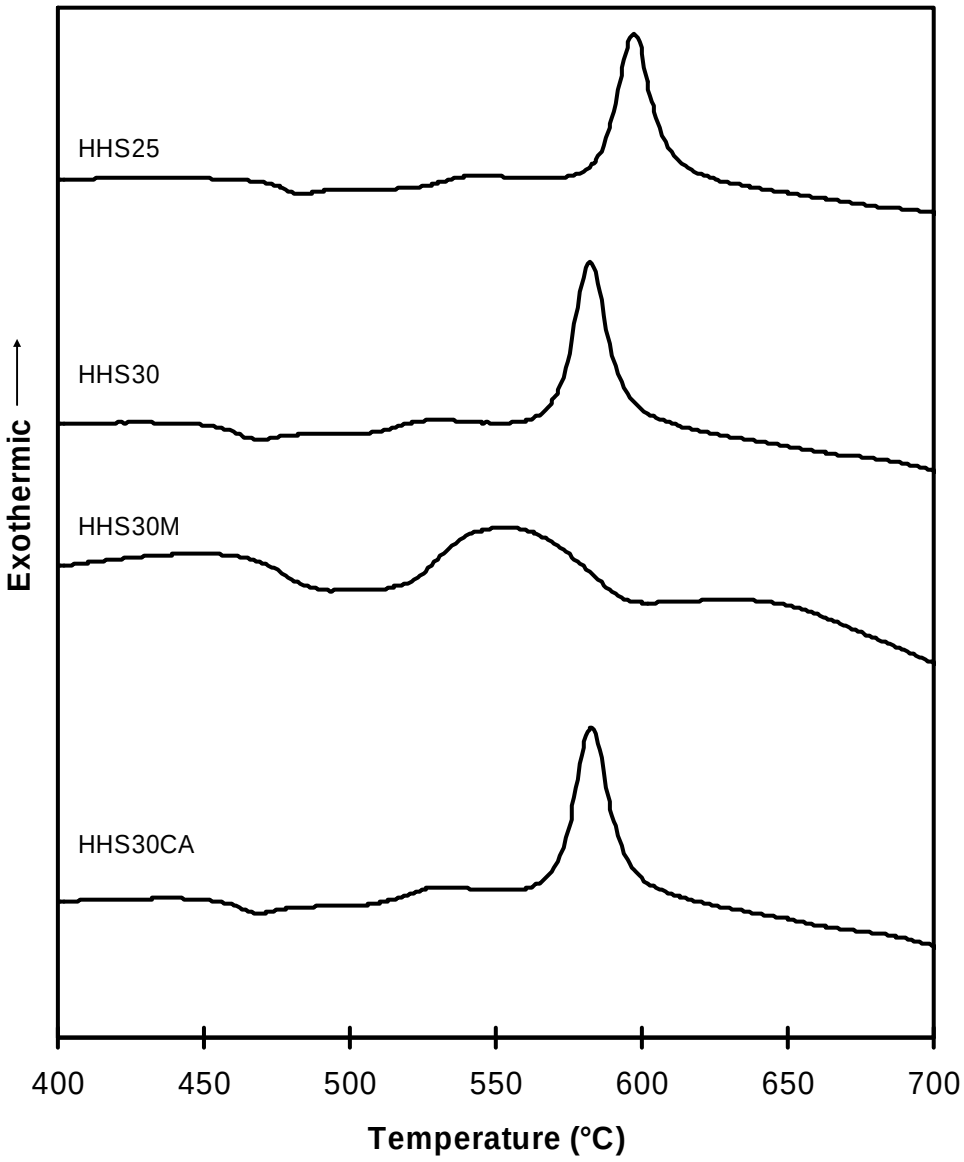

Fig. 6. Differential Thermal Analysis (DTA) of the HHS glasses measured at a heating rate of 10°C/min in air atmosphere.

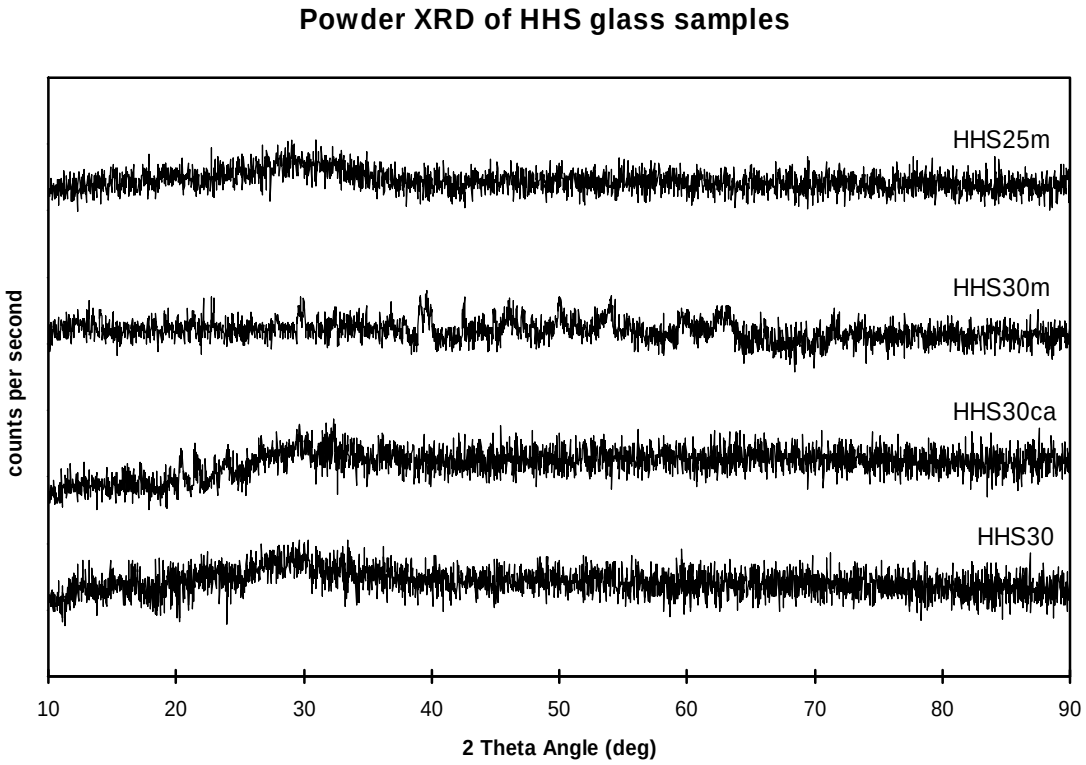

Fig. 7. Powder XRD patterns for iron phosphate glasses containing HHS waste after annealing at 400°C.

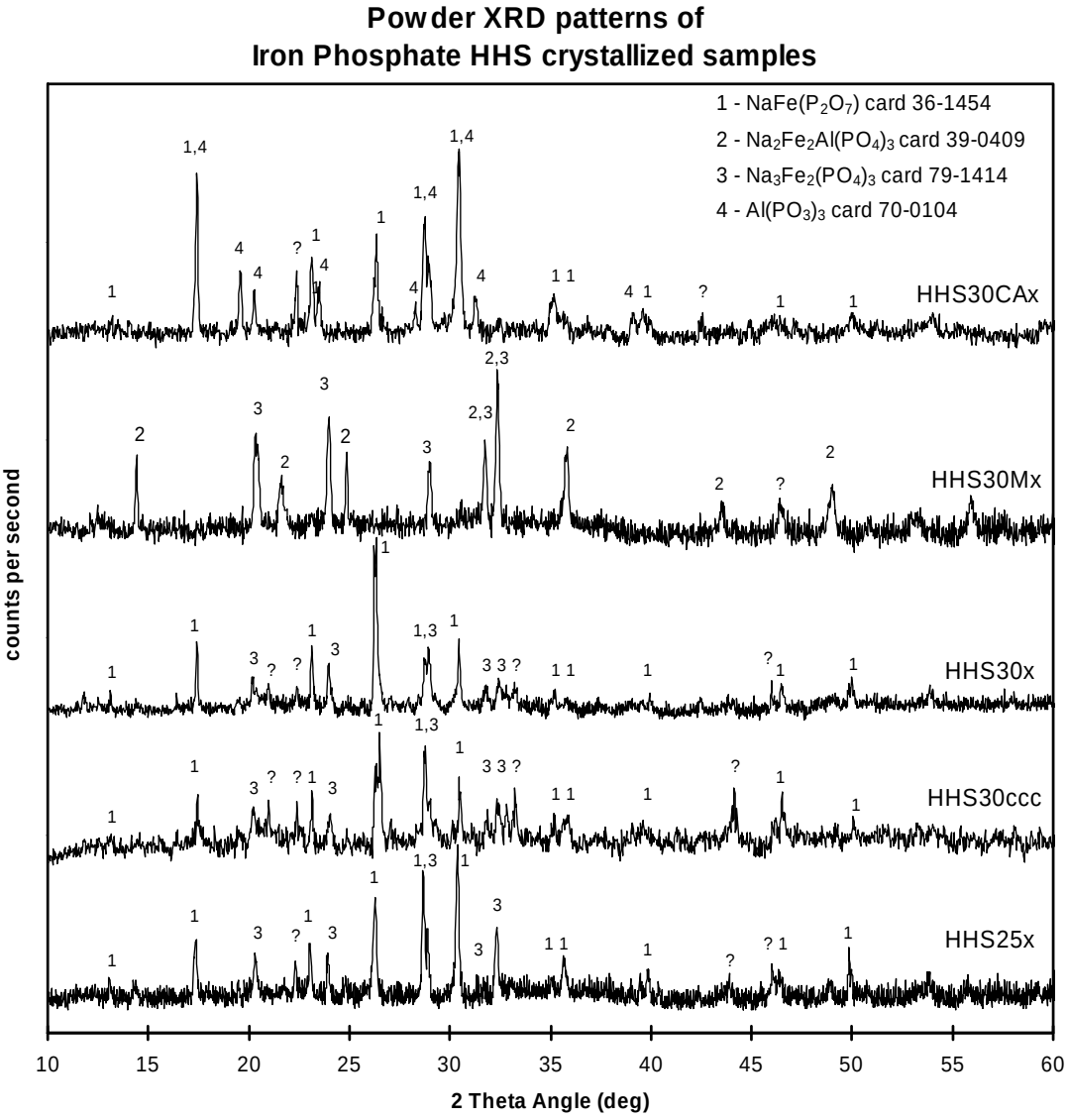

Fig. 8. Powder XRD patterns for iron phosphate HHS waste forms deliberately crystallized (24 hours at 560 to 580°C) and for the HHS30 melt that was slowly cooled from its melting temperature of 950°C (HHS30-CCC).

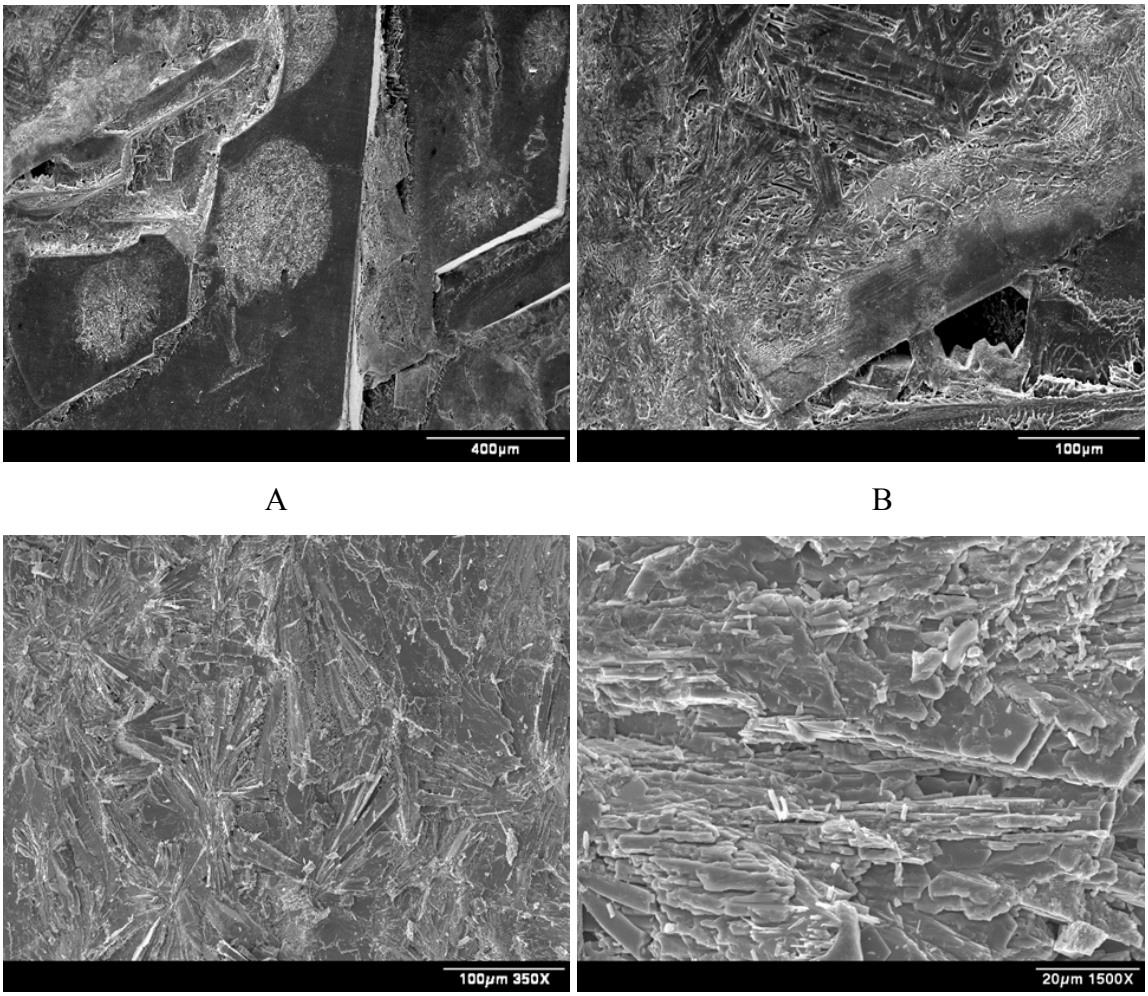

Fig. 9. SEM micrographs of the fracture surface of deliberately crystallized HHS30 samples

A and B) Simulated HHS30-CCC (cooled from 950°C to room temperature at 40°C/hr).

C and D) HHS30x (heat treated at 570°C for 24 hours).

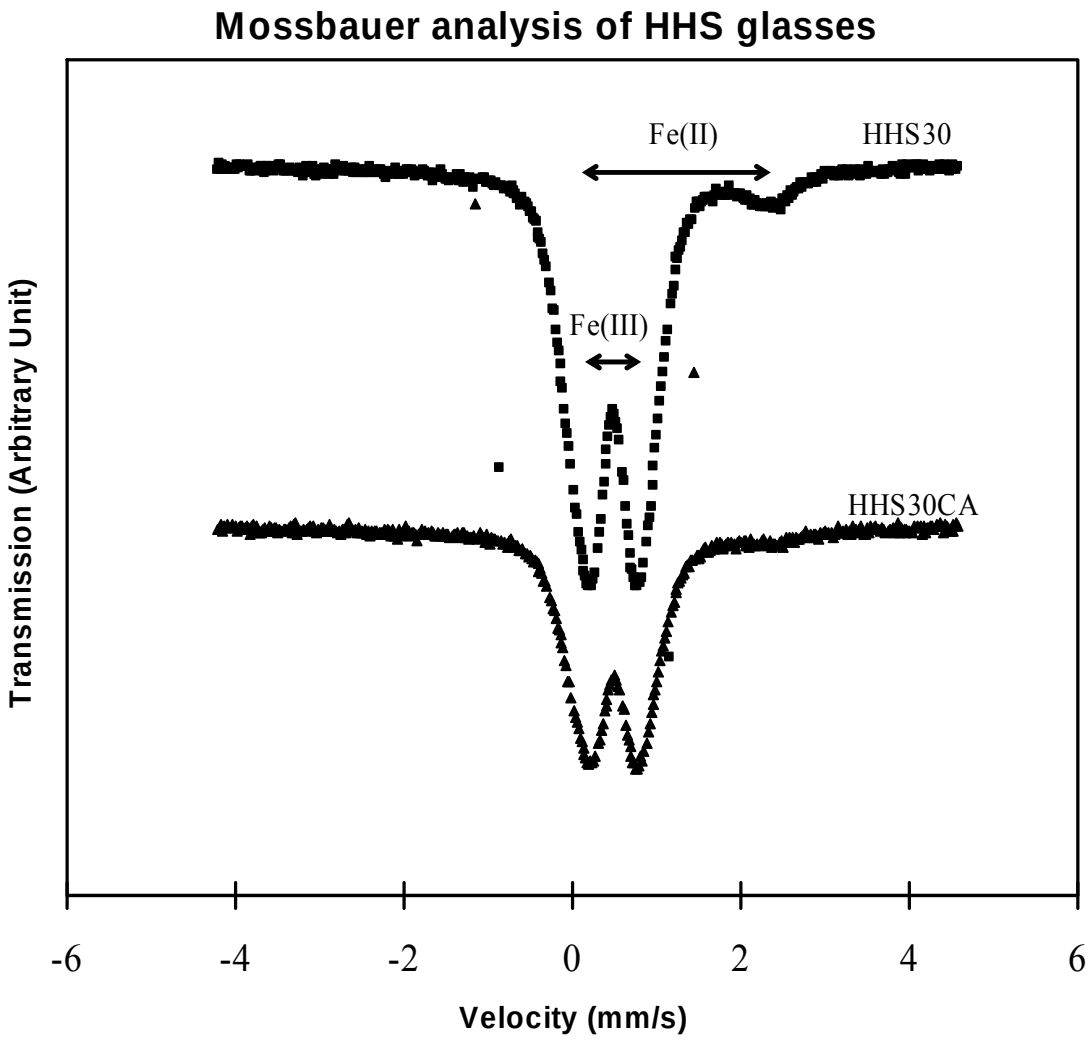

Fig. 10. Mössbauer spectra obtained at 23°C for HHS30 and HHS30CA iron phosphate glasses. The HHS30M spectra was nearly identical to the HHS30CA and is not shown here.

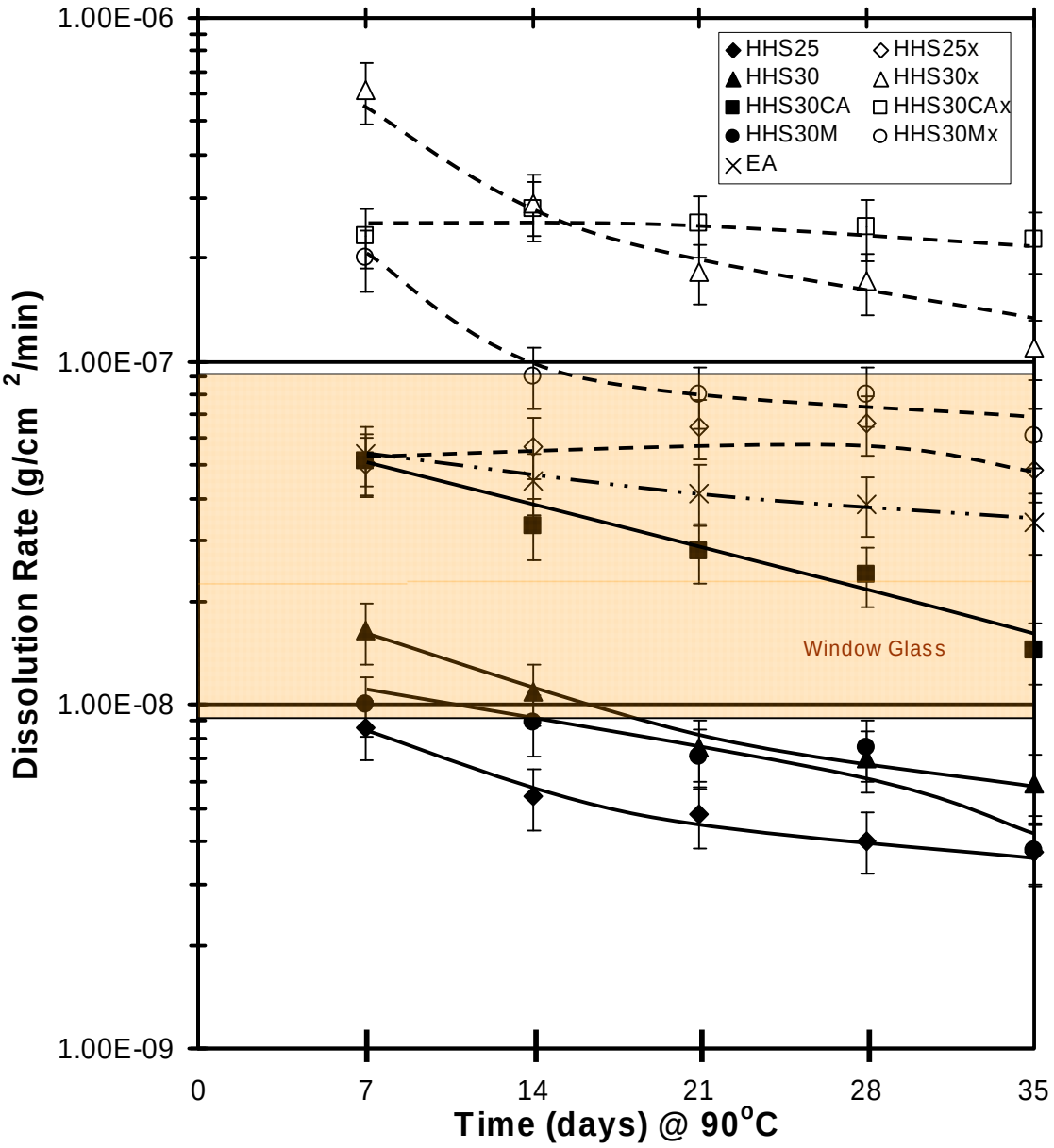

Fig. 11. Glass and crystallized sample dissolution rate as a function of time in 90°C DI water. Solid lines are for glassy samples, dashed lines are for crystallized samples. DR of EA glass (×) is included for comparison as well as the range for window glass in the shaded area. Lines are drawn as guides for the eye.

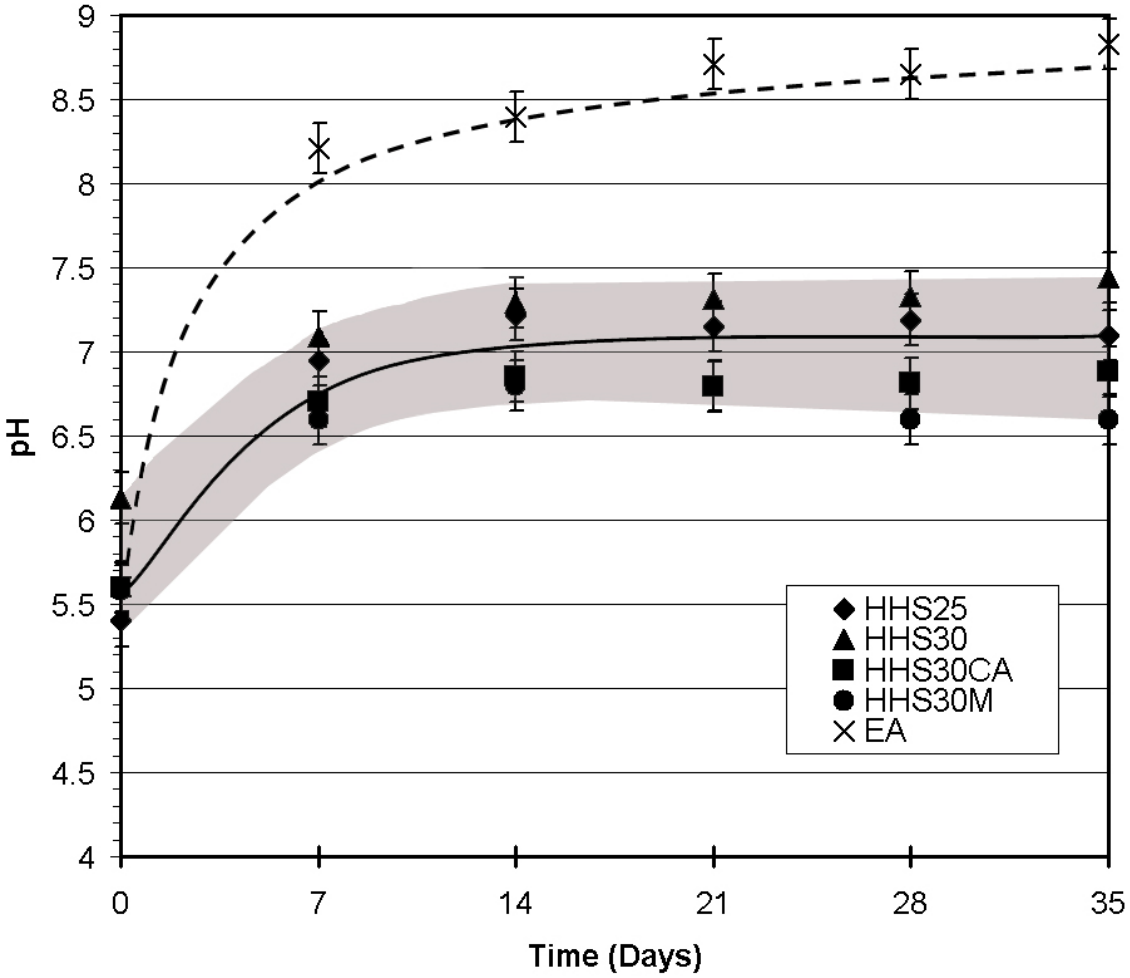

Fig. 12. Change in the pH of the DI water used for dissolution rate measurements of the iron phosphate HHS glasses (the average increase shown by the solid line with the shaded area denoting approximate range) as well as EA borosilicate glass (dashed line). Lines are drawn as guides for the eye.

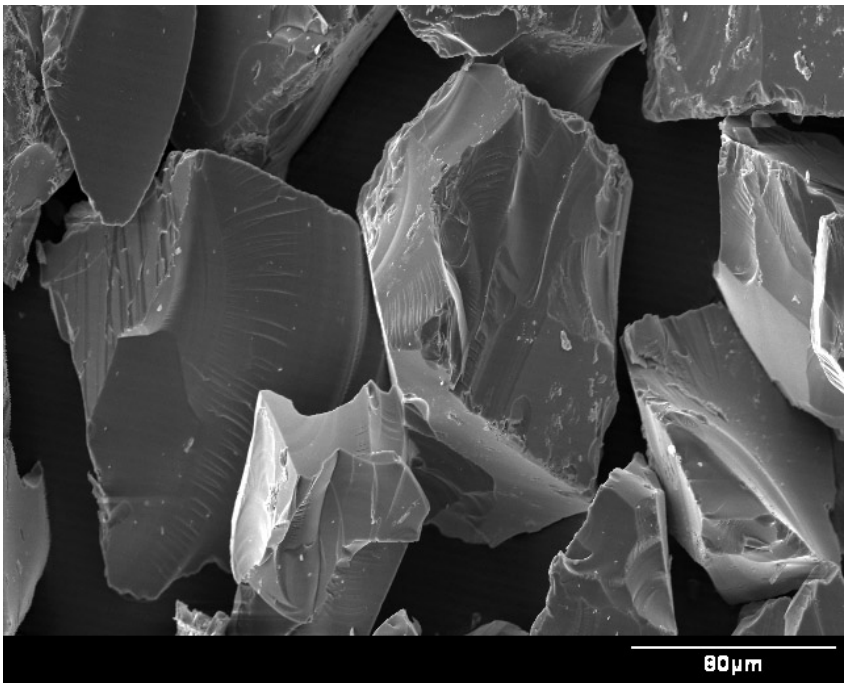

A

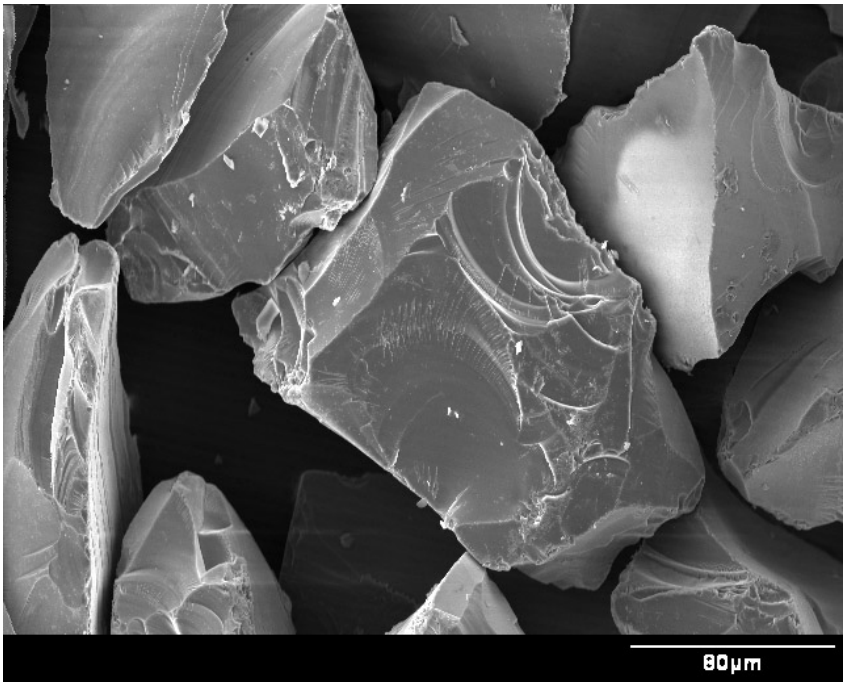

B

Fig. 13. A) SEM micrograph of uncorroded HHS30 glass particles at 500x.
B) HHS30 glass particles after immersion in deionized water at 90°C for seven days (PCT).

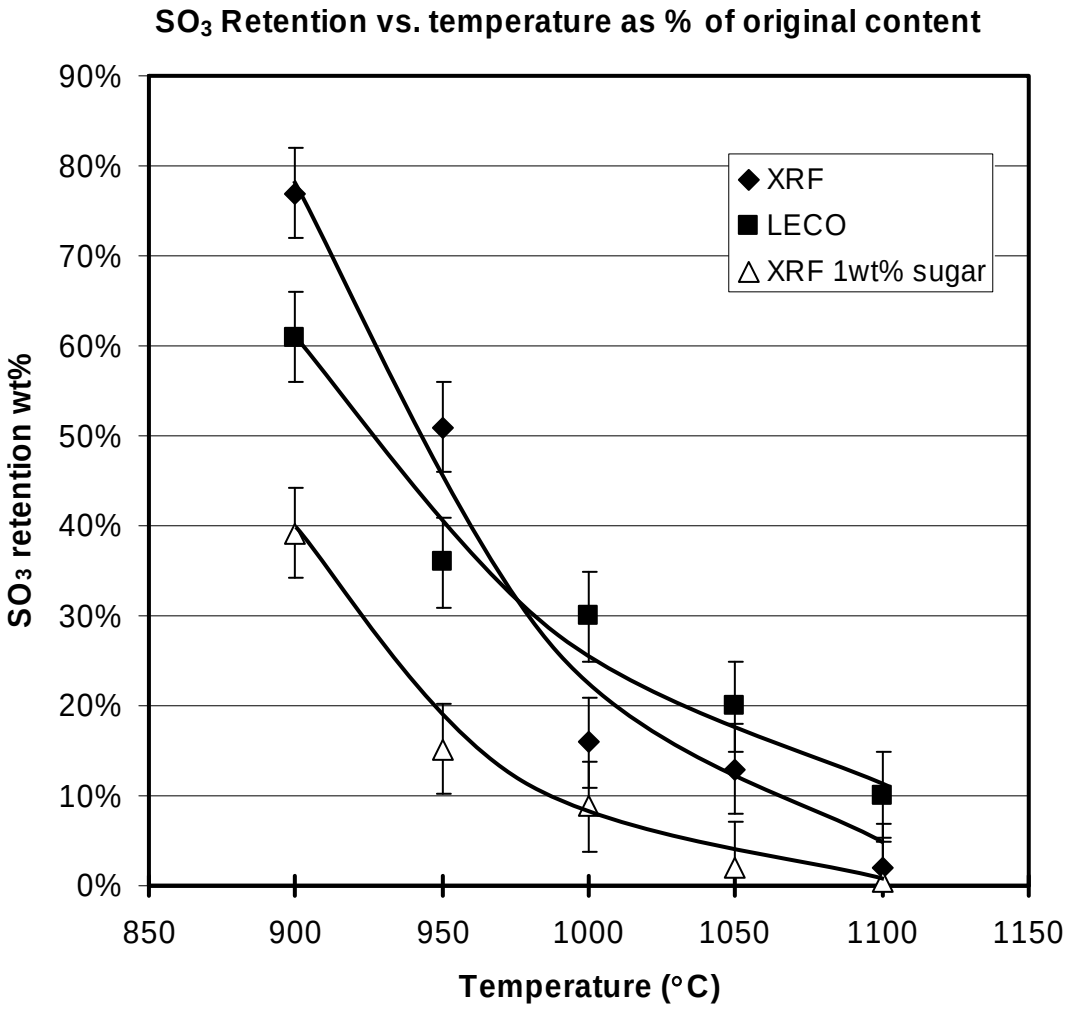

Fig. 14. Retention of SO_3 in a HHS30 glass after one hour at the temperatures shown. The SO_3 content of the starting batch was 2.85 wt%. Data for glasses made from batches containing 1 wt% sugar are denoted by open triangles (Δ). Lines are drawn as guides for the eye.

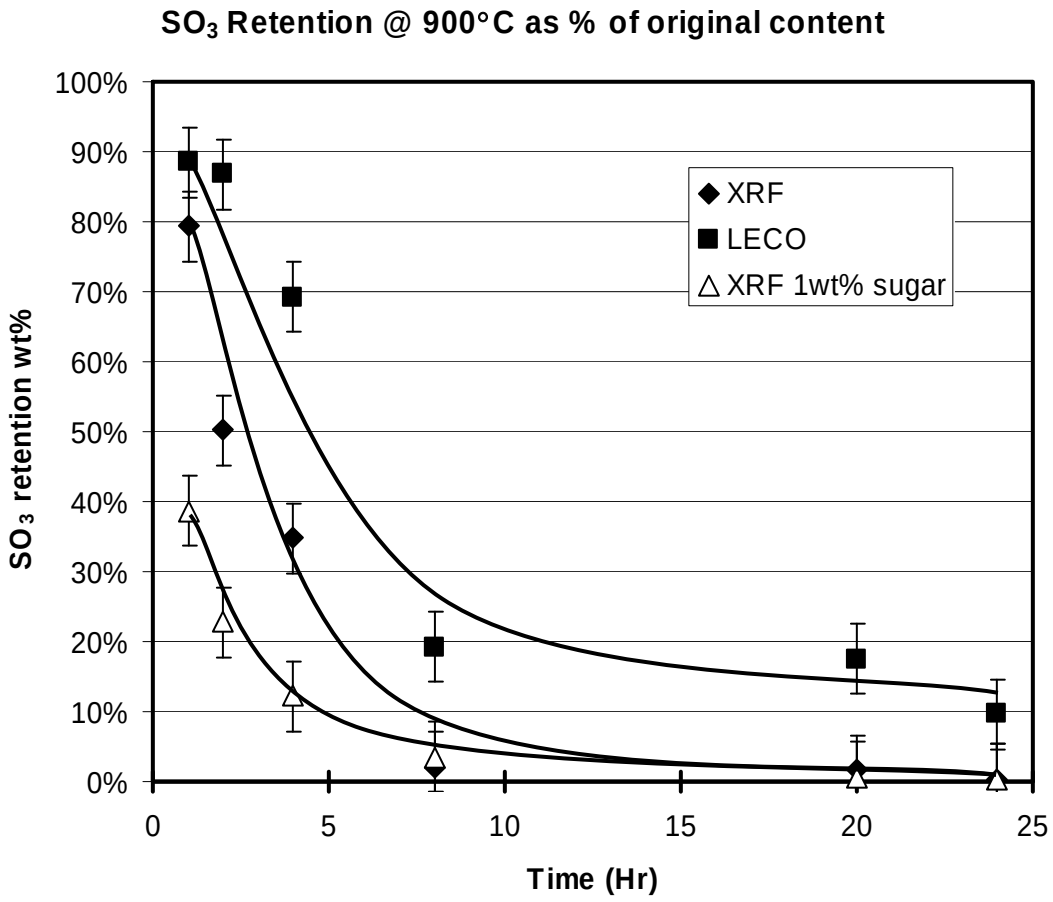

Fig. 15. Retention of SO_3 in a HHS30 glass after melting at 900°C for the time shown. The SO_3 content of the starting batch was 2.85 wt%. Data for glasses made from batches containing 1 wt% sugar are denoted by open triangles (Δ). Lines are drawn as guides for the eye.

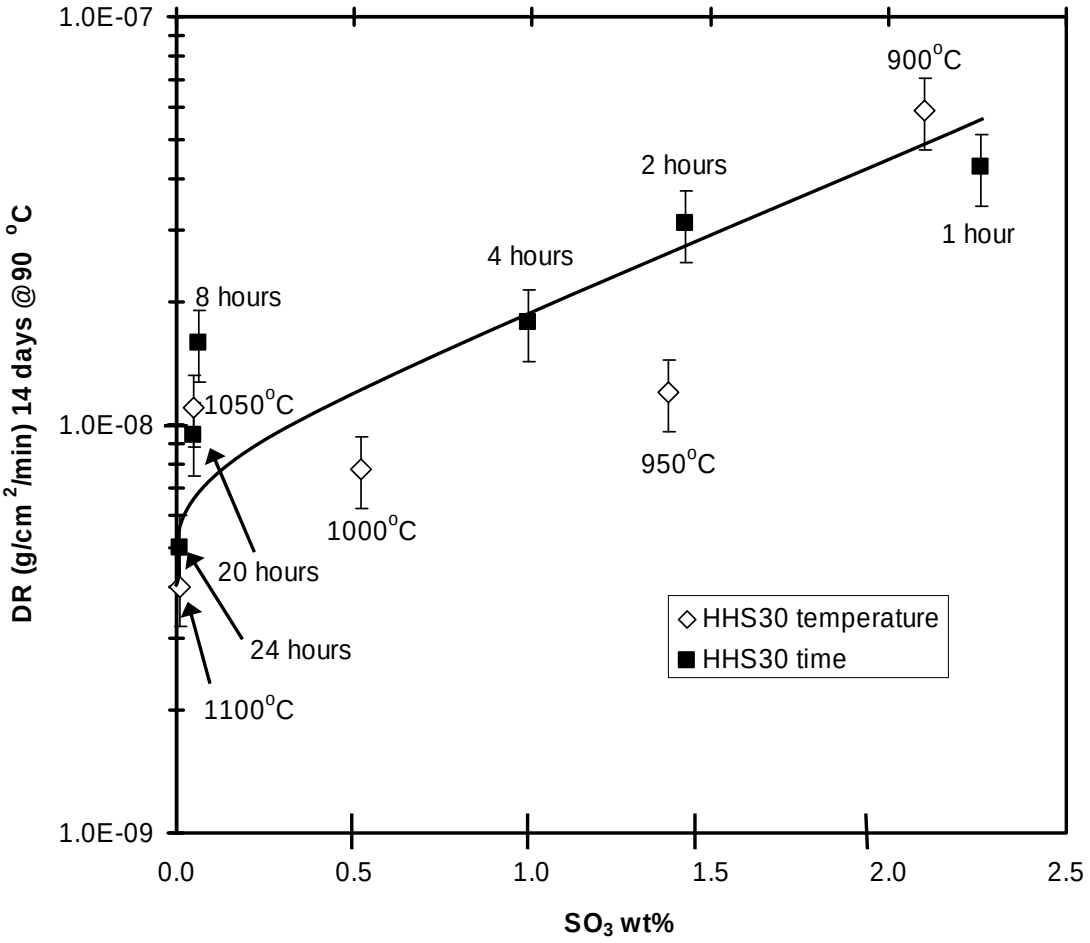

Fig. 16. Dependence of DR on SO_3 content (analyzed by XRF) for the HHS30 glass melted for varying times and temperatures, see Figs. 14 and 15. Sulfate content of starting batch was 2.85 wt%. The line is given as an indicator of the general trend.

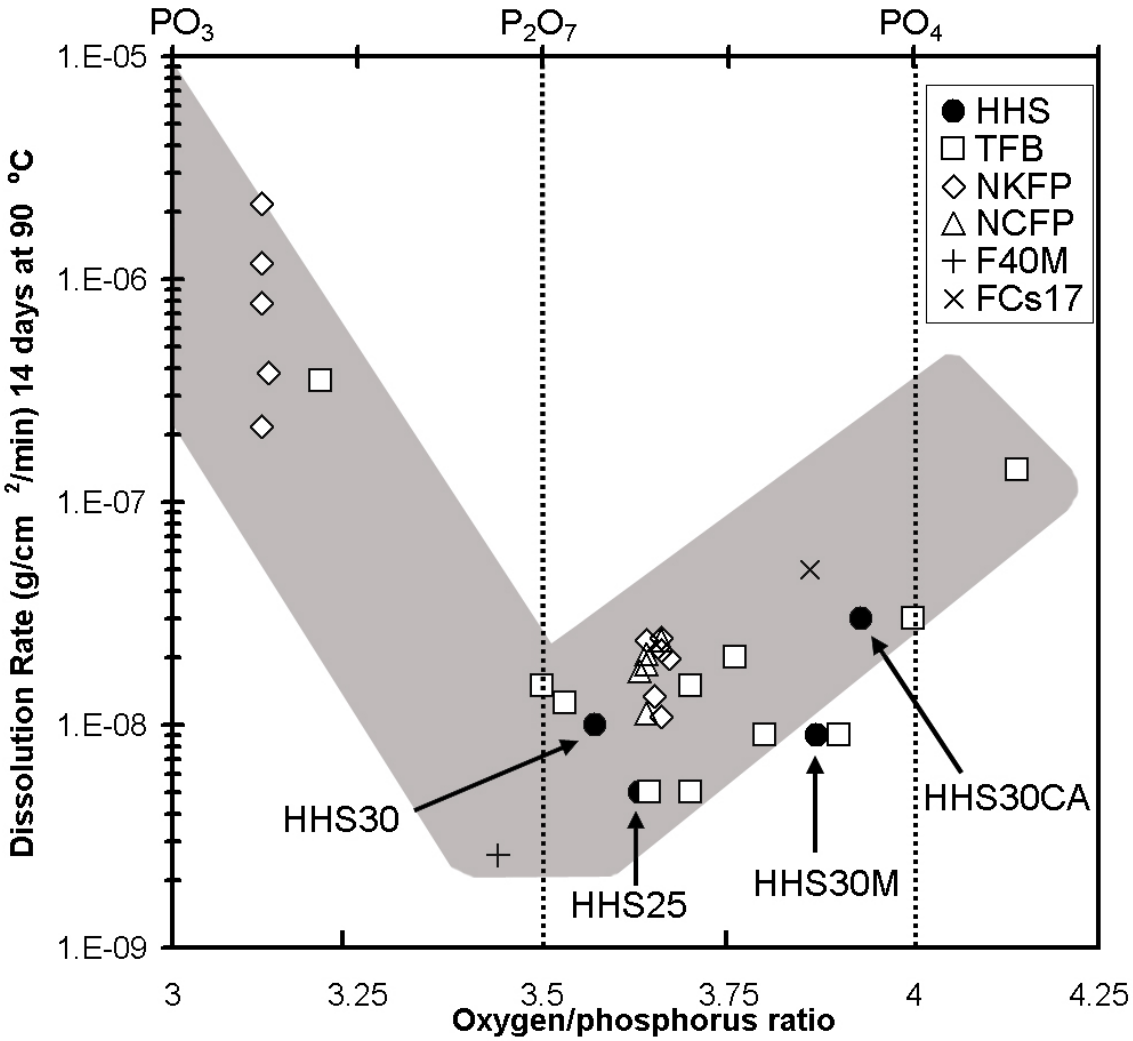

Fig. 17. Dissolution Rate as a function of O/P ratio for iron phosphate glasses containing HHS. Comparison data for iron phosphate glass containing (20 to 40 wt%) TFB waste from ref. [26]. NKFP and NCFP [36] which contain (20 mol% alkali, 20 to 32 mol% Fe_2O_3 and 48 to 60 mol% P_2O_5), F40M [36] (containing 40wt% Fe_2O_3 and 60 wt% P_2O_5) and FCs17 [38] (which contains 29 wt% Fe_2O_3, 38 wt% P_2O_5, and 33 wt% Cs_2O). Shaded area denotes general trend in DR with O/P ratio reported previously [26, 36].

APPENDIX A.

COMPLETE LIST OF IRON PHOSPHATE HHS GLASSES MELTED

Table A1
Compositions of Iron phosphate glasses containing HHS waste attempted.

Name	Composition	O/P	temp	time (hr)	DR*	Note
Trial Melts	W=SBW waste, F=Fe_2O_3, P=P_2O_5, U=UO_2, M=2%Bi2O3, 2%CaF2, 2%CaO, 2%PbO, 2%ZnO					
HHS30r	30W, 20F, 50P, 2 Sugar	3.7	950	2,7	Varies	Good glass
HHS30S	30W, 15F, 50P, 5SiO_2	3.6	950	2	-----	Silica unmelted
HHS30CA	30W, 10F, 50P, 5CaO, 5Al_2O_3	3.6	950	2	2.0E-08	Good glass
HHS30CaO	30W, 15F, 50P, 5CaO	3.6	950	2	1.8E-07	Good glass
HHS30(temp)	30W, 20F, 50P	3.7	up to 1200	1	varies	SO_3 vs temp
HHS30(time)	30W, 20F, 50P	3.7	up to 1200	1	varies	SO_3 vs time
HHS30Al	30W, 10F, 50P, 10Al_2O_3	3.7	1000	2	1.7E-07	Some alumina unmelted
HHS30Al2	30W, 15F, 50P, 5Al_2O_3	3.7	1000	2	8.9E-08	Good glass
HHS30Mn	30W, 15F, 50P, 5Mn_2O_3	3.7	950	2	7.6E-08	Good glass
HHS30MnB	30W, 10F, 50P, 10Mn_2O_3	3.7	950	2	2.3E-07	Good glass
HHS30MnC	30W, 15F, 45P, 10Mn_2O_3	3.7	950	2	5.9E-07	Good glass
HHS30Cr	30W, 15F, 50P, 5 Cr_2O_3	3.6	1000	2	1.2E-07	Green residue in crucible
HHS30U6	30W, 50P, 10F, 4U, 4CaF, 2Cr_2O_3	3.5	1000	2	9.0E-07	good glass
HHS30U5	30W, 52P, 15F, 3U	3.5	1000	2	Fell apart	partially crystallized
HHS30U4	30W, 52P, 12F, 6U	3.5	1000	2	Fell apart	Crystallized
HHS30U3	30W, 50P, 10F, 6U, 2ZrO_2, 2Cr_2O_3	3.6	1000	2	Fell apart	Uranium oxide unmelted
HHS30	30W, 20F, 50P	3.7	950	2	------	cooled to rt in furnace
HHS30HS	48g Na_2SO_4, 10F, 25P	3.8	950	2	------	cooled to rt in furnace
HHS30HS3	30W, 20F, 50P	3.7	up to 1200	1	Varies	some samples xtal
HHS30HS2	30W, 20F, 50P	3.7	950	2	Varies	Good glass
HHS30U2	30W, 10F, 50P 6UO2 4CaF	3.5	950	2	9.0E-08	
HHS25HS	25W, 20F, 55P.	3.5	up to 1200	1	Varies	higher temp samples better
HHS30U	30W, 10F, 50P 6UO_2	3.5	1000	2	4.0E-08	
HHS30ZCF	30W, 12F, 50P 4CaF	3.5	1000	2	-----	green glass
HHS25N	25W, 20F, 55P.	3.5	1000	2	Fell apart	crystallized
HHS25M(2)	25W, 20F, 45P 10M	3.8	1000	2	5.0E-09	
HHS30 Ca2	30W, 18F, 47P 5CaF	3.7	1000	2	1.2E-08	
HHS27.5	27.5W, 22.5F, 50P	3.7	1000	2	7.5E-09	
HHS25	25W, 25F, 50P	3.7	1000	2	-----	cracked on anneal
HHS25b	25W, 20F, 55P	3.1	51000	2	9.5E-09	Good glass
HHS25c	25W, 30F, 45P	4.0	1000	2	8.1E-08	
HHS20	20W, 35F, 45P	4.0	1000	2	9.5E-09	Glass
HHS30M(4)	30W, 20F, 40P, 10M	4.1	1000	2	------	small crystals in glass
HHS25j	25W, 15F, 50P, 5Mn, 2.5Pb, 2.5CaF_2	3.5	1000	2	------	Good glass
HHS25(2)	25W 25F, 50P	3.7	1000	2	------	Crystallized
HHS30G	30W, 20F, 42.5P, 7.5CaF_2	3.9	950	2	3.3E-07	

HHS30F	30W, 20F, 40P, 10CaF_2	4.0	950	2	9.3E-08	Good glass
HHS30M (2)	30W, 20F, 40P, 10M	4.1	950	14	------	
HHS25M	25W, 20F, 45P	3.8	950	2	8.2E-08	good glass
HHS35M (time)	35W, 20F, 35P	3.9	950	to 24	------	Some crystallized
HHS35M (temp)	45W, 14F, 41P	3.6	up to 1200	1	------	Some crystallized
HHS30M	30W, 20F, 40P	4.1	950	2	2.5E-09	good glass
HHS20	20W, 35F, 45P	4.0	1000	2	1.2E-09	good glass
HHS30C	30W, 25F, 45P	3.9	950	2	5.3E-10	good glass
HHS40 (time)	40W, 15F, 45P	4.0	950	to 24	------	good glass
HHS40 (temp)	40W, 15F, 45P	4.4	up to 1200	1	------	all but 900C made good glass
HHS35C	35W, 20F, 37.5P. 7.5B	5.0	950	2	2.8E-07	good glass
HHS35B	35W, 20F, 30P. 15B	5.0	950	2	3.0E-07	good glass
HHS25	25W, 30F, 45P	4	950	2	2.0E-08	good glass
HHS25B	25W, 25F, 50P	3.7	950	2	1.5E-08	good glass
HHS25c2	25W 30F 45P	3.5	1000	1	8.3E-08	good glass
HHS30	30W, 20F, 50P	3.7	1100	1	9.1E-09	Good Black Glass, Silver Color When Cut
HHS30B	30W, 30F, 40P	4.2	1000	1	------	Sample was in-homogenous
HHS30C2	30W, 25F, 45P	3.9	900	1	2.2E-06	Xtal
HHS30C3	30W, 25F, 45P	3.9	1000	1	7.5E-08	Sample Slightly Cracked in Annealing
HHS30(5)	30W,20F, 50P	3.7	1000	1	-----	cracked, Xtal @ Pour
HHS35	35W, 20F, 45P	3.9	950	1	1.1E-07	Glass w/ Small Xtal @ Pour
HHS35(2)	35W, 20F, 45P	3.9	1000	1	9.5E-08	Good Glass
HHS40	40W, 15F, 45P	3.9	950	1	1.0E-06	Good Glass
HHS40(2)	40W, 15F, 45P	3.9	1000	1	8.9E-07	Good Glass
HHS40(3)	40W, 15F, 45P	3.9	1050	1	4.8E-07	Good Glass
HHS45	45W,10F,45P	3.9	950	1	------	Good Green Glass
HHS45(2)	45W,10F,45P	3.9	1000	1	3.6E-06	Good Glass
HHS50	50W, 10F, 40P	4.2	950	1	------	Green Glass w/ Yellow xtals
HHS50B	50W, 5F, 45P	4.0	950	1	------	Good Green Glass
HHS55	55W, 10F, 35P	4.5	950	1	------	green glass partial xtal
HHS60	60W, 5F, 35P	4.5	950	1	------	xtal
Final Melts						
HHS30	30W, 20F, 50P	3.7	950	2	6.0E-09	Good glass
HHS30CA	30W, 10F, 50P, 5Al_2O_3, 5CaF_2	3.6	950	2	1.0E-08	Good glass
HHS30M	30W, 20F, 40P, 10P	3.7	950	2	4.1E-09	Good glass
HHS25	25W, 25F, 50P	3.7	950	2	4.0E-09	Good glass
HHS30x	30W, 20F, 50P	3.7	950	2	1.2E-07	Heat-treat @ 570
HHS30CAx	30W, 10F, 50P, 5Al_2O_3, 5CaF_2	3.6	950	2	2.3E-07	Heat-treat @ 580
HHS30Mx	30W, 20F, 40P, 10P	3.7	950	2	6.5E-07	Heat-treat @ 560
HHS25x	25W, 25F, 50P	3.7	950	2	5.2E-07	Heat-treat @ 570
HHS30-CCC	30W, 20F, 50P	3.7	950	2	1.5E-05	Cooled 40°C/min from melt temperature

*g/cm^2/min @ seven days in DI water at 90°C.

APPENDIX B.

COMPLETE DR DATA FOR IRON PHOSPHATE GLASSES CONTAINING HHS

Table B1

DR data for glasses measured from 7 to 35 days. Bold average values used in Fig. 11.

	Dissolution Rate g/cm^2/min				
	7 days	**14 days**	**21 days**	**28 days**	**35 days**
HHS25-1	1.0E-08	6.5E-09	5.4E-09	4.5E-09	4.5E-09
HHS25-2	7.1E-09	4.5E-09	4.0E-09	3.4E-09	3.1E-09
HHS25-3	8.4E-09	5.2E-09	5.0E-09	4.2E-09	3.6E-09
HHS25 avg	**8.6E-09**	**5.4E-09**	**4.8E-09**	**4.0E-09**	**3.7E-09**
HHS30-1	1.1E-08	9.1E-09	6.3E-09	5.8E-09	4.9E-09
HHS30-2	2.0E-08	1.3E-08	8.7E-09	8.4E-09	7.1E-09
HHS30-3	1.7E-08	1.1E-08	7.6E-09	6.9E-09	5.7E-09
HHS30 avg	**1.6E-08**	**1.1E-08**	**7.5E-09**	**7.0E-09**	**5.9E-09**
HHS30CA-1	5.3E-08	3.3E-08	3.0E-08	2.5E-08	1.4E-08
HHS30CA-2	4.2E-08	2.8E-08	2.3E-08	2.0E-08	1.2E-08
HHS30CA-3	5.9E-08	4.0E-08	3.2E-08	2.7E-08	1.7E-08
HHS30CA avg	**5.1E-08**	**3.3E-08**	**2.8E-08**	**2.4E-08**	**1.4E-08**
HHS30M-1	5.1E-09	4.3E-09	5.7E-09	6.9E-09	4.1E-09
HHS30M-2	2.3E-08	2.0E-08	1.3E-08	9.9E-09	4.5E-09
HHS30M-3	2.4E-09	2.8E-09	2.8E-09	5.7E-09	2.7E-09
HHS30M avg	**1.0E-08**	**8.9E-09**	**7.1E-09**	**7.5E-09**	**3.8E-09**
EA-1	6.5E-08	5.6E-08	5.0E-08	4.6E-08	3.7E-08
EA-2	4.5E-08	3.8E-08	3.3E-08	3.1E-08	3.0E-08
EA-3	5.2E-08	4.1E-08	4.0E-08	3.7E-08	3.4E-08
EA avg	**5.4E-08**	**4.5E-08**	**4.1E-08**	**3.8E-08**	**3.4E-08**

Table B2
pH values of water used in dissolution rate measurements for iron phosphate glasses containing HHS. Bold average values used in Fig. 12.

	Initial pH	**7 days**	**14 days**	**21 days**	**28 days**	**35 days**
HHS25-1	5.40	6.89	7.02	7.07	7.11	7.03
HHS25-2	5.40	6.94	7.35	7.25	7.31	7.23
HHS25-3	5.40	7.02	7.28	7.13	7.16	7.03
HHS25 avg	**5.40**	**6.95**	**7.22**	**7.15**	**7.19**	**7.10**
HHS30-1	6.13	6.93	7.14	7.17	7.21	7.32
HHS30-2	6.13	7.08	7.22	7.24	7.30	7.41
HHS30-3	6.13	7.25	7.52	7.53	7.49	7.59
HHS30 avg	**6.13**	**7.09**	**7.29**	**7.31**	**7.33**	**7.44**
HHS30CA-1	5.60	6.58	6.68	6.71	6.81	6.96
HHS30CA-2	5.60	6.79	6.96	6.89	6.92	6.87
HHS30CA-3	5.60	6.74	6.89	6.78	6.73	6.80
HHS30CA avg	**5.60**	**6.70**	**6.84**	**6.79**	**6.82**	**6.88**
HHS30M-1	5.58	6.69	6.78	6.80	6.67	6.67
HHS30M-2	5.58	6.76	6.81	6.86	6.62	6.62
HHS30M-3	5.58	6.35	6.56	6.68	6.54	6.57
HHS30M avg	**5.58**	**6.60**	**6.72**	**6.78**	**6.61**	**6.62**
EA-1	5.60	8.26	8.08	8.65	8.56	8.86
EA-2	5.60	8.02	8.54	8.75	8.78	8.93
EA-3	5.60	8.36	8.57	8.73	8.61	8.69
EA avg	**5.60**	**8.21**	**8.40**	**8.71**	**8.65**	**8.83**

Table B3
DR of deliberately crystallized HHS iron phosphate wasteforms. Bold average values used in Fig. 11.

	Dissolution Rate g/cm^2/min				
	7 days	**14 days**	**21 days**	**28 days**	**35 days**
HHS25x-1	2.1E-08	4.7E-08	5.4E-08	4.5E-08	4.1E-08
HHS25x-2	5.1E-08	5.4E-08	6.2E-08	7.2E-08	4.6E-08
HHS25x-3	7.8E-08	7.2E-08	7.9E-08	8.1E-08	6.1E-08
HHS25 avg	**5.0E-08**	**5.7E-08**	**6.5E-08**	**6.6E-08**	**4.9E-08**
HHS30x-1	6.4E-07	9.1E-08	7.3E-08	6.8E-08	5.0E-08
HHS30x-2	5.3E-07	3.6E-07	9.7E-08	9.0E-08	7.1E-08
HHS30x-3	7.3E-07	4.1E-07	3.6E-07	2.9E-07	2.7E-07
HHS30 avg	**6.2E-07**	**2.9E-07**	**1.8E-07**	**1.7E-07**	**1.1E-07**
HHS30CAx-1	1.3E-07	2.0E-07	1.9E-07	2.4E-07	1.5E-07
HHS30CAx-2	4.1E-07	3.8E-07	2.3E-07	2.0E-07	2.2E-07
HHS30CAx-3	2.4E-07	2.2E-07	3.3E-07	2.9E-07	3.3E-07
HHS30CA avg	**2.3E-07**	**2.8E-07**	**2.5E-07**	**2.5E-07**	**2.3E-07**
HHS30Mx-1	8.1E-08	6.3E-08	5.7E-08	6.9E-08	5.1E-08
HHS30Mx-2	2.3E-07	1.4E-07	1.1E-07	9.9E-08	7.6E-08
HHS30Mx-3	2.8E-07	3.0E-08	2.8E-08	5.7E-08	4.7E-08
HHS30M avg	**2.0E-07**	**9.1E-08**	**8.0E-08**	**8.1E-08**	**6.1E-08**

APPENDIX C.

DR AS A FUNCTION OF SO_3 RETENTION

Table C1
DR for HHS30 glasses melted for determination of SO_3 retention as a function of time and temperature. SO_3 wt% determined by XRF.

Temperature °C	**DR**	**wt% SO_3**	**% SO_3 Retention**
900	5.9E-08	2.10	74%
950	1.2E-08	1.38	48%
1000	7.8E-09	0.52	18%
1050	1.1E-08	0.05	2%
1100	4.0E-09	0.01	0%

Time (Hr)	**DR**	**wt% SO_3**	**% SO_3 Retention**
1	4.3E-08	2.26	79%
2	3.1E-08	1.43	50%
4	1.8E-08	0.99	35%
8	1.6E-08	0.06	2%
20	9.4E-09	0.05	2%
24	5.0E-09	0.01	0%

VITA

Robert Douglas Leerssen was born on November 22, 1977 in Fairbury, Nebraska to R. Douglas and Martha Leerssen. Robert grew up in Sedalia, Missouri but returned to Nebraska for high school; he graduated from Nebraska Evangelical Lutheran High School in Waco, Nebraska in 1996. He entered the University of Missouri – Rolla in the fall of 1996, and received his B.S. in Ceramic Engineering in December 2000. He began work on his M.S. in Ceramic Engineering under the guidance of Dr. Delbert Day in January 2001.

During his academic career at UMR, Robert was involved in a number of campus organizations including holding offices in Tau Kappa Epsilon fraternity, as well as in Keramos. He was also a member of the American Ceramic Society and Alpha Chi Sigma.